STUDIES ON SOME ASPECTS OF LIENARD LIKE DYNAMICAL SYSTEMS

A Thesis Submitted to the

UNIVERSITY OF NORTH BENGAL

for the Award of

DOCTOR OF PHILOSOPHY

in

MATHEMATICS

By

Aniruddha Palit

Under

the Supervision of

Prof. D. P. Datta

Department of Mathematics

University of North Bengal

Raja Rammohunpur, Siliguri

West Bengal - 734 013, India

May, 2016

DECLARATION

I declare that the thesis entitled **'STUDIES ON SOME ASPECTS OF LIENARD LIKE DYNAMICAL SYSTEMS'** has been prepared by me under the guidance of **Dr. D. P. Datta**, Professor, Department of Mathematics, University of North Bengal. No part of this thesis has formed the basis for the award of any degree or fellowship previously.

(Aniruddha Palit)
Department of Mathematics
University of North Bengal
Raja Rammohunpur
Siliguri, West Bengal - 734 013
INDIA

Date: 23.05.2016

CERTIFICATE

I certify that **Aniruddha Palit** has prepared the thesis entitled **'STUDIES ON SOME ASPECTS OF LIENARD LIKE DYNAMICAL SYSTEMS'**, for the award of Ph. D. degree of the University of North Bengal, under my guidance. He has carried out the work at the Department of Mathematics, University of North Bengal.

(Dr. D. P. Datta)
Professor
Department of Mathematics
University of North Bengal
Raja Rammohunpur
Siliguri, West Bengal - 734 013
INDIA

Professor
Department of Mathematics
University of North Bengal

Date: 23.05.2016

Abstract

David Hilbert proposed a list of 23 problems in Mathematics at the Paris conference of the International Congress of Mathematicians in 1900. The 16-th problem of his list consists of two similar problems in different branches of mathematics. The first problem is the investigation of the relative positions of the branches of real algebraic curves of degree n (and similarly for algebraic surfaces) and the second problem is the determination of the upper bound for the number of limit cycles in two-dimensional polynomial vector fields of degree n and an investigation of their relative positions. The second problem is known as Hilbert's sixteenth problem in the field of dynamical systems. Since then the problem remains unsolved for $n > 1$. However, some attempts are made by different authors in solving particular cases of this problem. So, it is evident that the study of limit cycle in dynamical system is still a vibrant field of current research.

In the field of dynamical system the Lienard equation is a second order differential equation, named after the French physicist Alfred-Marie Lienard. The well known classical Lienard's theorem ensures the uniqueness and existence of a limit cycle for this system under certain additional assumptions. One of the aims of this project is to find sufficient conditions ensuring existence of multiple limit cycles for Lienard like dynamical systems. We have generalized Lienard's theorem in different ways and found new results in this field.

The determination of shape, amplitude and other dynamical quantities of a limit cycle is another challenging field in the study of dynamical systems, especially in nonperturbative regime. Different asymptotic techniques have been developed to find an analytic solution and related dynamical quantities of nonlinear ordinary differential systems in which the Homotopy Analysis Method (HAM) is one such technique giving a

systematic approach to deal with this kind of problem. We used this technique to find the amplitude of the limit cycle as a uniformly valid function of the nonlinearity parameter for a particular Lienard like dynamical system viz., Rayleigh equation.

Another useful technique in this topic is Renormalization Group Method (RGM), which was originally formulated for managing divergences in the quantum field theory and later having deep applications in phase transitions and critical phenomena in statistical mechanics. Chen et al. (L.Y. Chen, N. Goldenfeld, and Y. Oono. Renormalization group and singular perturbations: Multiple scales, boundary layers, and reductive perturbation theory. *Physical Review E*, 54(1) : 376, 1996) translated this technique into the study of nonlinear differential equation. We used RGM to find the amplitude of limit cycle of two closely related systems viz., Van der Pol equation and Rayleigh Equation. We found that RGM is not capable in estimating amplitude of limit cycle in nonperturbative regime.

We have generalized the idea of RGM further by the introduction of control parameters similar to that used in HAM and also used a novel idea of nonlinear time leading to Improved Renormalization Group Method (IRGM). The use of IRGM enabled us to find good analytic approximation to the equation of the limit cycles for Van der Pol and Rayleigh differential equation exploiting multiple nonlinear scales associated with nonlinear time.

The publications during this study are listed below:

1. A. Palit and D.P. Datta. On a finite number of limit cycles in a lienard system. *International Journal of Pure and Applied Mathematics*, 59:469–488, 2010.

2. A. Palit and D.P. Datta. On the determination of exact number of limit cycles in lienard systems. *Bull. Cal. Math. Soc.*, 104:35–56, 2012.

3. A. Palit and D.P. Datta. Comparative Study of Homotopy Analysis and Renormalization Group Methods on Rayleigh and Van der Pol Equations. *Differential Equations and Dynamical Systems*, 1-

27, Available first online 26 July 2015, Doi: 10.1007/s12591-015-0253-y.

4. A. Palit and D.P. Datta. Existence of Limit Cycles in a Class of Non-symmetric Lienard Systems. *Indian Journal of Mathematics*, 58:59–93, 2016.

DEDICATION

To My Mamuni (Mother)

ACKNOWLEDGEMENTS

Completing a Doctoral thesis is certainly a matter of great delight to any person, especially to those who are engaged in educational ambience. In this especially opportune moment, I would like to express my wholehearted gratitude and deep regards to all the persons who helped me directly or indirectly to achieve this significant stage in my life.

First, I would like to express my profound appreciation to my respected supervisor Dr. Dhurjati Prasad Datta, Professor, Department of Mathematics, University of North Bengal for his magnificent supervision, heartiest cooperation and valuable suggestions throughout the entire course of this research work. He has supported me by his novel ideas, sound advice during different stages of my investigation. His sustained interest and delightful care in reviewing the thesis made my work easier and complete.

I would also like to express my genuine gratitude to my teachers of Department of Mathematics, University of North Bengal for their support in different occasions during my course of study. I wish to convey special note of appreciation to Dr. Kamal Kanti Nandi, Professor, Department of Mathematics, University of North Bengal for introducing Mathematica and Scientific Workplace which helped me a lot throughout my study.

Finally, my deepest gratitude goes to my Mamuni (Mother) Smt. Tapasi Palit for her unflagging love and unconditional support and constant inspiration throughout my life along with all the relatives and friends for their moral support and encouragement which enabled me to complete this investigation.

Date: 23.05.2016 Aniruddha Palit

Place: University of North Bengal (Aniruddha Palit)

List of Abbreviations

CGO:	Chen, Goldenfeld and Oono
DE:	Differential Equation
HAM:	Homotopy Analysis Method
IRGM:	Improved Renormalization Group Method
LPM:	Lins, Pugh and de Melo
NDE:	Nonlinear Differential Equation
ODE:	Ordinary Differential Equation
PDE:	Partial Differential Equation
QFT:	Quantum Field Theory
RG:	Renormalization Group
RGM:	Renormalization Group Method
VdP:	Van der Pol

Contents

Chapter 1

Preliminaries

1.1 Introduction

The study of nonlinear differential equations is of great interest in understanding the fundamental laws of nature. A basic fact of nature is that the laws governing the evolution of natural processes are generally described *locally* by differential equations. The local rate of variation of a relevant dynamical quantity in an infinitesimal neighbourhood of a point is related functionally to itself and other relevant dynamical variables so as to give an analytical (differential) representation of the law of variation of a given natural system. For a linear functional relationship involving the concerned dynamical variables, the natural law under study is linear and thus satisfies the principle of superposition; otherwise the concerned law and the associated differential equation is nonlinear. The theory of linear differential equations is fairly well understood in the sense that a linear differential equation with regular singularity is exactly solvable in the form of modified power series by the Frobenius method in the class of special functions at least locally in a neighbourhood of the singular point. In the case of an irregular singular point, on the other hand, a Frobenius series does not generally exists. One, however, is interested in estimating dominant asymptotic behaviour of the solution by well known asymptotic methods such as the method of dominance balance, WKB method, boundary layers method and so on [1, 2].

The difficulty with nonlinear DE (NDE) is that only a very few can admit exact solutions respecting general integrability criteria, thus ex-

posing special symmetry properties of the underlying dynamical problem. As an example, let us recall that the pendulum equation

$$\ddot{x} + \mu^2 \sin x = 0 \tag{1.1}$$

does admit exact solution involving elliptic integrals which in turn tells that the symmetry group of the nonlinear pendulum is much larger involving both librations or small oscillations about the stable centre and large rotations joining both the centre and unstable saddle, while the corresponding linearized orbit simply corresponds to small oscillations. Although study of possible exact solutions and integrability of NDEs is a topic of great interest, the class of exactly integrable equations using special functions is rather very small, that is to say a class of measure zero. Majority of NDEs are generally known to be non-integrable and can not be solved explicitly using known functions. As a consequence the study of qualitative methods to determine important features of a NDE without solving it exactly, in one hand, and also developing new efficient asymptotic methods to estimate accurately the approximate nature of the exact solutions and other relevant dynamical parameters, on the other, are both of great current interests in the literature of applied mathematics [1, 3, 4].

The main objective of the thesis is to study some aspects of qualitative theory of nonlinear differential equations in the context of a class of Lienard equations. The thesis also reports on an application of a new improved asymptotic method in estimating the periodic orbit and the corresponding amplitude for a class of Rayleigh-Van der Pol equations. The thesis is therefore divided into two parts. In Part I we present some simple but nevertheless interesting extensions of the classical Lienard theorem on the existence of unique limit cycle. In chapter 2 and 3, we present some theorems on the existence of exactly 2 and N number of distinct limit cycles for a class of generalized Lienard equations with symmetric potentials. In Chapter 4, the above theorem is extended for at least n limit cycles for more general class of Lienard equations with non-symmetric potential. In Part II of the thesis, we present analytic formula for amplitude of the unique limit cycle for both Rayleigh and Van der Pol equations in Chapter 5 using the Homotopy

Analysis Method (HAM). Similar results are discussed in Chapter 6 by Renormalization Group Method (RGM). In Chapter 7, we discuss applications of an Improved Renormalization Group Method (IRGM) in obtaining approximate formulae both for the periodic orbit and the corresponding amplitude for Rayleigh Van der pol system and the results are compared with those obtained by Homotopy Analysis method.

1.2 Qualitative Theory of Nonlinear Ordinary Differential Equations

The basic reason for studying nonlinear ODE stems from the fact that nature is inherently nonlinear; majority of natural processes and laws governing them are nonlinear. In fact, linear superposition principle can at best be considered to hold approximately for a realistic natural system. As for example, the (linear) simple harmonic oscillation is an approximate small amplitude oscillation of the nonlinear pendulum equation (1.1). Historically, the qualitative theory of NDE was founded by J. Henri Poincare around 1880s when he initiated his pioneering investigations of three body problem in celestial mechanics [5]. His work in this field laid down the foundation of various key concepts such as the (Poincare) first return maps, sensitive dependence on initial conditions of the late time asymptotic behaviour of a solution, the phenomenon of recurrence and others, in reinterpreting a NDE as a deterministic dynamical system. Poincare's original contributions on the dynamical system approach to NDE remains as an isolated masterpiece over a considerable period of time until the thread was taken up slowly by a number of physicists and mathematicians in the second quarter of twentieth century such as Balthazar Van der Pol [6] on the existence of stable nonlinear (self-excited) oscillation in vacuum tube electric circuit in 1920s, Mary Cartwright, John Littlewood, and N Levinson [7, 8] on the proof of existence of sensitive dependence on initial condition and random-like motion in a forced Van der Pol oscillator during 1940-1950 and others. The modern enthusiasm and interest in the theory of dynamical system and NDE was triggered by the path breaking paper of Edward Lorenz in 1962 on a low ($n = 3$) dimensional NDE model-

ing of convective fluid flow for the long time predictability problem of weather system, discovering numerically the butter-fly effect and what is presently known as Chaotic or strange attractor for a deterministic system [9].

In the following paragraphs, we present a short review of the basic facts of phase space (plane) analysis of a deterministic system in the context of planar systems relevant for this thesis, viz., the Rayleigh, Van der Pol and the Lienard differential systems. As the present work is limited to applications to limit curves (cycles) of a planar autonomous system (rather than higher dimensional chaotic attractors), our review will be rather elementary. We assume the basic facts and concepts of phase plane analysis [2,3]. We begin our review, following Ref. [2,3], as preparation for the statement of the Poincare-Bendixson theorem that establishes the existence of an isolated closed curve as the limit set of a planar nonlinear system.

Let us consider a general planar autonomous system

$$\begin{aligned} \dot{x} &= X(x,y) \\ \dot{y} &= Y(x,y), \end{aligned} \tag{1.2}$$

where $\dot{x} = \dfrac{dx}{dt}$, $\dot{y} = \dfrac{dy}{dt}$, the parameter t can be identified as time variable. We further assume that the system is regular [3] i.e., X and Y have continuous partial derivatives in the domain of definition which in general can be taken as entire phase plane.

Definition 1.2.1 (Half-Path) *Let Γ be a path of the system (1.2) and let $x = x(t)$ and $y = y(t)$ be a solution of (1.2) defining Γ. Then we shall call the set of all point of Γ for $t \geq t_0$, where t_0 is some value of t, a half-path of (1.2). In other words by a half-path of (1.2) we mean the set of all points with coordinates $(x(t), y(t))$ for $t_0 \leq t < \infty$. We denote such a half-path of (1.2) by Γ^+.*

It is well known that a linear planar autonomous system has a unique critical point i.e., the limit set of a linear system is a singleton set. The limit set of nonlinear system can, however, be more general; apart from the discrete set of critical points, a nonlinear system can also admit nontrivial limit set that is dense in $\mathbb{R}^2$ i.e. an isolated closed orbit. Such

isolated closed limit sets are called *limit cycles*. Here we introduce the precise definitions.

Definition 1.2.2 (Limit Set) [2] *Let Γ^+ be a half-path of (1.2) defined by $x = x(t)$ and $y = y(t)$ for $t \geq t_0$. Let (x_1, y_1) be a point in xy plane. If there exists a sequence of real numbers $\{t_n\}$, $n = 1, 2, \ldots$, such that $t_n \to +\infty$ and $(x(t_n), y(t_n)) \to (x_1, y_1)$ as $n \to +\infty$, then we call (x_1, y_1) a limit point of Γ^+. The set of all limit points of a half-path Γ^+ will be called the limit set of Γ^+ and will be denoted by $L(\Gamma^+)$.*

Definition 1.2.3 (Limit Cycles) *An isolated closed path Γ of the system (1.2) which is approached spirally from either the inside or the outside by a nonclosed half-path Γ' of the same system either as $t \to \infty$ or as $t \to -\infty$ is called a limit cycle of (1.2). The word 'isolated' has been used in the sense that there is no other closed path in its sufficiently close neighbourhood.*

In a planar autonomous system the asymptotic behaviour of a phase path is guided by the following well known Poincare-Bendixson theorem.

Theorem 1.2.1 (The Poincare-Bendixson Theorem) *Let R be a closed, bounded region that contains no critical point of a planar system (1.2) such that some positive half-path Γ of the system lies entirely within R. Then either Γ is itself a closed path, or it approaches asymptotically to a closed path as either $t \to \infty$ or $t \to -\infty$.*

It follows immediately that a planar nonlinear system can admit no limit set other than limit cycle or critical points. We consider the following example as an application of this theorem.

Example 1.2.1 *Consider the system*

$$\dot{x} = x\left(1 - x^2 - y^2\right) + y$$
$$\dot{y} = y\left(1 - x^2 - y^2\right) - x.$$

The equilibrium points are given by

$$\dot{x} = 0,\ \dot{y} = 0 \Rightarrow x = 0, y = 0$$

so that $(0,0)$ *is the only equilibrium point of the given system. In order to identify limit cycles of the system we consider the polar transformation*

$$x = r\cos\theta,\ y = \dot{x} = r\sin\theta$$

so that

$$r^2 = x^2 + y^2 \ \textit{and}\ \tan\theta = \frac{y}{x}.$$

The given system then becomes

$$\dot{r} = r\left(1 - r^2\right),\ \dot{\theta} = -1.$$

One particular solution to the system is

$$r = 1,\ \theta = -t$$

which corresponds to the limit cycle

$$x = \cos t,\ y = -\sin t.$$

Also,

$$\dot{r} > 0 \ \textit{when}\ 0 < r < 1 \ \textit{and}$$
$$\dot{r} < 0 \ \textit{when}\ r > 1,$$

showing that the phase paths approach the limit cycle $r = 1$ *from inside and outside the cycle. The equation for* $\dot{\theta}$ *shows that the phase points move in a spiral clockwise direction around the limit cycle. The phase plane diagram of the system is shown in Figure 1.1.*

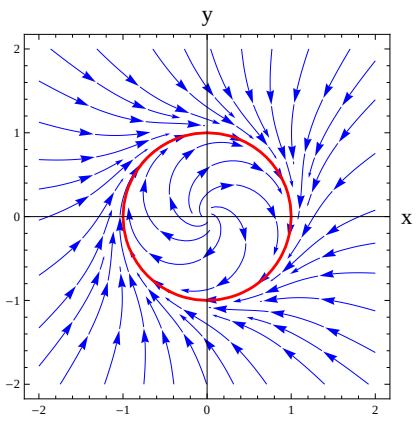

Figure 1.1: Stable Limit Cycle

The negatively directed system, on the other hand

$$\dot{x} = -x\left(1 - x^2 - y^2\right) - y$$
$$\dot{y} = -y\left(1 - x^2 - y^2\right) + x$$

has the phase plane diagram as shown in Figure 1.2.

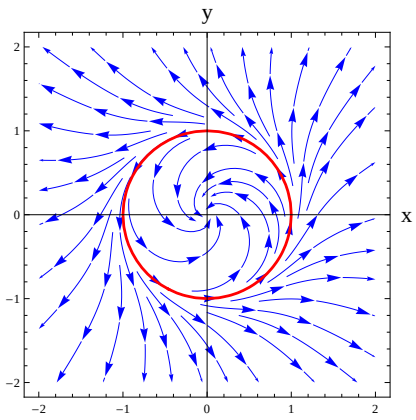

Figure 1.2: Unstable Limit Cycle

We observe that the positive half-path Γ is itself a closed path, or it approaches towards (or diverges from) a closed path, or it terminates at (or originates from) the equilibrium point $(0, 0)$. Example 1.2.1 gives us the concept of stable and unstable limit cycle the formal definition of which are given below.

Definition 1.2.4 (Stable Limit Cycle) *A limit cycle is said to be stable if the neighbouring positive half-paths approach asymptotically towards the cycle.*

Definition 1.2.5 (Unstable Limit Cycle) *A limit cycle is said to be unstable if the neighbouring positive half-paths approach asymptotically away from the cycle.*

Figure 1.1 and 1.2 respectively represent stable and unstable limit cycles. In Part I of this thesis we shall study sufficient conditions for the existence of single and multiple limit cycles for the Lienard equation (1.3). It should be mentioned here that the problem is closely related to the famous Hilbert's 16-th problem which asks about the maximum

number of limit cycles corresponding to the polynomial autonomous system (1.2) when X and Y are polynomials. We shall confine ourself to the Lienard equation introduced in the following subsection.

1.2.1 Lienard Equation

The Poincare-Bendixson theorem ensures the existence of at least one limit cycle in a bounded region. However it does not ensures the uniqueness of limit cycle for a given system. We shall restrict our study to generalized Lienard equation

$$\ddot{x} + f(x)\dot{x} + g(x) = 0 \tag{1.3}$$

and similar systems. This equation can be written as the autonomous system

$$\dot{x} = y - F(x), \qquad \dot{y} = -g(x), \tag{1.4}$$

known as Lienard system. This system has many applications in physical and engineering problems [6, 10, 11]. The Poincare-Bendixson theorem can ensure the existence of at least one limit cycle for the system (1.4). However, it does not always ensures the existence or the uniqueness of limit cycle for the system. One sufficient condition ensuring the existence and uniqueness of limit cycle for the Lienard system (1.4) is presented in the following theorem, which is well known as Lienard Theorem.

Theorem 1.2.2 (Lienard Theorem) *The equation (1.3) has a unique periodic solution if*

- (i) *f and g are continuous;*
- (ii) *F and $g(x)$ are odd functions with $g(x) > 0$ for $x > 0$;*
- (iii) *F is zero only at $x = 0$, $x = a$, $x = -a$ for some $a > 0$;*
- (iv) *$F(x) \to \infty$ as $x \to \infty$ monotonically for $x > a$.*

The detail of the theorem is reviewed in Chapter 2. The conditions are further generalized in remaining chapters of Part I of the thesis ensuring the existence of unique and multiple limit cycles for the system (1.4). The amplitude and shape of the limit cycles are also computed in Part II by applying Homotopy Analysis Method (HAM), Renormalization Group Method (RGM). Finally we complete this thesis by finding

analytic approximation of the amplitude and the equation of the limit cycle for two special kind of Lienard systems, viz. Rayleigh Equation and Van der Pol Equation, in the context of a new improved RGM in Chapter 7.

1.2.2 Rayleigh and Van der Pol Equations

Before the introduction of HAM and RGM we present the Rayleigh equation

$$\ddot{y} + \varepsilon \left(\frac{1}{3}\dot{y}^3 - \dot{y} \right) + y = 0. \tag{1.5}$$

and the Van der Pol equation

$$\ddot{x} + \varepsilon \, \dot{x} \left(x^2 - 1 \right) + x = 0 \tag{1.6}$$

where $\varepsilon > 0$ is a non-linearity parameter. Taking $x = \dot{y}$ one can generate (1.6) from (1.5). The equation (1.5) is used to model the dynamics of musical instruments such as the blown clarinet reed [4]. Rayleigh modeled the clarinet reed as a linear oscillator

$$\ddot{x} + kx = 0.$$

The effect of clarinetist is modeled by introducing a term $\alpha\dot{x} - \beta\dot{x}^3$, with $\alpha, \beta > 0$ on the right hand side, indicating negative damping for small $\dot{x}$ and positive damping for large $\dot{x}$. This gives rise to the model

$$\ddot{x} + kx = \alpha\dot{x} - \beta\dot{x}^3,$$

which is the dynamical model for the sustained oscillation of the blown clarinet reed. This system can be converted into the form (1.5) by the transformation

$$\tau = \sqrt{k}t, \;\; \beta = \frac{\varepsilon}{3\sqrt{k}}, \;\; \alpha = \varepsilon\sqrt{k} \text{ with } \varepsilon > 0.$$

The Van der Pol oscillator is also a non-conservative oscillator in which energy is dissipated at high amplitudes and generated at low amplitudes. Balthazar Van der Pol discovered this oscillator while he was working in the field of radio and telecommunication at Phillips in course of building electronic circuit models of human heart [6].

The Van der Pol circuit is composed of one inductor, one capacitor and one resistor arranged in a loop. A voltage is applied to the circuit and removed. The problem is to determine the resulting current and voltage behaviour. The diagram of the circuit is given below. The

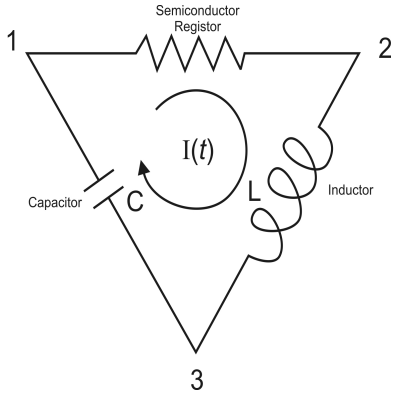

Figure 1.3: Van der Pol Circuit

problem is formulated under the following guiding laws:

Kirchhoff's first law on electrical circuit: It says that the current $I(t)$ through each of registor, inductor and capacitor are same at any time t.

Kirchhoff's second law on electrical circuit: It says that the sum of all voltage drops or voltage differences in a closed loop must vanish i.e.,

$$V_{12} + V_{23} + V_{31} = 0 \tag{1.7}$$

where V_{ij} is the voltage drop between nodes i and j; $i, j = 1, 2, 3$ and $i \neq j$.

We consider a semi-conductor as a registor so that a small voltage difference in one direction of the semi-conductor generates large current flow and in opposite direction it generates almost no current flow even if there is fairly large voltage difference between its ends 1 and 2. We take such a semi-conductor that the relation between the voltage difference V_{12} between the ends 1 and 2 and the current $I(t)$ through the registor be

$$V_{12} = I^3 - \mu I \tag{1.8}$$

where μ is a parameter which determines the sign of voltage difference V_{12} as I increases through the value $\sqrt{\mu}$. If $I < \sqrt{\mu}$ then $V_{12} > 0$ and if

$I > \sqrt{\mu}$ then $V_{12} < 0$.

The law stating the relationship between the inductance L of the inductor, the current flow $I(t)$ and the voltage difference V_{23} between the ends 2 and 3 is given by

$$V_{23} = L\frac{dI}{dt} = L\dot{I}(t). \tag{1.9}$$

The charge $q(t)$ at time t, the capacitance C of the capacitor and the voltage difference V_{31} between the ends 3 and 1 of the capacitor is related by the **Coulomb's law** as

$$\begin{aligned} C &= V_{31}q(t) \\ \text{i.e., } V_{31} &= \frac{q(t)}{C}. \end{aligned} \tag{1.10}$$

We know if $I(t)$ is the current flowing through the capacitor at time t, then

$$\dot{q}(t) = I(t). \tag{1.11}$$

We now construct a differential equation from the above relations. We suppose that

$$-V_{31} = V_{13} = V \tag{1.12}$$

so that (1.10) gives

$$V = V_{13} = -V_{31} = -\frac{q(t)}{C}.$$

Here C is constant. So, differentiating the relation with respect to time t and using (1.11) we get

$$\dot{V}(t) = -\frac{\dot{q}(t)}{C} = -\frac{I(t)}{C}. \tag{1.13}$$

Using (1.8), (1.9), (1.10) and (1.12) in (1.7) we get,

$$\left(I^3 - \mu I\right) + L\dot{I} - V = 0.$$

Differentiating again with respect to t we obtain,

$$\left(3I^2\dot{I} - \mu\dot{I}\right) + L\ddot{I} - \dot{V} = 0.$$

Using (1.13) we have,

$$\left(3I^2\dot{I} - \mu\dot{I}\right) + L\ddot{I} + \frac{I}{C} = 0$$
$$\Rightarrow \ddot{I} + \frac{\mu}{L}\left(\frac{3}{\mu}I^2 - 1\right)\dot{I} + \frac{I}{LC} = 0. \tag{1.14}$$

Applying the transformation

$$t = \sqrt{LC}\tau$$

so that

$$\dot{I} = \frac{dI}{d\tau}\frac{d\tau}{dt} = I'\frac{1}{\sqrt{LC}}$$
$$\text{and } \ddot{I} = \frac{d\dot{I}}{d\tau}\frac{d\tau}{dt} = \frac{d}{d\tau}\left(I'\frac{1}{\sqrt{LC}}\right)\frac{d\tau}{dt} = \frac{d}{d\tau}\left(I'\frac{1}{\sqrt{LC}}\right)\frac{1}{\sqrt{LC}} = I''\frac{1}{LC}$$

(1.14) reduces to

$$I''\frac{1}{LC} + \frac{\mu}{L}\left(\frac{3}{\mu}I^2 - 1\right)I'\frac{1}{\sqrt{LC}} + \frac{I}{LC} = 0$$
$$\Rightarrow I'' + \mu\sqrt{\frac{C}{L}}\left(\frac{3}{\mu}I^2 - 1\right)I' + I = 0.$$

Now taking further

$$I(\tau) = \sqrt{\frac{\mu}{3}}x(\tau)$$

the differential equation reduces to

$$\sqrt{\frac{\mu}{3}}x'' + \mu\sqrt{\frac{C}{L}}\left(x^2 - 1\right)\sqrt{\frac{\mu}{3}}x' + \sqrt{\frac{\mu}{3}}x = 0.$$

Writing

$$\varepsilon = \mu\sqrt{\frac{C}{L}}$$

we finally get

$$x'' + \varepsilon\left(x^2 - 1\right)x' + x = 0$$

which is the well known Van der Pol equation.

An important feature of this oscillator is that it has unique oscillation around a state at which energy generation and dissipation balance each

other and as a result we get a unique limit cycle. The existence of such limit cycle is confirmed by Lienard theorem. This unique characteristic of the oscillator makes the Van der Pol equation (1.6) a benchmark in the study of nonlinear oscillation and limit cycle. This equation has become a standard model for nonlinear oscillatory processes in physics, biology, sociology, economics and many more fields. For instance, electrical potential across the cell membranes of neurons in the gastric mill circuit of lobsters is modeled by Van der Pol equation [12, 13]. It is also used to model spike generation in giant squid axons [14, 15]. Due to its wide applications detailed understanding of the Van der Pol equation is still of considerable interest.

In the solution of a non linear ordinary differential equation (ODE) the study of asymptotic behaviour and the development of a compatible calculation technique is a topic of key interest in literature. HAM and RGM are two such techniques which are discussed in the following subsections.

1.2.3 Homotopy Analysis Method

In recent years there have been a lot of interests in the homotopy analysis method developed by S. Liao in his Ph.D. thesis [16]. The salient idea behind HAM is an extension of the topological concept of homotopy of paths into the function (solution) space of a given nonlinear differential equation, when the nonlinear differential operator ($\mathcal{N}$) itself is supposed to be a homotopic deformation of a simpler (linear) differential equation with well known solution set as the deformation parameter q is assumed to vary from the value 0 (corresponding to linear operator $\mathcal{L}$) to 1 (nonlinear operator $\mathcal{N}$). A known analytic solution of a simple (linear) problem is then continuously *deformed* into a solution of a more difficult (nonlinear) problem. Such deformation is called *homotopy*. A primary advantage of this approach is that the solution of the latter remains valid for all values of the small or large nonlinearity parameter that is present in the system. Moreover, HAM involves a free control parameter that makes the HAM generated solutions to converge generally to the exact solution of the nonlinear problem. A simple example of homotopy is $\mathcal{H}(x, q) = (1 - q) f(x) + q\, g(x)$ between

two functions $f(x)$ and $g(x)$. If $f(x)$ represents the solution of some simple problem and $g(x)$ represents that of a complicated problem then $\mathcal{H}(x,0) = f(x)$ undergoes through a continuous deformation or change and becomes $\mathcal{H}(x,1) = g(x)$ as q changes continuously from zero to 1. The parameter $q \in [0,1]$ is called homotopy parameter.

As pointed out by Liao [17], the homotopy analysis essentially depends on the implicit function theorem, which is a basic principle behind continuation and bifurcation analysis. Since HAM makes use of a rather simple but nevertheless attractive concept of topological homotopy of paths, the method gains much attentions in recent decades in the literature of differential equations in deriving correct analytic approximation of the solution of a large class of nonlinear differential equations. Although we shall apply this method to ODE only it can be applied to partial differential equation (PDE) as well [17]. Lopez et al. [18] computed an analytic approximation to the amplitude of the limit cycle for Van der Pol equation

$$\ddot{x} + \varepsilon\, \dot{x}\left(x^2 - 1\right) + x = 0 \tag{1.15}$$

which is uniformly valid for the nonlinearity parameter $\varepsilon > 0$. Although the HAM may fail for some typical systems as pointed out recently by Meijer [19], this method has many applications [20–25] which establish HAM as a convenient method to find analytic approximations of the solution and different parameters involved in the system, provided, of course, this method is at all applicable. Liao has pointed out some limitations of HAM in [17] such as lack of rigorous theories to choose initial approximations, auxiliary linear operators, auxiliary functions, and auxiliary parameter etc. involved in the computation scheme. However, we do not go into the study of mathematical rigor behind this method.

In the present thesis, we report approximate analytic formulas of the amplitude a of the limit cycle for both Van der Pol and the Rayleigh Equations

$$\ddot{y} + \varepsilon\left(\frac{1}{3}\dot{y}^3 - \dot{y}\right) + y = 0 \tag{1.16}$$

as a function of the nonlinearity parameter ε in the nonperturbative regime $0 < \varepsilon \leq 50$ which can be extended uniformly for all $\varepsilon > 0$.

The analytic formula of the amplitude for this system is computed in literature for $\varepsilon \to 0$. However, to the authors' best knowledge, this is the first analytic formula in literature for non-perturbative ε giving a good approximation with the exact values of the amplitude for Rayleigh system. The detail discussion on HAM is given in Chapter 5.

1.2.4 Renormalization Group Method

Theory of renormalization group (RG) has a hallowed history; originally invented as an efficient technique in eliminating undesired divergences in quantum electrodynamics, in particular, and quantum field theory (QFT), in general, by factoring out generic divergent terms in a perturbative expansion of the relevant physical (dynamical) quantity, for instance, the electron self-energy, order by order, leading finally to a finite well defined (renormalized) theory [26]. The original algorithmic formulation of RG theory was later put into a more rigorous framework by Wilson in the context of continuous phase transition that enjoys some sort of scale invariance and has the property of large scale cooperative behaviour [27]. Over the past few decades the theory of RG has been accepted as an efficient method of extracting finite measurable (observable) results from a basically nonlinear problem, for which the standard methods, such as perturbation theory or some of its variants, normally fail i.e. yield meaningless/divergent values or are of limited validity. It is reasonable that the RG method has got wide applications in a variety of nonlinear problems starting from quantum field theory [26], phase transitions in statistical mechanics [28], theory of fractals [29], turbulence and chaotic attractors in dynamical systems [30] and finally to nonlinear ordinary and partial differential equations. Chen et al. initiated the first successful application of the RG method in nonlinear differential equations [31].

In a renormalization theory one usually develops a scheme of viewing a system at different energy or distance scales. If we look at a large distance or time scale phenomena by smaller microscopic scale theory, such as in phase transitions or in nonlinear differential equations or if we want to explain low energy theory by high energy theory, as in QFT then we require to switch our view from one scale to another. Such

mathematical transformations involving switching of views is known as renormalization-group (RG) transformation [32]. If the theory remains unaltered, as in the case of fractals, then the underlying problem is scale invariant, otherwise special techniques are required to understand the precise law behind predicted variations in the proposed theory. RG theory provides one such approach which is generally known to answer such questions by means of RG flow equations which describe the exact patterns of variations of relevant dynamical quantities in a nonlinear problem. We shall discuss this problem in the context of nonlinear ODE.

In the study of nonlinear ODE solving an ODE in closed form is always a challenging problem. No general technique is available to obtain the solution of non linear ODEs in closed or finite form. The reason behind it is the class of standard functions (e.g., polynomials, exponential, logarithmic or trigonometric functions etc.) that we have in our hand is insufficient to accommodate the variety of differential equations those arise in practice. We therefore, investigate the qualitative characteristics of the solution, such as its existence, periodicity, regularity etc. and their behaviour in the form of long time asymptotics. Naive perturbation method in small nonlinear coupling parameter $|\varepsilon| << 1$ fails to give uniformly valid results for sufficiently large time, requiring for new approaches to obtain uniformly valid finite results. Another more severe problem is to obtain meaningful results even in sufficiently large coupling $\varepsilon \sim O(1)$ nonperturbative regime. Different singular perturbation technique such as method of multiple scales, boundary layers, averaging, WKB methods, central manifold theory are used to deal with this problem. However, each of these methods has its own drawback and does not produce uniformly valid solution for all values of the non linearity parameter involved in the ODE.

As remarked already, the renormalization group was initially devised in QFT [26] and it is widely applied in solid state physics, fluid mechanics, cosmology, quantum field theory and even nanotechnology to manage divergences that arise in the solution of nonlinear problems. The RG method (RGM) gives us an algorithmic approach to derive asymptotic expansion of the solution for a large class of singularly per-

turbed ODEs. A first significant application of the RGM in the solution of nonlinear ODEs is given by Chen, Goldenfeld, Oono [33, 34]. A brief introduction of RGM is given in Chapter 6 which is simplified latter by De Ville et al. [35] giving an algorithmic approach for achieving the solution. They studied interesting application of RGM for autonomous as well as nonautonomous systems. RGM is a technique which has many applications on differential equation in the recent past [35–39]. A major advantage of RGM is that it starts from naive perturbation expansion of a problem and is expected to yield automatically the gauge functions such as fractional powers of ε and logarithmic terms in ε in the renormalized expansion. One does not require to have any prior knowledge to prescribe these unexpected gauge functions in an ad hoc manner.

Although the RGM is formulated to give an analytic solution to a NDE and is based on naive perturbation expansion of a problem (which is formally possible for any system) and is expected to give an approximate solution for all values of the nonlinearity parameters involved in the problem, it is found in our work that the RG generated solution does not generally give good approximation uniformly for non-perturbative regime of the nonlinearity parameters.

To circumvent this undesired limitation of RGM, we present in the Part II of this these, a reformulation of RG method, called Improved RGM (IRGM), in the framework of a novel scale invariant extension of the ordinary analysis equipped with the so-called duality structure [40–42] and apply this scheme to calculate uniformly valid approximations for amplitudes for Rayleigh and Van der Pol equations for all values of the nonlinearity parameter. We have also shown the efficacy of the method by presenting efficient estimations of the limit cycle orbits of both these nonlinear oscillators.

Part I

Existence of Limit Cycles

Chapter 2

Existence of Exactly Two Limit Cycles in Lienard Systems

2.1 Introduction

The limit cycle of an autonomous system represents an isolated periodic motion. Its existence and number for a given planar system

$$\begin{aligned} \dot{x} &= X(x, y) \\ \dot{y} &= Y(x, y) \end{aligned} \tag{2.1}$$

remains a challenging problem of study for quite a long time. The problem is closely associated with Hilbert's 16-th problem which asks about the maximum number of limit cycles corresponding to the autonomous system (2.1) when X and Y are polynomials. Here we study a special form of the problem where the differential equation

$$\ddot{x} + f(x)\dot{x} + g(x) = 0, \tag{2.2}$$

known as Lienard Equation, is represented as the autonomous system

$$\dot{x} = y - F(x), \qquad \dot{y} = -g(x), \tag{2.3}$$

where $F(x) = \int_0^x f(u)\,du$. Different researchers [43–47] have already studied the existence, number, size, shape and location of the limit cycle of this system. One such well known result is the Lienard theorem which is discussed in Section 2.2 along with a brief sketch of its proof and some related observations. This theorem ensures the existence of

unique limit cycle for the system (2.3). We shall extend the Lienard theorem by applying some loose conditions and ensure the existence of multiple limit cycles for the system (2.3).

Many interesting results have been proved so far in literature regarding the existence of multiple limit cycles for the Lienard system (2.3). In the investigation of multiple limit cycles for the system (2.3) Lins, Pugh and de Melo [43] conjectured in 1977 that it has at most N limit cycles if $m = 2N + 1$ or $m = 2N + 2$. On the other hand, in the year 1975 G.S. Rychkov [44] proved that the maximal number of limit cycles of the system $\dot{y} = -x$, $\dot{x} = y - \left(a_1 x + a_3 x^3 + a_5 x^5\right)$ is equal to two. Holst and Sundberg [45] further extended Rychkov's theorem in 2006 for a class of $F(x)$ having 5-th degree polynomial like behaviour. The location of the limit cycles is another interesting problem for this system. Giacomini and Neukirch [46] have developed a general procedure for constructing a sequence of polynomials whose roots of odd multiplicity are related to the number and location of the limit cycles of equation (2.2) when $f(x)$ is an even degree polynomial. Odani [48] gave a proof on the existence of exactly N limit cycles of the Lienard equation (2.2) with $g(x) = x$. His method also gave an improved estimate of the amplitude of a limit cycle. Recently, in 2003, Chen and Chen [49] proved the Lins-Pugh-de Melo conjecture for Lienard system with function F odd. On the other hand, it has been shown [50] that for suitable polynomial F of degree 7, the system (2.3) has 4 limit cycles, contradicting the conjecture in [43]. Chen, Llibre and Zhang [47] proved a sufficient condition for existence of exactly N limit cycles for the system (2.3) with a general class of $F(x)$ functions where F is not necessarily a polynomial. We investigate an equivalent problem covering, however, a different class of functions F as compared to [47]. The investigation on the number of limit cycles for more general class of functions F is included in Chapter 4.

In this chapter we introduce a simple but, nevertheless, an important extension of the Lienard theorem for the unique limit cycle by removing the unbounded nature of the function F as $x \to \infty$. Next, in Theorem 2.4.1 we prove that the system (2.3) has exactly two limit cycles when the odd function $F(x)$ undergoes two sign changes in $x > 0$ and is

monotonic not only as $x \to \infty$, but also near (actually at the right of) the first zero. However, $g(x)$ ($g(x) > 0$ for $x > 0$) can be any odd continuous function. Analogous results have been proved in literature, viz. Theorem 5.1 of [51]. The statement of this theorem is given below.

Theorem 2.1.1 *Consider the differential equation (2.2) or its equivalent system*

$$\dot{x} = y, \qquad \dot{y} = -g(x) - f(x)\, y \tag{2.4}$$

with $g(x) = x$. Suppose that the following hypotheses are satisfied:

(i) $f(x) \in C^0(-d, d)$ *for sufficiently large* $d > 0$, $F(-x) = -F(x)$, *where* $\int_0^x f(x)\, dx = F(x)$;

(ii) there exists $0 < \beta_1 < \beta_2 < d$ *such that* $F(\beta_1) = F(\beta_2) = 0$, $F(x) \geq 0$ *if* $0 < x < \beta_1$, $F(x) \not\equiv 0$ *if* $0 < x \ll 1$, $F(x) \leq 0$ *if* $\beta_1 < x < \beta_2$ *such that* $f(\alpha_2) = 0$ *and* $f(x) \leq 0$ *if* $\beta_1 < x < \alpha_2$;

(iii) $f(x)$ *is nondecreasing as* x *increases for* $x \in [\alpha_2, d]$.

Then the system (2.4) has at most two limit cycles. (That is, if limit cycle(s) exist, either there are two simple limit cycles or one semistable limit cycle).

In this chapter we focus on the existence of unique or two limit cycles rather than their stability. We present Example 2.5.5 in support of Theorem 2.4.1, which clearly reveals the strength of this theorem over the Theorem 2.1.1. The *new insights* gained from Theorem 2.4.1 (and also from Theorem 2.3.1) then provide a general approach in obtaining an existence theorem for multiple limit cycles in a systematic manner. Moreover, as stated above, $g(x)$ in Theorem 2.4.1 is an odd function while for the theorem of [47] $g(x) = x$. The second important result that we find in section 2.3 is an efficient upper estimate of the amplitude of the limit cycle for the system (2.3). The values of the amplitudes for the Van der Pol equation are obtained in Example 2.3.1, which are much more accurate compared to those in [52] and [53].

In this chapter classical Lienard theorem is stated in Section 2.2 along with a brief sketch of its proof. Here some new notations are

introduced which will be useful in subsequent part of this chapter. An efficient upper estimate of the amplitude of the limit cycle is computed and an extension of the classical Lienard theorem is introduced ensuring existence of unique limit cycle in Section 2.3. This theorem is further extended in Section 2.4 ensuring existence of two limit cycles for the Lienard system (2.3). Some comparative examples are discussed in Section 2.5 showing the position of these two new theorems in the literature of qualitative theory of differential equation.

2.2 Classical Lienard Theorem

Here we present the well known Lienard's Theorem and a brief sketch of its proof in order to introduce necessary notations which will be used subsequently.

Theorem 2.2.1 *The equation (2.2) has a unique periodic solution if*

- (i) *f and g are continuous;*
- (ii) *F and $g(x)$ are odd functions with $g(x) > 0$ for $x > 0$;*
- (iii) *F is zero only at $x = 0$, $x = a$, $x = -a$ for some $a > 0$;*
- (iv) *$F(x) \to \infty$ as $x \to \infty$ monotonically for $x > a$.*

A Brief Sketch of the Proof. The general shape of the path can be obtained from the following observations.

(a) Because of the symmetry of the system(2.2) under the transformation $(x, y) \to (-x, -y)$ any periodic orbit is symmetric about the origin.

(b) The slope of a phase path is given by

$$\frac{dy}{dx} = \frac{-g(x)}{y - F(x)}. \tag{2.5}$$

Thus, a phase path is horizontal if $\dfrac{dy}{dx} = 0$, i.e. if $g(x) = 0$, i.e. if $x = 0$ (by (ii) above). Similarly, a phase path is vertical on the curve $y = F(x)$. Above the curve $y = F(x)$ we have $\dot{x} > 0$ and below $\dot{x} < 0$. Moreover, $\dot{y} < 0$ for $x > 0$ and $\dot{y} > 0$ for $x < 0$.

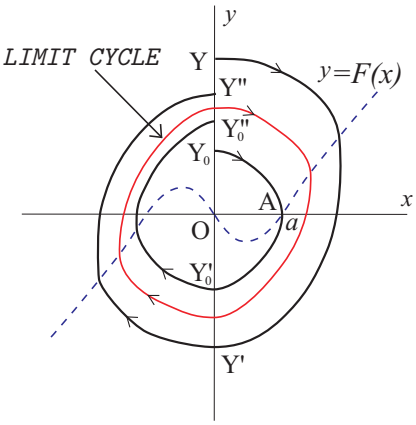

Figure 2.1: Orbits of the Lienard System (2.3).

A path $YY'Y''$ (Figure 2.1) is closed iff Y and Y'' coincide, which means by symmetry (a)

$$OY = OY'. \tag{2.6}$$

This is equivalent to

$$V_{YQY'} = 0, \tag{2.7}$$

where for a typical path YQY' in Figure 2.2

$$V_{YQY'} = v_{Y'} - v_Y = \int\limits_{YQY'} dv = \int\limits_{YQY'} F dy \tag{2.8}$$

and

$$v(x, y) = \int_0^x g(u)\, du + \frac{1}{2} y^2. \tag{2.9}$$

Writing

$$V_{YQY'} = V_{YB} + V_{BQB'} + V_{B'Y'},$$

where BB' is a line parallel to the y-axis and passing through the point $(0, a)$ when the function F changes its sign from negative to positive, one then proves that

(A) As Q moves out of the point $A(0, a)$ along the curve AC, the potentials $V_{YB} + V_{B'Y'}$ is positive and monotone decreasing.

(B) As Q moves out of the point $A(0, a)$ along the curve AC, $V_{BQB'}$ is monotone decreasing.

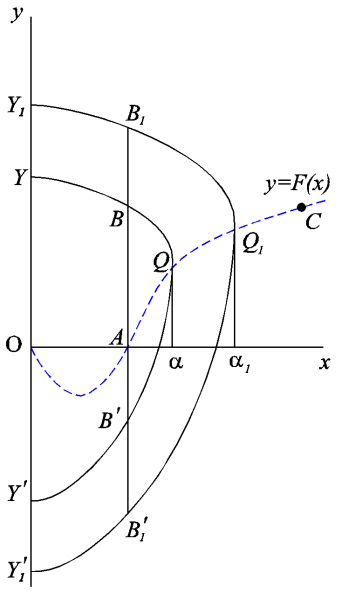

Figure 2.2: Typical paths for the Lienard Theorem

(C) From (A) and (B) it follows that $V_{YQY'}$ is monotone decreasing to the right of the point A, (Figure 2.2).

(D) The quantity $V_{BQB'}$ tends to $-\infty$ as the paths moves away to infinity.

(E) From (C) and (D), it follows that the quantity $V_{YQY'}$ is monotone decreasing to $-\infty$, at the right of the point A in Figure 2.2.

(F) $V_{YQY'} > 0$ when the point Q is at A or to the left of the point A.

It thus follows from (E) and (F) that $V_{YQY'}$ is monotone decreasing continuous function which changes its sign from positive to negative as the point Q moves out of $A\,(a, 0)$ along the curve. As a result, $V_{YQY'}$ will vanish once and only once. Thus, there is one and only one closed path and the proof is complete. ■

Remark 2.2.1 *In (2.8) we have defined the potential function V with three indices. More generally, if Γ is a directed curve in the phase plane of the system (2.3) then we define V_Γ by the line integral*

$$V_\Gamma = \int_\Gamma dv.$$

So, if Γ *denotes a curve joining more (or less) than three successive points the potential* V_Γ *will have more (or less) than three indices. For example, if we consider the curve* $\Gamma = YBQB'Y'$ *then*

$$V_{YBQB'Y'} = \int_{YBQB'Y'} dv.$$

Remark 2.2.2 *The unique limit cycle in the above theorem is* ***simple*** *in the sense that no (differentiable) perturbation satisfying the conditions* (i)*-*(iv) *can bifurcate the limit cycle into two or more number of limit cycles.*

Remark 2.2.3 *The condition* (E) *enables us to conclude that once* $V_{YQY'}$ *becomes negative, it can never be positive as* Q *moves to infinity through the curve of* $F(x)$*. This observation helps us to deduce the existence of a unique limit cycle. However, we see that the existence of the limit cycle is indeed ensured only if* $V_{YQY'}$ *becomes negative from positive i.e., if there is a change in sign of* $V_{YQY'}$*. Further, the unique value of* x *for which* $V_{YQY'} = 0$ *gives the* ***amplitude*** *of the limit cycle. Accordingly, if* $V_{YQY'}$ *becomes negative as* Q *moves out from origin through the curve of* $F(x)$ *then we get a limit cycle. This observation actually gives one with a possibility of weakening the conditions of the classical theorem, so as to accommodate a larger class of functions* $F(x)$ *but still having a unique limit cycle. Theorem 2.3.1 is one such realizations of a stronger version of the classical theorem, which shows that the existence of the (unique) limit cycle actually depends on the* ***local*** *monotonicity of* $F(x)$ *on a bounded interval containing the point where* $V_{YQY'}$ *vanishes. A limit cycle can indeed be realized even when* $F(x)$ *is bounded as* $|x| \to \infty$ *(c.f. Example 2.3.1)*
If it happens further that $V_{YQY'}$ *becomes positive from negative once more, then also, by an analogous argument as above we get a point* Q *on the curve* $F(x)$*, through which another limit cycle must pass. To prove this result we consider a function* $F(x)$ *(in Section 2.4) which is monotonically increasing to the right of the point* A *for a sufficiently large value of* x *and then it becomes decreasing for some subsequent values of* x *and ultimately become negative. The proof depends on an efficient estimate of the amplitude of the first limit cycle.*

2.3 Estimation of Amplitudes for the Van der Pol Equation

Let, $(\alpha, F(\alpha))$ be the coordinate of Q, as shown in Figure 2.2 and let $\alpha = \hat{\alpha}$ be the amplitude of the limit cycle of Theorem 2.2.1. It is well known that determining the exact value of the amplitude of the limit cycle of the Lienard system is a relatively difficult problem [52, 53]. We now find an estimate of $\hat{\alpha}$, for which the corresponding $V_{YQY'}$ just become negative from positive. Since, $V_{YQY'}$ is a monotone decreasing continuous function as the point moves out of the point $A(a, 0)$ along the curve, without any loss of generality we can say $V_{YQY'}$ can just become negative from positive if at least one of the following two cases hold, viz.,

(i) $V_{YQ} = 0$ but $V_{QY'} < 0$

(ii) $V_{QY'} = 0$ but $V_{YQ} < 0$.

The third possibility $V_{YQ} < 0$ and $V_{QY'} < 0$ can be reduced to either of the above two cases by monotonicity and continuity of $V_{YQY'}$, i.e. by taking an α closer to $\hat{\alpha}$, (i.e., $\alpha \to \hat{\alpha} + 0$) either one of V_{YQ} and $V_{QY'}$ can be made to vanish. Similarly, the possibility that either one of V_{YQ} and $V_{QY'}$ is positive while their sum is negative, can also be eliminated by choosing α far from $\hat{\alpha}$ $(\alpha > \hat{\alpha})$.

Case (i)

Here $V_{YQ} = 0$ is possible if

$$V_{YB} + V_{BQ} = 0. \tag{2.10}$$

In step (A) of the proof of Theorem 2.2.1 it has been proved that $V_{YB} > 0$.

We are now going to show that $V_{BQ} < 0$.

On the path BQ, we have $F(x) \geq 0$ and $\dfrac{dy}{dt} = \dot{y} = -g(x) < 0$.

Therefore,

$$V_{BQ} = \int_{BQ} F dy = \int_{BQ} F \frac{dy}{dt} dt$$
$$= -\int_{BQ} F\left(x\left(t\right)\right) g\left(x\left(t\right)\right) dt < 0. \tag{2.11}$$

Thus, we can say that (2.10) is true if $|V_{YB}| = |V_{BQ}|$

i.e., if $|v\left(a, y_+\left(a\right)\right) - v\left(0, y_+\left(0\right)\right)| = |v\left(\alpha, F\left(\alpha\right)\right) - v\left(a, y_+\left(a\right)\right)|$,

where $y_+\left(0\right) = OY$ (Figure 2.2). It is possible if

$$\int_0^a g\left(u\right) du + \frac{1}{2} y_+^2\left(a\right) - \frac{1}{2} y_+^2\left(0\right) = -\int_a^\alpha g\left(u\right) du - \frac{1}{2} F^2\left(\alpha\right) + \frac{1}{2} y_+^2\left(a\right).$$

So, we have

$$G\left(\alpha\right) = \frac{1}{2} y_+^2\left(0\right) - \frac{1}{2} F^2\left(\alpha\right), \tag{2.12}$$

where $G\left(x\right) = \int_0^x g\left(u\right) du$.

Let $\alpha = \alpha'$ be a root of (2.12) (existence of which is assured by construction) so that

$$G\left(\alpha'\right) = \frac{1}{2} y_+^2\left(0\right) - \frac{1}{2} F^2\left(\alpha'\right). \tag{2.13}$$

Case (ii)

Here, $V_{QY'} = 0$ is possible if

$$V_{QB'} + V_{B'Y'} = 0. \tag{2.14}$$

In step (A) of the proof of the Theorem 2.2.1 it is proved that $V_{B'Y'} > 0$.

Proceeding analogous to case (i) one establishes that $V_{QB'} < 0$ and consequently (2.14) is true provided

$$G\left(\alpha\right) = \frac{1}{2} y_-^2\left(0\right) - \frac{1}{2} F^2\left(\alpha\right), \tag{2.15}$$

where $OY' = -y_-(0)$, $y_-(0) < 0$ (Figure 2.2). If $\alpha = \alpha''$ be a root of (2.15) we have

$$G(\alpha'') = \frac{1}{2}y_-^2(0) - \frac{1}{2}F^2(\alpha''). \tag{2.16}$$

It now follows that if we take

$$\bar{\alpha} = \max\{\alpha', \alpha''\} \tag{2.17}$$

then for any value of $\alpha > \bar{\alpha}$, $V_{YQY'} \leq 0$ since, $V_{YQY'} = V_{YQ} + V_{QY'}$. Thus, the function F should be monotonic increasing in the interval $a < x \leq \bar{\alpha}$. Notice that the classical Lienard theorem already ensures the existence of such an $\bar{\alpha}$. In the light of the above discussion we can now *extend* the classical Lienard theorem by weakening the unbounded nature of the function F as stated in the following theorem and cover a more large class of functions.

Theorem 2.3.1 *The equation (2.2) has a unique limit cycle if*

- (*i*) *f and g are continuous in $(-d, d)$ for sufficiently large d;*
- (*ii*) *F and g are odd functions with $g(x) > 0$ for $x > 0$;*
- (*iii*) *F is zero only at $x = 0$, $x = a$, $x = -a$ for some a, where $0 < a < d$;*
- (*iv*) *$\exists$ a number $\bar{\alpha}$ defined by (2.17) such that F is monotonic increasing in $a < x \leq \bar{\alpha}$ and nondecreasing in $\bar{\alpha} < x < d$.*

The existence of $\bar{\alpha}$ ensures a sign change in $V_{YQY'}$ whereby we get the existence of a unique limit cycle in the finite phase plane. The rest of the proof of this theorem remains same as that of classical Lienard theorem. Also, from the above discussion and the proof of classical Lienard theorem it follows that $V_{YQY'}$ does not change its sign any more if the function F is simply *monotone nondecreasing* in $\bar{\alpha} < x < \infty$. In such cases the function F can *even be bounded and even attain a constant value as $x \to \infty$*, but still we get a unique limit cycle for such a bounded Lienard system. Thus, we can indeed cover a larger class of functions than those covered by the Lienard theorem (c.f. Example 2.3.1).

In the beginning of the proof of Theorem 2.2.1 we observed that above the curve $y = F(x)$ we have $\dot{x} > 0$ and below $\dot{x} < 0$. So, the x-coordinate of a point on a limit cycle will achieve its maximum

absolute value on the curve $y = F(x)$. Therefore, the amplitude of a limit cycle for the Lienard system is the abscissa of the point Q lying on the curve $y = F(x)$. Since, for a limit cycle we have $V_{YQY'} = 0$, so by the construction of $\bar{\alpha}$ it follows that it is an *efficient upper estimate of the amplitude* of the limit cycle. In the following example we find the values of $\bar{\alpha}$ for the well known Van der Pol equation against different values of μ and compare them with the results obtained in [52] and [53]. This also gives an example of a *bounded* Van der Pol equation having same amplitude as that of the standard Van der Pol equation.

Example 2.3.1 *Here, in the following table we present estimates of the amplitude of the limit cycle for Van der Pol equation in which* $F(x) = \mu\left(\frac{x^3}{3} - x\right)$ *and* $g(x) = x$ *for different values of* μ. *It is clear that our estimates are reasonably close to the exact (numerically computed) values (as reported in* [52]*). Our values also appear to be much better than the upper bound* 2.3233 *of* [52] *(the estimated values of* [53] *are valid only for small* μ*). From our numerical estimates it follows that although the estimated values of the amplitude seem to vary irregularly for the moderately large values of* $\mu \in [0, 10]$*, these are nevertheless*

bounded above by 2.05.

μ	$y_+(0)$ *and* $y_-(0)$	$\bar{\alpha}$
0.1	2.00117	2.0000586437166383
0.2	2.007076	2.002540101136999
0.3	2.015912	2.0054678254782505
0.4	2.028253	2.0091503375996034
0.5	2.044065	2.013278539452526
1	2.1727135	2.0327736318429275
1.5	2.3710897	2.0436704679281523
2	2.6149725	2.04739132291152
2.5	2.8844602	2.047213463900291
3	3.1687156	2.045311842105752
3.5	3.462322	2.0427848260891426
4.5	4.06701715	2.037557405718347
5	4.3752293	2.035154629371522
10	7.5528123	2.020095969119061

We get the same result if we consider the bounded function

$$F(x)=\begin{cases}\mu\left(\dfrac{x^3}{3}-x\right), & x\in(-2.4,2.4)\\ \mu\left(\dfrac{(2.4)^3}{3}-2.4\right)-\dfrac{4.76\mu}{\sin(0.6)}\left(\cos(0.6)-\cos(x-3)\right), & x\in(-3,-2.4]\cup[2.4,3)\\ \mu\left(\dfrac{(2.4)^3}{3}-2.4\right)-\dfrac{4.76\mu}{\sin(0.6)}\left(\cos(0.6)-1\right), & x\in(-\infty,-3]\cup[3,\infty)\end{cases}$$

in the whole phase plane or the following function in ***finite*** *phase plane.*

$$F(x)=\begin{cases}\mu\left(\dfrac{x^3}{3}-x\right), & x\in(-2.4,2.4)\\ \mu\left(\dfrac{(2.4)^3}{3}-2.4\right)-\dfrac{4.76\mu}{\sin(0.6)}\left(\cos(0.6)-\cos(x-3)\right), & x\in(-3,-2.4]\cup[2.4,3)\end{cases}.$$

This also tells that the value of d need not be too large. A limit cycle is assured even for a moderately large d.

It follows from this example that the amplitude of the unique limit cycle is independent of the asymptotic behaviour of $F(x)$ as $x\to\infty$. Indeed, the amplitude corresponds to the point $Q(\hat{\alpha},F(\hat{\alpha}))$ on the limit cycle for which the integral $V_{YQY'}=\int\limits_{YQY'}F\,dy$ vanishes and clearly

depends on the form of $F(x)$ in the finite interval $(0, \hat{\alpha})$. To the best of author's knowledge, this result apparently is not recorded clearly in the literature. We therefore state this observation as the following corollary.

Corollary 2.3.1 *Amplitude of the unique limit cycle of the Lienard system (2.3) is independent of the asymptotic behaviour of $F(x)$ as $|x| \to \infty$.*

2.4 Extension of Lienard Theorem for Two Limit Cycles

By the observations discussed in last section it is clear that, in the interval $a < \alpha < \bar{\alpha}$ we obtain the limit cycle as mentioned in Theorems 2.2.1 and 2.3.1. Moreover, because of the condition (iv) we see that the limit cycle remains unique. However, if the function does not satisfy this condition, then the limit cycle may not be unique. We now present our new theorem ensuring the existence of two limit cycles for the equation (2.2).

Theorem 2.4.1 *Let f and g be two functions satisfying the following properties.*

- (i) *f and g are continuous;*
- (ii) *F and g are odd functions and $g(x) > 0$ for $x > 0$.;*
- (iii) *F has positive simple zeros only at $x = a_1$, $x = a_2$ for some $a_1 > 0$ and some $a_2 > \bar{\alpha}$, $\bar{\alpha}$ being defined by (2.17) and $\bar{\alpha} < L$, where L is the first local maxima of $F(x)$ in $[a_1, a_2]$;*
- (iv) *F is monotonic increasing in $a_1 < x \leq \bar{\alpha}$ and $F(x) \to -\infty$ as $x \to \infty$ monotonically for $x > a_2$;*

Then the equation (2.2) has exactly two limit cycles around the origin.

Proof: We can get exactly the same observations as we get in observations (a) and (b) in the beginning of the proof of Theorem 2.2.1.

By the observations in section 2.3 we can ensure the existence of inner limit cycle. So, we shall now prove the existence of one more limit cycle by showing that

$$OY = OY'$$

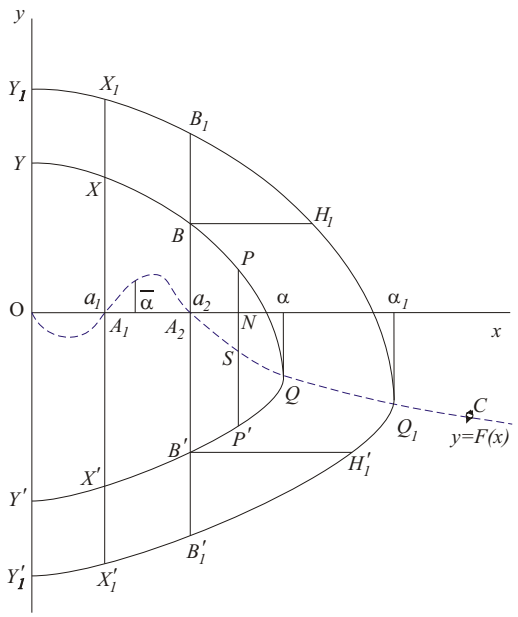

Figure 2.3:

once more when $x > \bar{\alpha}$. To prove the result we shall consider the function $v(x, y)$ as in (2.9), and write,

$$V_{YQY'} = V_{YX} + V_{XB} + V_{BQB'} + V_{B'X'} + V_{X'Y'}, \tag{2.18}$$

where XX' is a line parallel to the y-axis passing through the point $(0, a_1)$ where the function F changes its sign from negative to positive and BB' is a line parallel to the y-axis passing through the point $(0, a_2)$ where the function F changes its sign from positive to negative. The proof is carried out through the steps (A) to (F) below. Here we refer to the Figure 2.3.

Step (A) : **As** Q **moves out from** A_2 **along** A_2C, $V_{YX} + V_{X'Y'}$ **is positive and monotonic decreasing.**

We choose two points $Q(\alpha, F(\alpha))$ and $Q_1(\alpha_1, F(\alpha_1))$ on the curve of $F(x)$ where $\alpha_1 > \alpha$. Let YQY' and $Y_1Q_1Y_1'$ be two paths through Q and Q_1 respectively. On the segments YX and Y_1X_1 we have

$$y > 0,\ F(x) < 0 \text{ and } y - F(x) > 0.$$

Now,

$$\begin{aligned} & (y-F(x))_{YX} < (y-F(x))_{Y_1X_1} \\ \Longrightarrow \quad & \left(\frac{1}{y-F(x)}\right)_{YX} > \left(\frac{1}{y-F(x)}\right)_{Y_1X_1}. \end{aligned}$$

Since $g(x) > 0$ for $x > 0$, we have

$$\left(\frac{-g(x)}{y-F(x)}\right)_{YX} < \left(\frac{-g(x)}{y-F(x)}\right)_{Y_1X_1}.$$

So by (2.5) we get

$$\left(\frac{dy}{dx}\right)_{YX} < \left(\frac{dy}{dx}\right)_{Y_1X_1} < 0. \tag{2.19}$$

Therefore,

$$V_{YX} = \int_{YX} F dy = \int_{YX} (-F)\left(-\frac{dy}{dx}\right) dx.$$

Using (2.19) we get

$$V_{YX} > \int_{Y_1X_1} (-F)\left(-\frac{dy}{dx}\right) dx.$$

Since, F and dy are positive on Y_1X_1 we have

$$V_{YX} > \int_{Y_1X_1} F dy = V_{Y_1X_1} > 0. \tag{2.20}$$

Next, on the segments $X'Y'$ and $X_1'Y_1'$ we have

$$y < 0,\ F(x) < 0 \text{ and } y - F(x) < 0.$$

Now,

$$\begin{aligned} & (y-F(x))_{X'Y'} > (y-F(x))_{X_1'Y_1'} \\ \Longrightarrow \quad & \left(\frac{-g(x)}{y-F(x)}\right)_{X'Y'} > \left(\frac{-g(x)}{y-F(x)}\right)_{X_1'Y_1'}. \end{aligned}$$

So, by (2.5)

$$\left(\frac{dy}{dx}\right)_{X'Y'} > \left(\frac{dy}{dx}\right)_{X_1'Y_1'} > 0. \tag{2.21}$$

Therefore,

$$V_{X'Y'} = \int\limits_{X'Y'} F dy = \int\limits_{Y'X'} (-F)\,\frac{dy}{dx} dx.$$

Using (2.21) we get

$$V_{X'Y'} > \int\limits_{Y_1'X_1'} (-F)\,\frac{dy}{dx} dx.$$

Since, F and dy are negative on $X_1'Y_1'$ we have

$$V_{X'Y'} > \int\limits_{X_1'Y_1'} F dy = V_{X_1'Y_1'} > 0. \tag{2.22}$$

From (2.20) and (2.22) we have

$$V_{YX} + V_{X'Y'} > V_{Y_1X_1} + V_{X_1'Y_1'} > 0.$$

Therefore, $V_{YX}+V_{X'Y'}$ is positive and monotonic decreasing as the point Q moves out from A_2 along A_2C.

Step (B) **: As** Q **moves out from** A_2 **along** A_2C**,** $V_{XB} + V_{B'X'}$ **is negative and monotonic increasing.**

On the segments XB and X_1B_1 we have

$$y > 0,\ F(x) < 0 \text{ and } y - F(x) > 0.$$

Now,

$$\begin{aligned} & (y - F(x))_{XB} < (y - F(x))_{X_1B_1} \\ \Longrightarrow \quad & \left(\frac{-g(x)}{y - F(x)}\right)_{XB} < \left(\frac{-g(x)}{y - F(x)}\right)_{X_1B_1}. \end{aligned}$$

So, by (2.5) we get

$$\left(\frac{dy}{dx}\right)_{XB} < \left(\frac{dy}{dx}\right)_{X_1B_1} < 0. \tag{2.23}$$

Therefore,

$$V_{XB} = \int\limits_{XB} F dy = \int\limits_{XB} F \frac{dy}{dx} dx.$$

Using (2.23) we get

$$V_{XB} < \int\limits_{X_1B_1} F\frac{dy}{dx}dx = \int\limits_{X_1B_1} Fdy = V_{X_1B_1} < 0 \tag{2.24}$$

since, $F > 0$ and $dy < 0$ on XB and X_1B_1.

Next, on the segments $B'X'$ and $B'_1X'_1$ we have

$$y < 0,\ F(x) > 0 \text{ and } y - F(x) < 0.$$

Now,

$$\begin{aligned} & (y - F(x))_{B'X'} > (y - F(x))_{B'_1X'_1} \\ \Longrightarrow \quad & \left(\frac{-g(x)}{y - F(x)}\right)_{B'X'} > \left(\frac{-g(x)}{y - F(x)}\right)_{B'_1X'_1}. \end{aligned}$$

Using (2.5) we get

$$\left(\frac{dy}{dx}\right)_{B'X'} > \left(\frac{dy}{dx}\right)_{B'_1X'_1} > 0. \tag{2.25}$$

Therefore,

$$V_{B'X'} = \int\limits_{B'X'} Fdy = -\int\limits_{X'B'} F\frac{dy}{dx}dx = \int\limits_{X'B'} F\left(-\frac{dy}{dx}\right)dx.$$

So, by (2.25) we have

$$V_{B'X'} < \int\limits_{X'_1B'_1} F\left(-\frac{dy}{dx}\right)dx \ = \int\limits_{B'_1X'_1} Fdy = V_{B'_1X'_1} < 0 \tag{2.26}$$

since, $F > 0$ and $dy < 0$ on $B'X'$ and $B'_1X'_1$.

From (2.24) and (2.26) we have

$$V_{XB} + V_{B'X'} < V_{X_1B_1} + V_{B'_1X'_1} < 0.$$

Therefore, $V_{XB} + V_{B'X'}$ is negative and monotonic increasing as the point Q moves out from A_2 along A_2C.

Step (C) : **As** Q **moves out from** A_2 **along** A_2C, $V_{BQB'}$ **is positive and monotonic increasing and tends to** $+\infty$ **as the path recedes to infinity.**

On BQB' and $B_1Q_1B_1'$, we have $F(x) < 0$. We draw BH_1 and $B'H_1'$ parallel to x-axis.

Therefore,

$$\begin{aligned} V_{B_1Q_1B_1'} &= \int\limits_{B_1Q_1B_1'} F dy \\ &= \int\limits_{B_1'Q_1B_1} (-F)\, dy \\ &\geq \int\limits_{H_1'Q_1H_1} (-F)\, dy \end{aligned}$$

since, $F(x) < 0$ and $dy > 0$ for points on $H_1'Q_1H_1$. Again since,

$$F(x)]_{B'QB} \geq F(x)]_{H_1'Q_1H_1}$$

for same value of y we get

$$\begin{aligned} V_{B_1Q_1B_1'} &\geq \int\limits_{H_1'Q_1H_1} (-F)\, dy \geq \int\limits_{B'QB} (-F)\, dy \\ &= \int\limits_{BQB'} F dy \\ &= V_{BQB'} \\ \implies V_{B_1Q_1B_1'} &\geq V_{BQB'}. \end{aligned} \tag{2.27}$$

Next, let S be a point on the curve of $F(x)$, to the right of A_2, and let BQB' be an arbitrary path, with Q to the right of S. The straight

line $PNSP'$ is parallel to the y-axis. Then,

$$\begin{aligned} V_{BQB'} &= \int\limits_{BQB'} F(x)\, dy \\ &= \int\limits_{B'QB} (-F(x))\, dy \\ &\geq \int\limits_{P'QP} (-F(x))\, dy \end{aligned} \tag{2.28}$$

since, $(-F(x)) \geq 0$ and $dy \geq 0$ along $B'QB$. Now by condition (iv) of this theorem it follows that F is monotonic decreasing for $x > a_2$ and so we have $|F(x)| \geq NS$ on $P'QP$ and since further $F(x) \leq 0$ on $P'QP$ so this implies $-F(x) \geq NS$ on $P'QP$. Again, $PP' \geq NP'$. Thus we get

$$V_{BQB'} \geq \int\limits_{P'QP} NS\ dy = NS \int\limits_{P'QP} dy = NS \cdot PP' \geq NS \cdot NP' \ .$$

But as Q goes to infinity towards the right , $NP' \to \infty$. Hence, we can conclude that $V_{BQB'}$ is positive and monotonic increasing and tends to $+\infty$ as the paths recede to infinity.

Step (D) :

From steps (A) and (B) it follows that the quantities $V_{YX} + V_{X'Y'}$ and $V_{XB} + V_{B'X'}$ are bounded quantities. Thus by (2.18) and by step (C) it follows that $V_{YQY'}$ is monotonic increasing to $+\infty$ to the right of A_2.

Step (E) :

By the construction of $\bar{\alpha}$ it is clear that $V_{YQY'} < 0$ in $\bar{\alpha} \leq x < a_2$ i.e., to the left of A_2. Again from step (D) we conclude that $V_{YQY'}$ ultimately becomes positive as Q moves out of A_2 along the curve of $F(x)$. Therefore, by the same reason given in conclusion of the Theorem 2.2.1, it follows that there is one and only one path in the region $x > \bar{\alpha}$ such that

$$V_{YQY'} = 0.$$

Also, by (2.7) and the symmetry of the path it is clear that the path is closed.

Step (F) :

By the construction of $\bar{\alpha}$ and by step (E) it is clear that equation (2.2) has exactly two limit cycles around the origin, the second limit cycle surrounds the first one. This completes the proof of the Theorem 2.4.1.

Remark 2.4.1 *It also follows from the proof that both the limit cycles are simple* (*c.f., Remark 2.2.2*) *that neither can bifurcate under any small* C^1 *perturbation satisfying the conditions of the theorem.*

Remark 2.4.2 *One cannot assume that* $V_{YQY'} < 0$ *if* $\bar{\alpha} \geq L$. *We give a Counter Example 2.5.2 below.*

Remark 2.4.3 *It is well known that two consecutive limit cycles cannot both be stable* (*unstable*). *Because of our choice of the function* $F(x)$ (*negative and monotone decreasing at the right of and near the origin and infinity*), *the inner limit cycle is stable and outer limit cycle is unstable* (*in reverse to those of reference* [45, 48]).

2.5 Examples and Comparisons

Here some examples are presented which help us to understand the importance of the Theorem 2.4.1 and 2.3.1 in the literature of qualitative theory of differential equation. It is shown in section 3.3 of [45] that the limit cycles of the autonomous system

$$\left.\begin{aligned} \dot{x} &= y \\ \dot{y} &= -x - \mu h(x, \dot{x}) \end{aligned}\right\} \tag{2.29}$$

are asymptotic to the circle $x^2 + y^2 = r^2$ as $\mu \to 0$ where the values of r are the roots of the equation

$$\Phi(r) := \int_0^{2\pi} h(r \sin u, r \cos u) \cos u \; du = 0. \tag{2.30}$$

We note that this is not the Lienard system. It is the canonical autonomous system for the Lienard equation. The phase diagram of above

system and the Lienard system, however, should be similar. Here we take $\mu = 0.1$, $h(x, \dot{x}) = \left(-4 + 75x^2 - 50kx^4\right)\dot{x}$, $k \neq 0$ so that

$$f(x) = \mu\left(-4 + 75x^2 - 50kx^4\right) = -0.4 + 7.5x^2 - 5kx^4,$$

$$F(x) = -0.4x + 2.5x^3 - kx^5$$

and

$$\begin{aligned}\Phi(r) &= \int_0^{2\pi} \left(-4 + 75r^2\sin^2 u - 50kr^4\sin^4 u\right) r\cos u \cdot \cos u \; du \\ &= -\frac{1}{4}\pi r\left(25kr^4 - 75r^2 + 16\right).\end{aligned}$$

Therefore, (2.30) reduces to

$$-\frac{1}{4}\pi r\left(25kr^4 - 75r^2 + 16\right) = 0$$

giving

$$r^2 = \frac{1}{10k}\left(15 \pm \sqrt{225 - 64k}\right).$$

So, (2.30) has real and distinct roots if $225 > 64k$ i.e., if $k < 3.515625$, real and repeated if $k = 3.515625$ and imaginary if $k > 3.515625$. Therefore it follows that we will get two distinct limit cycles, which are asymptotic to the circles corresponding to the above two distinct values of r if $k < 3.515625$. Similarly, we will get only one limit cycle when $k = 3.515625$ and no limit cycle when $k > 3.515625$. It can be verified that the system undergoes a saddle node bifurcation at $k = 3.515625$.

We note that the point $(\bar{\alpha}, F(\bar{\alpha}))$ on the limit cycle in the Lienard plane gets transformed to the point $(-\bar{\alpha}, 0)$ lying on the almost circular limit cycle of radius $r \gtrsim r_1$ (in the canonical phase plane) where $r_1^2 = \frac{1}{10k}\left(15 - \sqrt{225 - 64k}\right)$ (r_1 corresponds to the first limit cycle) under the transformation

$$x = -u, \; y = -v + F(u),$$

(u, v) and (x, y) being the corresponding points in Lienard plane and canonical phase plane with f an even function. We thus have

$$\bar{\alpha} \gtrsim \sqrt{\frac{1}{10k}\left(15 - \sqrt{225 - 64k}\right)}.$$

We now present the phase diagrams of the above systems in Lienard plane in the following examples for different values of k. These examples justify our new theorem. We used Mathematica 5.1 in plotting the limit cycles discussed in these examples.

Example 2.5.1 *Here we consider the autonomous system (2.3) with* $k = 3.65$, $f(x) = -0.4 + 7.5x^2 - 5kx^4$, $g(x) = x$ *and* $F(x) = -0.4x + 2.5x^3 - kx^5$. *The phase diagram in Lienard plane is shown in Figure 2.4(a) which* ***does not*** *have any limit cycle. Again we take* $k = 3.57$ *in*

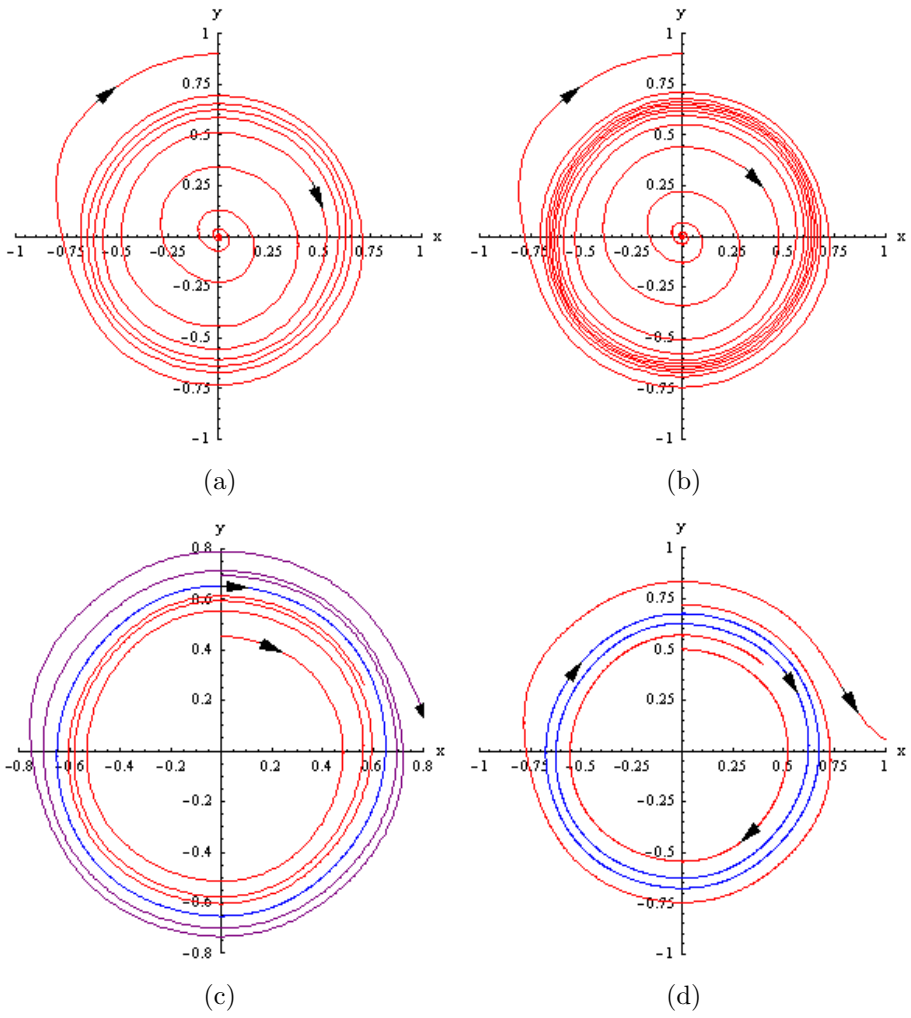

Figure 2.4: The phase diagram of the system (2.3) in Lienard plane
(a) with $k = 3.65$, and center as a repelling node in Example 2.5.1,
(b) with $k = 3.57$ in Example 2.5.1,
(c) with $k = 3.515625$, and one limit cycle in Example 2.5.2,
(d) with $k = 3.5$, and two limit cycles in Example 2.5.3.

the above system. The corresponding phase diagram is shown in Figure

2.4(b). This phase diagram also ***does not*** *contain any limit cycle, but we see that the path is concentrating in a certain circular region.*

Example 2.5.2 *Here we consider the autonomous system (2.3) discussed above with* $k = 3.515625$ *so that* $a_1 \simeq 0.49307$, $a_2 \simeq 0.68410$, $y_+(0)$ *and* $y_-(0)$ *both are approximately equal to* 0.652287 *and* $\bar{\alpha} \simeq 0.65204$. *Let* L_1 *be the point of minima of* F *in* $(0, a_1)$ *and* L_2 *be the point of maxima of* F *in* (a_1, a_2). *Here* $F(x)$ *is increasing in*

$$(-L_2, -L_1) \cup (L_1, L_2)$$

and decreasing in

$$(-\infty, -L_2) \cup (-L_1, L_1) \cup (L_2, \infty),$$

where $L_1 \simeq 0.24997$ *and* $L_2 \simeq 0.60348$. *In this case we obtain* ***only one*** *limit cycle as shown in Figure 2.4(c). Here,* F *is not monotone increasing throughout the interval* $a_1 < x \leq \bar{\alpha}$, *violating the condition (iv) of Theorem 2.4.1 (since* $\bar{\alpha} > L_2$*) (c.f. Remark 2.4.2).*

Example 2.5.3 *We now take* $k = 3.5$. *Here,* $y_+(0)$ *and* $y_-(0)$ *are approximately equal to* 0.624499. *The equations (2.12) and (2.15) both reduce to*

$$\frac{x^2}{2} = \frac{1}{2}(0.624499)^2 - \frac{1}{2}\left(-0.4x + 2.5x^3 - 3.5x^5\right)^2$$

having real roots $x = \pm 0.62393$ *so that* $\bar{\alpha} \simeq 0.62393$. *Here,* $a_1 = 0.4919$ *and* $a_2 = 0.68725$ *showing that* $a_1 < \bar{\alpha} < a_2$. *Next,* $L_1 \simeq 0.24985$, $L_2 \simeq 0.60510$. *Here, all the conditions of Theorem 2.4.1 are satisfied except condition (iv). However, we still get two limit cycles as shown in Figure 2.4(d) drawn in Lienard plane. This example and the above example show that the conditions of Theorem 2.4.1 are sufficient but not necessary.*

Example 2.5.4 *Finally we take* $k = 3$. *Here,* $y_+(0)$ *and* $y_-(0)$ *are approximately equal to* 0.5552 *and* $\bar{\alpha} \simeq 0.55324$. *Here,* $a_1 = 0.46473$ *and* $a_2 = 0.78572$ *showing that* $a_1 < \bar{\alpha} < a_2$. *Next,* $L_1 \simeq 0.24638$, $L_2 \simeq 0.66279$. *Here, all the conditions of Theorem 2.4.1 are satisfied*

and so we get ***exactly two*** *limit cycles. The phase diagram in Lienard plane is shown in Figure 2.5.*

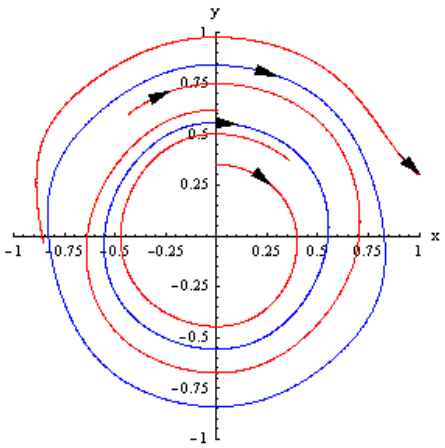

Figure 2.5: The phase diagram of the system (2.3) in Lienard plane with $k = 3$, and two limit cycles in Example 2.5.4.

Remark 2.5.1 *Although in the above examples the value of μ is sufficiently small (so as to satisfy the amplitude analysis of [45]) our theorem should be applicable for large values of $|\mu|$. More detailed bifurcation analysis in the (μ, k) parametric plane will be considered separately.*

Example 2.5.5 *We now consider the function*

$$F_+(x) = \begin{cases} -0.1\sin(10\pi x), & 0 \le x < 0.15 \\ 0.01\sqrt{1-\left(\dfrac{x-0.15}{0.01}\right)^2}, & 0.15 \le x < 0.15 + \dfrac{1}{\sqrt{101}} \\ 0.02099503719021 - 2\sqrt{0.1\,(x-0.239503719021)}, & x \ge 0.15 + \dfrac{1}{\sqrt{101}} \end{cases}.$$

Then we have $a_1 = 0.1$, $a_2 = 0.250523508686456 45$, $L = 0.15$. Here,

$$\begin{aligned} f(L) = 0 &< f(0.2395037190209989) \\ &= 0.2006848039831627 > f(a_2) = 0.9526060763219791, \end{aligned}$$

though

$$L < 0.2395037190209989 < a_2$$

showing that the function is not monotone nonincreasing in $[L, a_2]$ and so it does not satisfy the condition (3) of Theorem 5.1 in chapter 4 in the book [51]. However for the inner limit cycle we have $y_+(0) =$

$y_{-}(0) = 0.12238318$. *So,* $\bar{\alpha} = 0.12221435874426823 < L$ *satisfying the conditions of Theorem 2.4.1. This example clearly shows that the Theorem 2.4.1 covers a larger class of functions than those covered by Theorem* 5.1 *in chapter* 4 *in* [51]. *The function* F *alongwith two limit cycles are shown in Figure 2.6.*

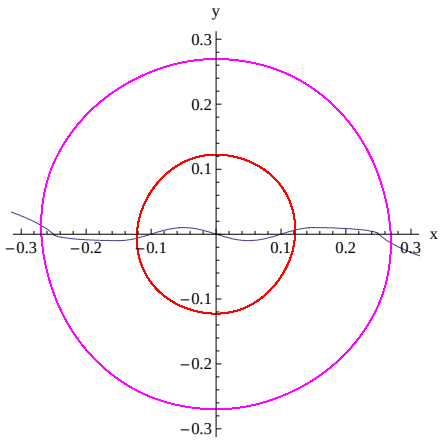

Figure 2.6: The phase diagram of (2.3) in Lienard plane for Example 2.5.5.

2.6 Concluding Remarks

Many interesting new results have been proved on the existence of an exact number of multiple limit cycles [45, 47, 48] in the recent past. Odani has proved a sufficient condition in [48] using a choice function ϕ_k which can be exploited to obtain better estimates of amplitudes of the limit cycles. We used a straight forward method depending on the geometry of phase diagram. We have proved a similar result with more general class of functions $F(x)$ by a simpler method. In the present approach a strict monotonicity of $F(x)$ is required only in the intervals $a_1 < x < \bar{\alpha}$ and $x > a_2$. Consequently, $F(x)$ can accommodate "small scale" oscillations in the interval $\bar{\alpha} < x < a_2$. Odani, for instance, considered an $F(x)$ which is not only C^1 but also has a unique extremum in the interval $a_1 < x < a_2$. Further, this new theorem is valid for a more general class of the function $g(x)$. Odani's theorem, however, is valid only for $g(x) = x$. An interesting problem will be to establish the relation between $\bar{\alpha}$ of our approach and the function ϕ_k. We note that $\hat{\alpha}_i$ corresponds to the amplitude of the limit cycles. Our estimates

of amplitude of the limit cycle of the Van der pol equation constitute an improvement over those available in the literature [52, 53]. Example 2.5.5, on the other hand, show the difference between the present theorem and those of [51]. The calculations are accurate upto the accuracy level $O\left(10^{-7}\right)$. The existence of limit cycles in a Lienard system *allowing discontinuity* (see, for instance, [54]) is an interesting problem for further study.

Before finishing this chapter we note that the value $\bar{\alpha}$, in general, is a function of the parameters of $F(x)$ in the parametric space. For instance, in Examples 2.5.1-2.5.4, $\bar{\alpha}$ is a function of the parameters μ and k. The study of the variation of $\bar{\alpha}$ in the parametric space seems to offer interesting insights into the bifurcation and related issues of the multiple limit cycles in a Lienard system. The relationship with Poincare's return map also needs to be studied. We wish to investigate these problems in future.

Chapter 3

Existence of Exactly N Limit Cycles in Lienard Systems

3.1 Introduction

We have gone through a brief study on existence of unique and two limit cycles for the Lienard equation

$$\ddot{x} + f(x)\dot{x} + g(x) = 0 \tag{3.1}$$

in Chapter 2 by extending the well known Classical Lienard theorem. In this chapter we shall study the existence of multiple limit cycles for the above equation in the Lienard plane given by the autonomous system

$$\dot{x} = y - F(x), \qquad \dot{y} = -g(x) \tag{3.2}$$

where $F(x) = \int_0^x f(u)\,du$. It is already mentioned in Chapter 2 as a conjecture by Lins, Pugh and de Melo [43] (LPM) that the system (3.2) has at most N limit cycles if $m = 2N + 1$ or $m = 2N + 2$. However, it has been shown [50] that for suitable polynomial F of degree 7, the system (3.2) has 4 limit cycles, contradicting the conjecture in [43]. Recently, in 2003 Chen and Chen [49], proved the LPM conjecture for Lienard system with function F odd.

Although LPM conjecture ensures the maximum N number of limit cycles in the system (3.2), considerably large amount of study in literature ensures the existence of exactly N limit cycles for the equation (3.1). In the study on the number of limit cycles several authors have

studied the equation (3.1) in the usual phase plane (viz. Theorem 7.10 − 7.12, Chapter 4 in [51]) whereas some considered the Lienard plane [47]. In Theorem 7.10, Chapter 4 [51] the function f is taken as a periodic function. Its statement is given below without proof.

Theorem 3.1.1 *Consider the differential equation*

$$\ddot{x} + f(x)\dot{x} + x = 0 \tag{3.3}$$

or its equivalent system

$$\dot{x} = v,\ \dot{v} = -x - f(x)v. \tag{3.4}$$

Let

(A) $f(x) \in C^0(-\infty, \infty)$, *and* $\exists\ l > 0$ *such that* $f(x) \leq 0$ *for* $0 \leq x \leq l$, $f(x) \not\equiv 0$ *for* $0 < x \ll 1$, $f(2l \pm x) = -f(x)$ *for* $-\infty < x < \infty$.

(B) $f(x)$ *is nondecreasing when* x *increases, for* $0 \leq x \leq l$.

Assertion (i) : *Suppose that hypothesis* (A) *is satisfied, then the system* (3.4) *has at least* n *limit cycles in the strip* $|x| \leq 2(n+1)l$, $n = 1, 2, 3, \ldots$.

Assertion (ii) : *Suppose that hypotheses* (A) *and* (B) *are satisfied, then system* (3.4) *has exactly* n *limit cycles in the strip* $|x| \leq 2(n+1)l$, $n = 1, 2, 3, \ldots$, *with stable and unstable limit cycles lying alternately between each other.*

We must note that $g(x) = x$ in Theorem 3.1.1. This theorem is further generalized as Theorem 7.11 in, Chapter 4 of [51] in which the function $F'(x) = f(x)$ is a monotone function in certain regions. However, Theorem 2.4.1 in Chapter 2 and Theorem 3.2.1 in the present chapter do not depend upon the monotonicity of f. Rather, we have used the monotonicity of its primitive F. As a consequence, merely the sign of the function f determines the monotonic nature of F, and hence determines the number of limit cycles in Lienard system (3.2). Moreover, F has better smoothness relative to f. Thus our results cover a different class of functions than those covered by Theorems 7.10 and 7.11 in [51] as mentioned above. We must observe that these theorems

in [51] were proved in classical phase plane given by the system (3.4). However, Theorem 7.12 of Chapter 4 in [51] and the theorem in [47] have been proved on Lienard plane. Both of these results have assumed the existence of $\beta_j \in [a_j, a_{j+1}]$, $j = 2, 3, 4, \ldots$ such that $F(\beta_j) = F(L_{j-1})$ where, a_j's are positive roots of F and L_j's are unique extremum of F in $[a_j, a_{j+1}]$ for $j = 1, 2, 3, \ldots$. However, if we do not get any such β_j then these results are not applicable. In such situations Theorem 3.2.1 is still applicable to determine the exact number of limit cycles. Example 3.4.1 is such evidence showing the strength of Theorem 3.2.1 over other similar results as mentioned earlier.

In Chapter 2 we have presented a new method for proving the existence of exactly two limit cycles of a Lienard system [55]. Recall that the proof of Lienard theorem depends on the existence of an odd function $F(x)$ with zeros at $x = 0$ and $x = \pm a$ $(a > 0)$ and that $F(x) > 0$ for $x > a$ and tends to ∞ as $x \to \infty$. To weaker this assumption, we note at first that the existence of a limit cycle is still assured if there exists a value $\bar{\alpha} > a$ (called an efficient upper estimate of the amplitude of the limit cycle) such that $F(x)$ is increasing for $a \leq x < \bar{\alpha} < L_1$, where L_1 is the first extremum of $F(x)$, $x > a$. Based on this observation we are then able to generalize the standard theorem for the existence of exactly two limit cycles. Our theorem [56] not only extends the class of $F(x)$ considered by Odani [48, 52], but also that of the more recent work of Chen et al. [47]. Although we are dealing with odd functions F only, there are certain odd functions as shown in Example 3.4.1, which satisfy the conditions of Theorem 3.2.1 but do not satisfy the theorem of [47]. This establishes our claim that the present theorems cover different classes of functions F than those covered in [47].

In this chapter we prove the theorem for the existence of exactly N limit cycles for the system (3.1). Here, we present an algorithm to generate any desired number of limit cycles around the origin, which is the only critical point for the system (3.1). Existence of limit cycles have been established in various natural and biological systems [3, 51, 57]. It is well known that mammalian heartbeats may follow a nonlinear oscillatory patterns under certain (physiological) constraints [57]. However, sometimes it becomes very difficult to obtain total information

about a nonlinear system due to various natural constraints, as a result of which we obtain only a partial or incomplete data [58]. Our objective is to fill up those gaps and construct a Lienard system that may be considered to model the dynamics of the missing part of the phenomena in an efficient manner.

To state this in another way, let us suppose that the Lienard system is defined only on a bounded region $[-a_1, a_1]$, $a_1 > 0$ having one (or at most a finite number of) limit cycles in that region. Our aim is to develop an algorithm to extend the Lienard system minimally throughout the plane accommodating a given number of limit cycles in the extended region. By minimal extension we mean that the graph $(x, F(x))$, of the function F which is initially defined only in $|x| < a_1$ is extended beyond the line $x = a_1$ iteratively as an action induced by two suitably chosen functions $\phi(x)$ and $H(x)$ so that ϕ acts on the abscissa x and H acts on the ordinate $F(x)$ respectively. Accordingly the desired extension $\tilde{F}(x)$ of $F(x)$, $x > a_1$ is realized as $H \circ F(x) = \tilde{F} \circ \phi(x)$. The choice of ϕ and H is motivated by the Theorem 3.2.1 so that the extension $\tilde{F}$ satisfies the conditions of the said theorem. It turns out that ϕ can simply be a bijective function, while H may be any monotonic function admitting $\bar{\alpha} < L$ (c.f. equation (2.17) in Chapter 2), L being the unique extremum of $\tilde{F}(x)$, $x \in [a_1, a_2]$, $\tilde{F}(a_1) = \tilde{F}(a_2) = 0$.

The chapter is organized as follows. In Section 3.2 we have proved an extension of the Theorem 2.4.1 for existence of exactly N limit cycles in the Lienard equation [55,56]. In Section 3.3 we present the construction by which we can get a system of the form (3.1) having any desired number of limit cycles around a single critical point. Examples in support of this algorithm are studied in Section 3.4 in order to compare the newly proved results with those available in literature. Finally, Section 3.5 contains some concluding remarks.

3.2 Existence of Exactly N limit cycles for Lienard System

In Chapter 2 we have extended the Classical Lienard Theorem as Theorem 2.4.1 ensuring existence of exactly two limit cycles along with

necessary notations. In order to avoid repetition we shall frequently refer them in the proof of the following theorem ensuring existence of exactly N (≥ 2) limit cycles.

Theorem 3.2.1 *Let f and g be two functions satisfying the following properties.*

- (i) *f and g are continuous;*
- (ii) *F and g are odd functions and $g(x) > 0$ for $x > 0$;*
- (iii) *F has N number of $+ve$ simple zeros only at $x = a_i$, $i = 1, 2, \ldots, N$, where $0 < a_1 < a_2 < \ldots < a_N$ such that in each interval $I_i = [a_i, a_{i+1}]$, $i = 1, 2, \ldots, N-1$, there exists $\bar{\alpha}_i$, satisfying properties given by (2.17), such that $\bar{\alpha}_i < L_i$ where L_i is the unique extremum in I_i, $i = 1, \ldots, N-2$ and L_{N-1}, the first local extremum in $[a_{N-1}, a_N]$;*
- (iv) *F is monotonic in $a_i < x \leq \bar{\alpha}_i \ \forall \ i$ and $|F(x)| \to \infty$ as $x \to \infty$ monotonically for $x > a_N$.*

Then the equation (3.1) has exactly N limit cycles around the origin, all are simple.

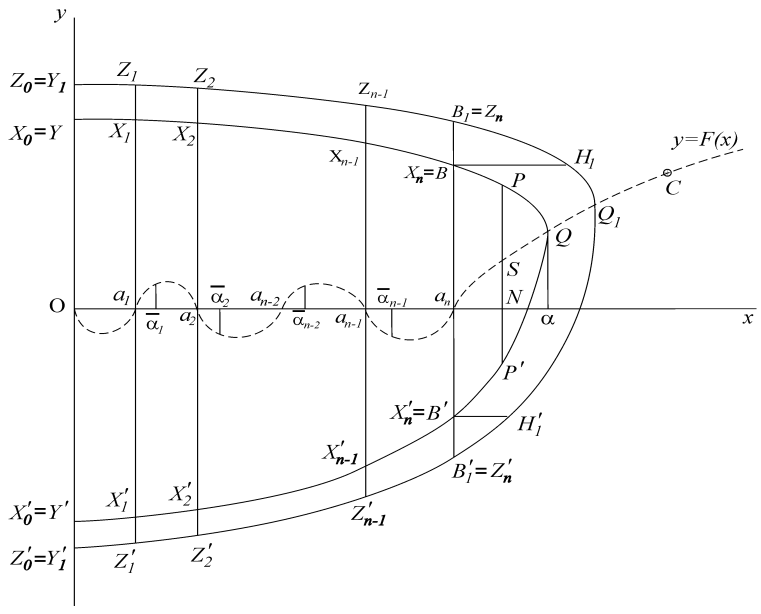

Figure 3.1:

Proof: We shall prove the theorem by showing the result that each limit cycle intersects the x-axis at a point lying in the interval $(\bar{\alpha}_i, \bar{\alpha}_{i+1}]$, $i = 0, 1, 2, \ldots, N-1$, where $\bar{\alpha}_0 = L_0$ is the local minima of $F(x)$ in

$[0, a_1]$. By Classical Lienard Theorem and Theorem 2.4.1 it follows that the result is true for $N = 1$ and $N = 2$. We shall now prove the theorem by the method of induction. We assume that the theorem is true for $N = n - 1$ and we shall prove that it is true for $N = n$. We prove the theorem by taking n as an odd $+ve$ integer so that $(n - 1)$ is even. The case for which n is even can similarly be proved and so is omitted. It can be shown that [3], $V_{YQY'}$ changes its sign from $+ve$ to $-ve$ as Q moves out of $A_1\,(a_1, 0)$ along the curve $y = F\,(x)$ and hence vanishes there due to its continuity and generates the first limit cycle around the origin. Next, in [55] we see $V_{YQY'}$ again changes its sign from $-ve$ to $+ve$ and generates the second limit cycle around the first. Also, we see that for existence of second limit cycle we need the existence of the point $\bar{\alpha}$, which we denote here as $\bar{\alpha}_1$.

Since by induction hypothesis the theorem is true for $N = n - 1$, so it follows that in each and every interval $(\bar{\alpha}_k, \bar{\alpha}_{k+1}]$, $k = 0, 1, 2, \ldots, n-2$ the system (3.2) has a limit cycle and the outermost limit cycle cuts the x-axis somewhere in $(\bar{\alpha}_{n-1}, \infty)$. Also $V_{YQY'}$ changes its sign alternately as the point Q moves out of a_i's, $i = 1, 2, \ldots, n - 1$. Since $(n - 1)$ is even, it follows that $V_{YQY'}$ changes its sign from $+ve$ to $-ve$ as Q moves out of a_{n-2} along the curve $y = F\,(x)$. Since there is only one limit cycle in the region $(\bar{\alpha}_{n-1}, \infty)$, so it is clear that $V_{YQY'}$ must change its sign from $-ve$ to $+ve$ once and only once as Q moves out of $A_{n-1}\,(a_{n-1}, 0)$ along the curve $y = F\,(x)$. Also it follows that once $V_{YQY'}$ becomes $+ve$ so that it does not vanish further, otherwise we would get one more limit cycle, contradicting the hypothesis so that total number of limit cycle become n. We now try to find an estimate of α for which $V_{YQY'}$ vanishes for the last time.

We shall now prove that the result is true for $N = n$ and so we assume that all the hypotheses or conditions of this theorem are true for $N = n$. So, we get one more point $\bar{\alpha}_n$ and another root a_n, ensuring the fact that $V_{YQY'}$ vanishes as Q moves out of A_{n-1} through the curve $y = F\,(x)$, thus accommodating a unique limit cycle in the interval $(\bar{\alpha}_{n-1}, \bar{\alpha}_n]$.

By the result discussed so far it follows that $V_{YQY'} > 0$ when α lies in certain suitable small right neighbourhood of $\bar{\alpha}_{n-1}$. We shall prove

that $V_{YQY'}$ ultimately becomes $-ve$ and remains $-ve$ as Q moves out of $A_n\,(a_n, 0)$ along the curve $y = F\,(x)$ generating the unique limit cycle and hence proving the required result for $N = n$.

We draw straight line segments X_kX_k', $k = 1, 2, 3, \ldots, n$, passing through A_k and parallel to y-axis as shown in Figure 3.1. For convenience, we shall call the points X_n, X_n', Y, Y' as B, B', X_0, X_0' respectively. We write the curves

$$\Gamma_k = X_{k-1}X_k, \quad \Gamma_k' = X_k'X_{k-1}', \quad k = 1, 2, 3, \ldots, n$$

so that

$$YQY' = X_0QX_0' = \sum_{k=1}^{n}\Gamma_k + X_nQX_n' + \sum_{k=1}^{n}\Gamma_k' = \sum_{k=1}^{n}\left(\Gamma_k + \Gamma_k'\right) + BQB'$$

and

$$V_{YQY'} = \sum_{k=1}^{n}\left(V_{\Gamma_k} + V_{\Gamma_k'}\right) + V_{BQB'}. \tag{3.5}$$

We shall prove the result through the following steps.

Step (A) : **As** Q **moves out of** A_n **along** A_nC, $V_{\Gamma_k} + V_{\Gamma_k'}$ **is** $+ve$ **and monotonic decreasing for odd** k**.**

We choose two points $Q\,(\alpha, F\,(\alpha))$ and $Q_1\,(\alpha_1, F\,(\alpha_1))$ on the curve of $F\,(x)$, where $\alpha_1 > \alpha > a_n$. Let YQY' and $Y_1Q_1Y_1'$ be two phase paths through Q and Q_1 respectively. We have already taken $Y = X_0$, $Y' = X_0'$, $B = X_n$ and $B' = X_n'$. We now take $Y_1 = Z_0$, $Y_1' = Z_0'$, $B_1 = Z_n$, $B_1' = Z_n'$ and Z_kZ_k' as the extension of the line segment X_kX_k' $\forall$ k. Also we write $Z_{k-1}Z_k = \Lambda_k$ and $Z_k'Z_{k-1}' = \Lambda_k'$. If k is odd, then on the segments Γ_k and Λ_k we have $y > 0$, $F\,(x) < 0$ and $y - F\,(x) > 0$. Now,

$$0 < [y - F\,(x)]_{\Gamma_k} < [y - F\,(x)]_{\Lambda_k}.$$

Since $g\,(x) > 0$ for $x > 0$ so we have

$$\left[\frac{-g\,(x)}{y - F\,(x)}\right]_{\Gamma_k} < \left[\frac{-g\,(x)}{y - F\,(x)}\right]_{\Lambda_k} < 0.$$

So, by (3.2) we get

$$\left[\frac{dy}{dx}\right]_{\Gamma_k} < \left[\frac{dy}{dx}\right]_{\Lambda_k} < 0. \tag{3.6}$$

Therefore, by (3.6) we have

$$V_{\Gamma_k} = \int_{\Gamma_k} F\ dy = \int_{\Gamma_k} (-F)\left(-\frac{dy}{dx}\right) dx$$
$$> \int_{\Lambda_k} (-F)\left(-\frac{dy}{dx}\right) dx = \int_{\Lambda_k} F\ dy = V_{\Lambda_k}.$$

Since $F(x)$ and $dy = \dot{y}dt = -g(x)\,dt$ are both $-ve$ along Λ_k for odd k, so we have

$$V_{\Gamma_k} > V_{\Lambda_k} = \int_{\Lambda_k} F\ dy > 0. \tag{3.7}$$

Next, on the segments Γ'_k and Λ'_k we have $y < 0$, $F(x) < 0$ and $y - F(x) < 0$. Now,

$$0 > [y - F(x)]_{\Gamma'_k} > [y - F(x)]_{\Lambda'_k}.$$

So, by (3.2) we get

$$\left[\frac{dy}{dx}\right]_{\Gamma'_k} > \left[\frac{dy}{dx}\right]_{\Lambda'_k} > 0. \tag{3.8}$$

Therefore by (3.8) we have

$$V_{\Gamma'_k} = \int_{\Gamma'_k} F\ dy = \int_{-\Gamma'_k} (-F)\frac{dy}{dx}dx > \int_{-\Lambda'_k} (-F)\frac{dy}{dx}dx = \int_{\Lambda'_k} F\ dy = V_{\Lambda'_k}.$$

Since $F(x)$ and $dy = \dot{y}dt = -g(x)\,dt$ are both $-ve$ along Λ'_k for odd k, so we have

$$V_{\Gamma'_k} > V_{\Lambda'_k} = \int_{\Lambda'_k} F\ dy > 0. \tag{3.9}$$

From (3.7) and (3.9) we have

$$V_{\Gamma_k} + V_{\Gamma'_k} > V_{\Lambda_k} + V_{\Lambda'_k} > 0.$$

Therefore $V_{\Gamma_k} + V_{\Gamma'_k}$ is $+ve$ and monotone decreasing as the point Q moves out of A_n along A_nC.

Step (B) : **As** Q **moves out from** A_n **along** A_nC, $V_{\Gamma_k}+V_{\Gamma'_k}$ **is** $-ve$ **and monotonic increasing for even** k**.**

On the segments Γ_k and Λ_k we have $y>0$, $F(x)>0$ and $y-F(x)>0$. Now,

$$0<\left[y-F(x)\right]_{\Gamma_k}<\left[y-F(x)\right]_{\Lambda_k}.$$

Since $g(x)>0$ for $x>0$ so we have

$$\left[\frac{-g(x)}{y-F(x)}\right]_{\Gamma_k}<\left[\frac{-g(x)}{y-F(x)}\right]_{\Lambda_k}<0.$$

So, by (3.2) we get

$$\left[\frac{dy}{dx}\right]_{\Gamma_k}<\left[\frac{dy}{dx}\right]_{\Lambda_k}<0. \tag{3.10}$$

Therefore by (3.10) we have

$$V_{\Gamma_k}=\int\limits_{\Gamma_k}F\ dy=\int\limits_{\Gamma_k}F\frac{dy}{dx}dx<\int\limits_{\Lambda_k}F\frac{dy}{dx}dx=\int\limits_{\Lambda_k}F\ dy=V_{\Lambda_k}.$$

Since $F(x)>0$ and $dy=\dot{y}dt=-g(x)\,dt<0$ along Λ_k for even k, so we have

$$V_{\Gamma_k}<V_{\Lambda_k}=\int\limits_{\Lambda_k}F\ dy<0. \tag{3.11}$$

Next, on the segments Γ'_k and Λ'_k we have $y<0$, $F(x)>0$ and $y-F(x)<0$. Now,

$$0>\left[y-F(x)\right]_{\Gamma'_k}>\left[y-F(x)\right]_{\Lambda'_k}$$

so that by (3.2) we get

$$\left[\frac{dy}{dx}\right]_{\Gamma'_k}>\left[\frac{dy}{dx}\right]_{\Lambda'_k}>0. \tag{3.12}$$

Therefore by (3.12) we have

$$V_{\Gamma'_k}=\int\limits_{\Gamma'_k}F\,dy=\int\limits_{-\Gamma'_k}F\left(-\frac{dy}{dx}\right)dx<\int\limits_{-\Lambda'_k}F\left(-\frac{dy}{dx}\right)dx=\int\limits_{\Lambda'_k}F\,dy=V_{\Lambda'_k}.$$

Since $F(x)>0$ and $dy=\dot{y}dt=-g(x)\,dt<0$ along Λ'_k for even k, so

we have

$$V_{\Gamma'_k} < V_{\Lambda'_k} = \int\limits_{\Lambda'_k} F\ dy < 0. \tag{3.13}$$

From (3.11) and (3.13) we have

$$V_{\Gamma_k} + V_{\Gamma'_k} < V_{\Lambda_k} + V_{\Lambda'_k} < 0.$$

Therefore $V_{\Gamma_k} + V_{\Gamma'_k}$ is $-ve$ and monotone increasing as the point Q moves out of A_n along A_nC.

Step (C) : $V_{BQB'}$ **is** $-ve$ **and monotone decreasing and tends to** $-\infty$ **as** Q **tends to infinity along** A_nC**.**

On BQB' and $B_1Q_1B'_1$ we have $F(x) > 0$. We draw BH_1 and $B'H'_1$ parallel to x-axis. Since $F(x) > 0$ and $dy = \dot{y}dt = -g(x)\,dt < 0$ along $B_1Q_1B'_1$, so

$$V_{B_1Q_1B'_1} = \int\limits_{B_1Q_1B'_1} F\ dy \leq \int\limits_{H_1Q_1H'_1} F\ dy.$$

Since $[F(x)]_{H_1Q_1H'_1} \geq [F(x)]_{BQB'}$ and $F(x) > 0$, $dy = \dot{y}dt = -g(x)\,dt < 0$ along BQB', so we have

$$V_{B_1Q_1B'_1} \leq \int\limits_{H_1Q_1H'_1} F\ dy \leq \int\limits_{BQB'} F\ dy = V_{BQB'} < 0. \tag{3.14}$$

Let S be a point on $y = F(x)$, to the right of A_n and let BQB' be an arbitrary path, with Q to the right of S. The straight line $PSNP'$ is parallel to the y-axis. Since $F(x) > 0$ and $dy = \dot{y}dt = -g(x)\,dt < 0$ along BQB' and PQP' is a part of BQB', so we have

$$V_{BQB'} = \int\limits_{BQB'} F\ dy = -\int\limits_{B'QB} F\ dy \leq -\int\limits_{P'QP} F\ dy. \tag{3.15}$$

By hypothesis F is monotone increasing on A_nC and so $F(x) \geq NS$ on PQP' and hence (3.15) gives

$$V_{BQB'} \leq -\int\limits_{P'QP} NS \cdot dy = -NS \int\limits_{P'QP} dy = -NS \cdot PP' \leq NS \cdot NP.$$

But as Q goes to infinity towards the right, so $NP \to \infty$ and hence by

the above relation it follows that $V_{BQB'} \to -\infty$.

Step (D) :

From steps (A) and (B) it follows that $\sum_{k=1}^{n} \left(V_{\Gamma_k} + V_{\Gamma'_k}\right)$ in (3.5) is bounded. Therefore as Q moves to infinity from the right of A_n ultimately the quantity $V_{BQB'}$ dominates and hence $V_{YQY'}$ monotonically decreases to $-\infty$ to the right of A_n. The monotone decreasing nature of $V_{BQB'}$ inherits the same nature to $V_{YQY'}$ as Q moves out of A_n along the curve $y = F(x)$.

By the construction of $\bar{\alpha}_n$ it is clear that $V_{YQY'} > 0$ at a point on the left of A_n and ultimately it becomes $-ve$ when the point Q is at the right of A_n. So, by monotonic decreasing nature of $V_{YQY'}$ it can vanish only once as the point Q moves out of A_n along the curve $y = F(x)$. Thus, there is a unique path for which $V_{YQY'} = 0$. We recall that [3] by symmetry of paths, a typical phase path YQY' of the system (3.2) becomes a limit cycle iff $OY = OY'$ and in Chapter 2 it is shown in (2.7) that

$$OY = OY' \Longleftrightarrow V_{YQY'} = 0.$$

Therefore, it follows that the path is closed and the proof is complete.

3.3 Construction of a Lienard System with Desired Number of Limit Cycles

We now present an algorithm by which we can form a Lienard system with as many limit cycles as required. We present the technique for two limit cycles around a single critical point. This technique can similarly be extended for n number of limit cycles. As stated in the introduction, this algorithm is expected to become relevant in a physical model with partial or incomplete data [58].

Suppose in a given physical or dynamical problem, the function F of the Lienard equation (3.1) is well defined only within a finite interval $[-a_1, a_1]$ denoting $F(x) = f_1(x)$ for $x \in [-a_1, a_1]$ and satisfying the conditions:

(*i*) f_1 is a continuous odd function having only one $+ve$ zero a_1;
(*ii*) $xf_1(x) < 0 \ \forall \ x \in [-a_1, a_1]$;
(*iii*) f_1 has a unique local minimum at the point L_0 within (a_0, a_1), where $a_0 = 0$.

Suppose it is also known that the system has a (first or smallest) limit cycle crossing x-axis just outside the interval $[-a_1, a_1]$ in the Lienard plane. We have no information about $F(x)$ beyond the interval. Our aim is to develop an algorithm to determine a function f_2 as a restriction of F in an interval of the form $[a_1, a_2]$ so that it satisfies the conditions of the Theorem 3.2.1, ensuring the second limit cycle crossing x-axis outside the interval $[-a_2, a_2]$. The function F outside this interval can be defined as a monotonic function ensuing the existence of the second limit cycle by Theorem 3.2.1. Now to determine f_2 precisely from the information of f_1 in $[a_0, a_1]$ we need to define two functions ϕ_1 and H_1 so that we get the abscissa and ordinates of f_2 in the interval $[a_1, a_2]$ respectively. The choice of ϕ_1 is motivated by Odani's Choice function [48] (c.f. Remark 3.4.1 for further details). The functions ϕ_1 and H_1 are defined as follows:
the functions ϕ_{1L} and ϕ_{1R} are bijective such that

$$\phi_{1L} : [a_0, L_0] \to [a_1, L_1], \quad \phi_{1L}(a_0) = a_1, \phi_{1L}(L_0) = L_1$$
$$\phi_{1R} : [L_0, a_1] \to [L_1, a_2], \quad \phi_{1R}(L_0) = L_1, \phi_{1R}(a_1) = a_2$$
$$\phi_1(s) = \begin{cases} \phi_{1L}(s), & s \in [a_0, L_0] \\ \phi_{1R}(s), & s \in [L_0, a_1] \end{cases}$$

and H_1 is monotone decreasing on $[0, f_1(L_0)]$ such that

$$H_1 \circ f_1 := f_2 \circ \phi_1. \tag{3.16}$$

To make the definition (3.16) explicit we define at first two monotone functions f_{2L}^* and f_{2R}^* and then introduce H_1 parametrically by the help

of two monotone decreasing functions H_{1L} and H_{1R} on $[0, f_1(L_0)]$ as

$$\begin{aligned} H_{1L} &: f_{1L}(s) \to f_{2L}^*(\phi_{1L}(s)), \quad s \in [a_0, L_0] \\ H_{1R} &: f_{1R}(s) \to f_{2R}^*(\phi_{1R}(s)), \quad s \in [L_0, a_1] \\ H_1(x) &= \begin{cases} H_{1L}(x), & \text{if } x = f_{1L}(s),\ s \in [a_0, L_0] \\ H_{1R}(x), & \text{if } x = f_{1R}(s),\ s \in [L_0, a_1] \end{cases}. \end{aligned}$$

The choice of f_2^* is made on the basis of $f_1(x)$ defined on $[-a_1, a_1]$ and the second zero a_2 of $F(x)$ that must lie close to but nevertheless, less than the expected amplitude of the second limit cycle. We define the functions f_{2L} and f_{2R} as

$$\begin{aligned} f_{2L} &: \phi_{1L}(s) \to H_{1L}(f_{1L}(s)), \quad s \in [a_0, L_0] \\ f_{2R} &: \phi_{1R}(s) \to H_{1R}(f_{1R}(s)), \quad s \in [L_0, a_1]. \end{aligned}$$

We should note that in the definition of ϕ_{1L} and ϕ_{1R} we have used the conditions $\phi_{1L}(a_0) = a_1, \phi_{1L}(L_0) = L_1$ and $\phi_{1R}(L_0) = L_1, \phi_{1R}(a_1) = a_2$. We could also have used the conditions $\phi_{1L}(a_0) = L_1, \phi_{1L}(L_0) = a_1$ and $\phi_{1R}(L_0) = a_2, \phi_{1R}(a_1) = L_1$ instead, but in that case the function H_1 and H_2 must be monotone increasing.
If $x \in [a_1, L_1]$, then $x = \phi_{1L}(s)$ for some $s \in [a_0, L_0]$. Therefore,

$$f_{2L}(x) = f_{2L}(\phi_{1L}(s)) = H_{1L}(f_{1L}(s)) = f_{2L}^*(\phi_{1L}(s)) = f_{2L}^*(x).$$

So,

$$f_{2L} = f_{2L}^*.$$

Next, if $x \in [L_1, a_2]$, then $x = \phi_{1R}(s)$ for some $s \in [L_0, a_1]$. Therefore,

$$f_{2R}(x) = f_{2R}(\phi_{1R}(s)) = H_{1R}(f_{1R}(s)) = f_{2R}^*(\phi_{1R}(s)) = f_{2R}^*(x).$$

So,

$$f_{2R} = f_{2R}^*.$$

Thus, the unknown functions f_{2L} and f_{2R} can be expressed by known

functions f_{2L}^* and f_{2R}^* so that we have

$$f_2(x) = \begin{cases} f_{2L}(x), & x \in [a_1, L_1] \\ f_{2R}(x), & x \in [L_1, a_2] \end{cases}$$
$$= \begin{cases} f_{2L}^*(x), & x \in [a_1, L_1] \\ f_{2R}^*(x), & x \in [L_1, a_2]. \end{cases}$$

Next we construct the restriction f_3 of the function F in $[a_2, a_3]$ having unique local maximum at L_2 (say) in (a_2, a_3). We assume two bijective functions

$$\phi_{2L} : [a_1, L_1] \to [a_2, L_2], \quad \phi_{2L}(a_1) = a_2, \phi_{2L}(L_1) = L_2$$
$$\text{and } \phi_{2R} : [L_1, a_2] \to [L_2, a_3], \quad \phi_{2R}(L_1) = L_2, \phi_{2R}(a_2) = a_3$$

and two more functions f_{3L}^* and f_{3R}^*. We define two monotone decreasing functions H_{2L} and H_{2R} on $[0, f_2(L_1)]$ parametrically as

$$H_{2L} : f_{2L}(s) \to f_{3L}^*(\phi_{2L}(s)), \quad s \in [a_1, L_1]$$
$$H_{2R} : f_{2R}(s) \to f_{3R}^*(\phi_{2R}(s)), \quad s \in [L_1, a_2].$$

We define

$$f_{3L} : \phi_{2L}(s) \to H_{2L}(f_{2L}(s)), \quad s \in [a_1, L_1]$$
$$f_{3R} : \phi_{2R}(s) \to H_{2R}(f_{2R}(s)), \quad s \in [L_1, a_2]$$

so that as shown above we have

$$f_{3L} = f_{3L}^* \text{ and } f_{3R} = f_{3R}^*.$$

Therefore,

$$f_3(x) = \begin{cases} f_{3L}(x), & x \in [a_2, L_2] \\ f_{3R}(x), & x \in [L_2, a_3] \end{cases}$$
$$= \begin{cases} f_{3L}^*(x), & x \in [a_2, L_2] \\ f_{3R}^*(x), & x \in [L_2, a_3]. \end{cases}$$

We observe that

$$f_{3L} : \phi_{2L}(\phi_{1L}(s)) \to H_{2L}(f_{2L}(\phi_{1L}(s))), \quad s \in [a_0, L_0]$$
$$f_{3R} : \phi_{2R}(\phi_{1R}(s)) \to H_{2R}(f_{2R}(\phi_{1R}(s))), \quad s \in [L_0, a_1].$$

We can similarly proceed and construct all the restrictions f_k of the function F in $[a_{k-1}, a_k]$ for $k = 4, 5, 6, \ldots, N$ so that the corresponding Lienard system have exactly N limit cycles. Thus an incomplete Lienard system can be extended iteratively over larger and larger intervals of x, having as many (simple) limit cycles as desired. We note, however, that the choice of iterated functions has as large arbitrariness except for the required minimal conditions of monotonicity satisfying Theorem 3.2.1. The number of limit cycles for each such choices remain invariant. The problem of reconstructing data with a given number of limit cycles and having specified shapes is left for future study. We now illustrate the above construction by the following examples.

3.4 Examples

First we consider an example in which the function F is chosen to satisfy Theorem 3.2.1 but not the Theorem 7.12 in chapter 4 of the book [51] nor Theorem 1 in [47]. Here the figures have been drawn using Mathematica.

Example 3.4.1 *We define*

$$F_+(x) = \begin{cases} 0.005 - 0.025\sqrt{1 - \left(\dfrac{x - 0.048989794}{0.05}\right)^2}, & 0 \le x < a_1 \\ -0.0008137888130718 + 0.01\sqrt{1 - \left(\dfrac{x - 0.14781375}{0.05}\right)^2}, & a_1 \le x < a_2 \\ 0.0009168416064002765 - 0.015\sqrt{1 - \left(\dfrac{x - 0.29746094}{0.1}\right)^2}, & a_2 \le x < a_3 \\ -0.0003265987749816556 + 0.04\sqrt{x - 0.3972073012751128}, & x \ge a_3, \end{cases}$$

where

$$a_1 = 0.097979588$$
$$a_2 = 0.197647912$$
$$\text{and } a_3 = 0.397273968.$$

and

$$F(x) = \begin{cases} F_+(x) & x \geq 0 \\ -F_+(-x) & x < 0 \end{cases}$$

The function $F_+(x)$ *is obtained by matching three ellipses and a parabola successively in the intervals* $(0, a_1)$, (a_1, a_2), (a_2, a_3), *and* (a_3, ∞) *such that*

$$F_+(a_i + 0) = F_+(a_i - 0) \text{ and } F'_+(a_i + 0) = F'_+(a_i - 0), \qquad (3.17)$$

where a_i*'s are zeros of* F_+. *The unique extremum of* F *in* $(0, a_1)$, (a_1, a_2), (a_2, a_3) *are respectively*

$$L_0 = 0.048989794$$
$$L_1 = 0.14781375$$
$$\text{and } L_2 = 0.29746094.$$

We obtain three limit cycles which meet the positive y*-axis at the points* $(0, y_1(0))$, $(0, y_2(0))$, $(0, y_3(0))$ *where*

$$y_1(0) = 0.1332869$$
$$y_2(0) = 0.212146685$$
$$\text{and } y_3(0) = 0.4630114.$$

The matching conditions (3.17) are used to make $F \in C^1(R)$ *with accuracy level* $O\left(10^{-7}\right)$. *This function is constructed in a trial and error method and numerical data with large significant digits arise in this fashion. Examples with lower significant digits and lower and higher accuracy are possible in principle. Here we get* $\bar{\alpha}_1 = 0.133002186$ *and* $\bar{\alpha}_2 = 0.21203506657$. *The function* F *satisfies all the conditions of Theorem 3.2.1 (for example* $\bar{\alpha}_i < L_i$ *etc.) and so the existence of the above three limit cycles are ensured by this theorem, the proof of which is presented separately* [56]. *However, the function* F *is defined in such a manner that* $|F(L_0)| > |F(L_2)|$ *implying that* β_2 *mentioned in Theorem* 1 *of* [47] *or in Theorem* 7.12, *chapter* 4 *of the book* [51] *does not exist and hence these theorems are not applicable for the corresponding Lienard system. The limit cycles of the Lienard system in Lienard plane and the graph of the function* F *have been shown separately in the*

Figure 3.2. To conclude, Theorem 1 *of* [47] *or Theorem* 7.12, *Chapter* 4 *in the book* [51] *fail to predict the existence of the exact number of limit cycles for the above function* $F(x)$.

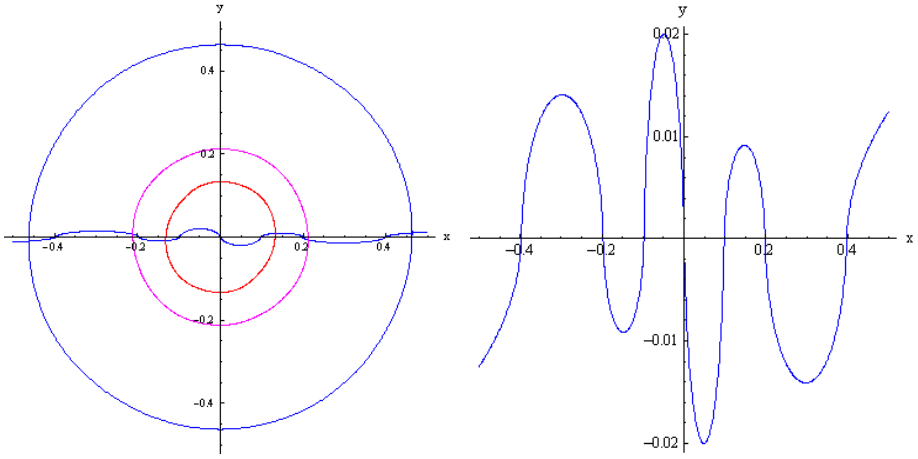

(a) (b)

Figure 3.2:
(a) The phase diagram of the system (3.2) in Lienard plane with three limit cycles.
(b) Graph of the function F in Example 3.4.1.

We now present some examples following the construction described in Section 3.3.

Example 3.4.2 *Let* $a_1 = 0.2$, $a_2 = 0.5$ *and*

$$f_1(x) = 0.15 - 0.25\sqrt{1 - \frac{(x-0.1)^2}{0.125^2}}, \quad -0.2 \leq x \leq 0.2.$$

Here, $L_0 = 0.1$. *Let* $L_1 = 0.3$. *Let us choose*

$$f_{2L}^*(x) = -0.15 + 0.25\sqrt{1 - \frac{(x-0.3)^2}{(0.125)^2}}$$

$$f_{2R}^*(x) = -0.15 + 0.25\sqrt{1 - \frac{(x-0.3)^2}{(0.25)^2}}.$$

Also, let

$$\phi_{1L}(s) = \sqrt{As^2 + B}.$$

To determine the unknown parameters A *and* B *we assume that* $\phi_{1L}(a_0) =$

a_1, $\phi_{1L}(L_0) = L_1$. *Then* $A = 5$ *and* $B = 0.04$. *Next, let*

$$\phi_{1R}(s) = \sqrt{A's^2 + B'}$$

with $\phi_{1R}(L_0) = L_1$ *and* $\phi_{1R}(a_1) = a_2$. *Then,* $A' = \frac{16}{3}$ *and* $B' = \frac{11}{300}$. *Then following the algorithm in Section 3.3 we have*

$$f_{2L} = f_{2L}^* \text{ in } [a_1, L_1]$$
$$\text{and } f_{2R} = f_{2R}^* \text{ in } [L_1, a_2]$$

so that

$$f_2(x) = \begin{cases} f_{2L}(x), & x \in [a_1, L_1] \\ f_{2R}(x), & x \in [L_1, a_2]. \end{cases}$$

We now define

$$F_+(x) = \begin{cases} f_1(x), & 0 \le x < a_1 \\ f_2(x), & a_1 \le x < a_2 \\ -\frac{4}{3}(x - 0.5), & x \ge a_2 \end{cases}$$

to make F_+ *continuously differentiable in* $[0, \infty)$. *The last part of the function* F_+ *is taken to make* F_+ *monotone decreasing for* $x \ge a_2$ *so that the function* F *defined below satisfy the condition that* $|F(x)| \to \infty$ *as* $x \to \infty$ *monotonically for* $x \ge a_2$. *We take*

$$F(x) = \begin{cases} F_+(x), & x \ge 0 \\ F_-(x), & x < 0. \end{cases}$$

We find two limit cycles which cross the +ve y-axis at the points $(0, 0.26731065)$ *and* $(0, 0.5749823)$ *respectively. So,* $y_+(0) = y_-(0) = 0.26731065$ *and* $\bar{\alpha}_1 = 0.254219124$. *So, the conditions* $\bar{\alpha}_1 \le L_1$ *are satisfied in this example. Thus the existence of limit cycles are ensured by the Theorem 3.2.1 with* $g(x) = x$ *establishing the construction in Section 3.3. The limit cycles alongwith the curve of* $F(x)$ *has been shown in Figure 3.3.*

Remark 3.4.1 *From condition* $(C2)$ *in* [48] *we see that*

$$g(\phi_k(x))\,\phi_k'(x) \ge g(x).$$

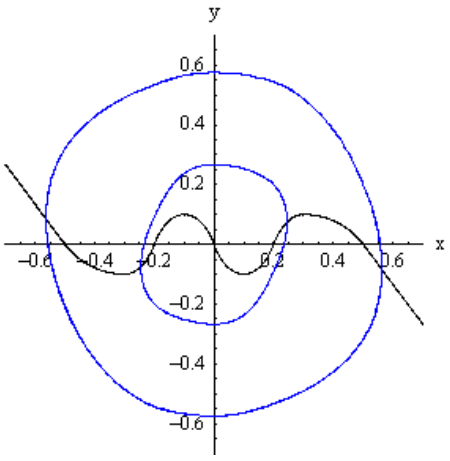

Figure 3.3: Limit cycles for the system in Example 3.4.2 with the curve of $F(x)$.

If $g(x) = x$, *then it gives*

$$\phi_k(x)\,\phi_k'(x) \geq x.$$

Thus, in Example 3.4.2 if we take $\phi_k(s) = \phi_{1L}(s) = \sqrt{As^2 + B}$, *then the above inequality gives*

$$\begin{aligned} & \sqrt{As^2+B} \cdot \frac{2As}{2\sqrt{As^2+B}} \geq s \\ i.e., \quad & As \geq s \\ i.e., \quad & A \geq 1. \end{aligned}$$

By the definition of f_{2L}^* *and* f_2 *it follows that the remaining part of the condition* $(C2)$ *is satisfied if*

$$|F(\phi_{1L}(s))| \geq |F(s)|, \quad s \in [a_0, L_0]$$

and in particular

$$|F(\phi_{1L}(0))| = |F(0)|.$$

Since, $\phi_{1L}(s) \in [a_1, a_2]$ *and* $s \in [a_0, L_0]$ *so it gives*

$$\begin{aligned} & |f_2(\phi_{1L}(s))| \geq |f_1(s)|, \quad s \in [a_0, L_0] \\ i.e., \quad & |H_{1L}(f_{1L}(s))| \geq |f_{1L}(s)|, \quad s \in [a_0, L_0]. \end{aligned} \tag{3.18}$$

Next, in particular the equality occurs at $s = a_0 = 0$ *and so we have*

$$\begin{aligned} & |F(\phi_{1L}(0))| = |F(0)| \\ \Rightarrow\ & |H_{1L}(f_{1L}(0))| = 0 \\ \Rightarrow\ & |H_{1L}(0)| = 0 \\ \Rightarrow\ & H_{1L}(0) = 0 \end{aligned} \tag{3.19}$$

since $F(0) = 0$ *and* $f_{1L}(0) = 0$. *By our construction we also see*

$$s \cdot H_1(s) < 0 \quad \forall\ s.$$

Thus, ϕ_{1L} *behaves like choice function described by Odani. Here, the condition (3.18) does not hold for the system discussed in Example 3.4.2. In fact, here*

$$|H_{1L}(f_{1L}(s))| \leq |f_{1L}(s)| \quad s \in [a_0, L_0].$$

However, the conditions (viz. $\bar{\alpha}_i < L_i$, *etc.) of Theorem 3.2.1 are satisfied ensuring the existence of exactly two limit cycles. This shows that the Theorem 3.2.1 and the construction presented above covers a larger class of functions* F *than those covered in* [48]. *The equality in (3.18) occurs in Example 3.4.2 only at the point* $s = a_0 = 0$. *However, the equality can occur at points where* $s \neq a_0$. *We present Example 3.4.3 below to show this kind of behaviour.*

Remark 3.4.2 *The function* f_2 *in Example 3.4.2 is obtained from* f_1 *by reflection and translation along* x*-axis. However, it is clear from the construction of Section 3.3, that there is a plenty of freedom in the possible extensions of* f_1 *having a fixed number of limit cycles, as illustrated in Examples 3.4.3 and 3.4.4. In these examples we consider more general transformations so that the limit cycles are obtained having amplitudes close to those expected from the given physical (dynamical) problem.*

Example 3.4.3 *Here, our target is to construct an example in which*

$$F_{+}(x)=\begin{cases}0.055518-0.08\sqrt{1-\dfrac{(x-0.144)^2}{0.04}}, & 0\leq x\leq 0.144\\ 0.148506-0.172988\sqrt{1-\dfrac{(x-0.144)^2}{(0.206686)^2}}, & 0.144<x\leq 0.34\\ 0.0910146+0.0209854\sqrt{1-\dfrac{(x-0.407)^2}{(0.06751554)^2}}, & 0.34<x\leq 0.407\\ -0.2280727+0.340073\sqrt{1-\dfrac{(x-0.407)^2}{(0.125376)^2}}, & 0.407<x\leq 0.5\\ -3.0000372\,(x-0.5), & x>0.5\end{cases}$$

and

$$F(x)=\begin{cases}F_{+}(x), & x\geq 0\\ F_{-}(x), & x<0.\end{cases}$$

Here, $a_1=0.2$, $a_2=0.5$, $L_0=0.144$ *and* $L_1=0.407$. *It is easy to show that*

$$\phi_{1L}(s)=\sqrt{4.974392361\cdot s^2+0.0625}$$
$$\text{and } \phi_{1R}(s)=\sqrt{2.019706\cdot s^2+0.12376838}.$$

Here,

$$f_1(x)=\begin{cases}0.055518-0.08\sqrt{1-\dfrac{(x-0.144)^2}{0.04}}, & 0\leq x\leq 0.144\\ 0.148506-0.172988\sqrt{1-\dfrac{(x-0.144)^2}{(0.206686)^2}}, & 0.144<x\leq 0.2\end{cases}$$

$$f_2(x)=\begin{cases}0.148506-0.172988\sqrt{1-\dfrac{(x-0.144)^2}{(0.206686)^2}}, & 0.2<x\leq 0.34\\ 0.0910146+0.0209854\sqrt{1-\dfrac{(x-0.407)^2}{(0.06751554)^2}}, & 0.34<x\leq 0.407\\ -0.2280727+0.340073\sqrt{1-\dfrac{(x-0.407)^2}{(0.125376)^2}}, & 0.407<x\leq 0.5\end{cases}$$

The second part of the condition $(C2)$ *in* [48] *i.e., the condition* (*3.18*)

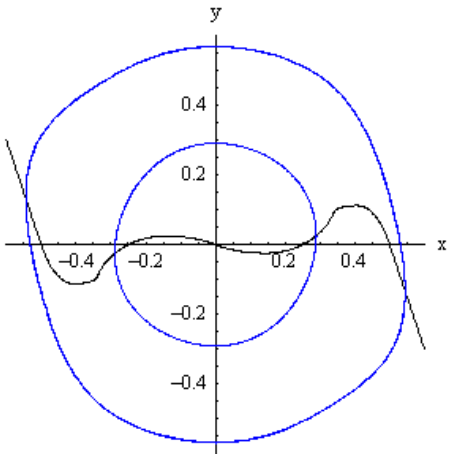

Figure 3.4: Limit cycles for the system in Example 3.4.3 with the curve of $F(x)$.

does not hold. In fact,

$$|H_{1L}(f_{1L}(s))| < |f_{1L}(s)| \ \text{ in } \ (0, 0.05290111)$$
$$\text{and } |H_{1L}(f_{1L}(s))| > |f_{1L}(s)| \ \text{ in } \ (0.05290111, 0.144).$$

The equality occurs at $s = 0$ *and* $s = 0.05290111$. *Here, we get two limit cycles crossing the +ve y-axis at the points* $(0, 0.29039755)$ *and* $(0, 0.567249)$ *respectively so that* $y_+(0) = y_-(0) = 0.29039755$ *and* $\bar{\alpha}_1 = 0.2892792083$. *Consequently,* $\bar{\alpha}_1 \leq L_1$ *and the other conditions of Theorem 3.2.1 with* $g(x) = x$ *are satisfied justifying the existence of exactly two limit cycles. These two limit cycles alongwith the curve of* $F(x)$ *has been shown in Figure 3.4.*

Example 3.4.4 *We now consider an example involving three limit cycles by taking* $a_1 = 0.1$, $a_2 = 0.2$, $a_3 = 0.4$ *and*

$$f_1(x) = 0.04422166 - 0.08\sqrt{1 - \frac{(x - 0.05)^2}{(0.06)^2}}, \quad -0.1 \leq x \leq 0.1.$$

Here $L_0 = 0.05$ *and let* $L_1 = 0.15$, $L_2 = 0.3$. *We take*

$$f_{2L}^*(x) = -0.04422166 + 0.08\sqrt{1 - \frac{(x - 0.15)^2}{(0.06)^2}},$$
$$f_{2R}^*(x) = -0.04422166 + 0.08\sqrt{1 - \frac{(x - 0.15)^2}{(0.06)^2}}.$$

It is easy to construct

$$\phi_{1L}(s) = \sqrt{5s^2 + 0.01}, \quad s \in [a_0, L_0],$$
$$\phi_{1R}(s) = \sqrt{\frac{7}{3}s^2 + \frac{5}{300}}, \quad s \in [L_0, a_1].$$

Next, we take

$$f^*_{3L}(x) = 0.0043819183 - 0.03\sqrt{1 - \frac{(x-0.3)^2}{(0.101084111)^2}},$$
$$f^*_{3R}(x) = 0.0043819183 - 0.03\sqrt{1 - \frac{(x-0.3)^2}{(0.101084111)^2}}.$$

We can similarly construct

$$\phi_{2L}(s) = \sqrt{4s^2} = 2s, \quad s \in [a_1, L_1],$$
$$\phi_{2R}(s) = 2s, \quad s \in [L_1, a_2].$$

so that $\phi_{2L}(a_1) = a_2$, $\phi_{2L}(L_1) = L_2$, $\phi_{2R}(L_1) = L_2$ *and* $\phi_{2R}(a_2) = a_3$. *We define*

$$F_+(x) = \begin{cases} 0.04422166 - 0.08\sqrt{1 - \frac{(x-0.05)^2}{(0.06)^2}}, & 0 \le x < 0.1 \\ -0.04422166 + 0.08\sqrt{1 - \frac{(x-0.15)^2}{(0.06)^2}}, & 0.1 \le x < 0.2 \\ 0.0043819183 - 0.03\sqrt{1 - \frac{(x-0.3)^2}{(0.101084111)^2}}, & 0.2 \le x < 0.4 \\ 2.0100758\,(x - 0.4), & 0.4 \le x \end{cases}$$

and

$$F(x) = \begin{cases} F_+(x), & x \ge 0 \\ F_-(x), & x < 0 \end{cases}$$

to make F *continuously differentiable. We can easily calculate that* $\bar{\alpha}_1 = 0.12418214965$ *and* $\bar{\alpha}_2 = 0.2354818163$ *and consequently* $\bar{\alpha}_i < L_i$ *for* $i = 1, 2$. *All the other conditions of Theorem 3.2.1 with* $g(x) = x$ *are satisfied and hence we get three distinct limit cycles as shown in Figure* 3.5 *alongwith the curve of* $F(x)$ *defined above.*

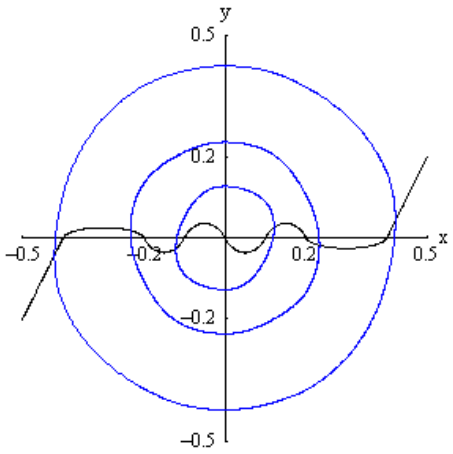

Figure 3.5: Three limit cycles for the system in Example 3.4.4 with the curve of $F(x)$.

Remark 3.4.3 *Here the function F is defined in such a manner that $|F(L_0)| > |F(L_2)|$ implying that β_2 mentioned in Theorem 3 of* [47] *or in Theorem 7.12, chapter 4 of the book* [51] *does not exist and hence these theorems are not applicable for the corresponding Lienard system.*

3.5 Concluding Remarks

In this chapter we extended Lienard Theorem for multiple limit cycles by computing an efficient upper estimate of the amplitude of each cycle. Examples in Section 3.4 establish that the Theorem 3.2 can be used on Lienard systems for which the existence of limit cycles cannot be ensured by similar results available in Literature [47, 51]. An algorithm for the reconstruction of Lienard systems with incomplete information has been proposed [56]. It has been referred further by other authors in recent past [59]. This algorithm is merely proposed to reconstruct Lienard system with specified number of limit cycles. However, similar problem with a given number of limit cycles and having specified shapes is left for future study.

Chapter 4

Existence of Limit Cycles in Non-symmetric Lienard Systems

4.1 Introduction

We have completed a brief study on the existence of unique or multiple limit cycles for the Lienard equation

$$\ddot{x} + f(x)\dot{x} + g(x) = 0 \tag{4.1}$$

in the previous chapters representing it as the well known Lienard autonomous system

$$\dot{x} = y - F(x), \qquad \dot{y} = -g(x), \tag{4.2}$$

where $F(x) = \int_0^x f(x)\,dx$. Obtaining a sufficient condition for existence, number, shapes and amplitudes of limit cycles of this system have been considered to be an interesting problem over the past few decades. Various classical results have been proved considering F and g as odd functions [43, 44, 46, 47, 49, 52, 60]. We studied few new results in the previous chapters. However, some attempts have also been made to cover a more general class of functions [47, 51, 52]. We call a Lienard system *non-symmetric* when F is not an odd function. In this context, let us mention here the interesting contributions from the Italian school led by Sansone [61], Sabatini and Villari [62] and other co-workers, for instance, [63]. The work of Sabatini and Villari [62], in particular, gives uniqueness theorems for a large class of so called generalized Lienard systems.

The well known Lienard theorem [3, 51] gives a set of sufficient con-

ditions for the existence of unique limit cycle of the system (4.2). In this theorem the functions F and g are odd and $g(x) > 0$ for $x > 0$. Recently, Llibre et al. have proved a sufficient condition for the existence of N number of limit cycles [47]. An important aspect of their result is that the function $F(x)$ need not be odd. They proved the result by using the Filipov transformation and the applications of annular region theorem [51]. Here, we consider a class of functions $F(x)$ which have different signs in a sufficiently small neighbourhood of the origin analogous to odd functions [64]. However, the exact symmetry of odd functions about the origin is broken so as to make them non-symmetric. An example of polynomial function satisfying the necessary conditions (Theorem 4.4.1, say) may be given as $F(x) = \frac{1}{3}x^3 + \frac{1}{2}x^2 - x$. The functions which keep the same sign in the sufficiently small neighbourhood of the origin, as in the case of even functions, are not considered here.

In our previous studies [55, 56], we have extended the classical Lienard theorem in two ways. At the first level, we succeeded to weaken the sufficient conditions on $F(x)$ based on a simple observation that the existence of the unique limit cycle is assured even when $F(x)$ is *monotonic only in an interval* $(0, \bar{\alpha}]$ *where* $\bar{\alpha}$ *is determined as an efficient upper estimate of the amplitude of the limit cycle.* Using this insight we then *generalized* the standard Lienard theorem to prove the existence of multiple limit cycles [55, 56]. The strength of the approach is that it uses essentially similar arguments as that of the classical theorem (for one limit cycle), but by using careful upper estimates of amplitudes, a stronger result is derived. One could therefore avoid the technicalities that are usually encountered in the literature [47, 51, 52, 60]. Another aspect that is needed to be mentioned is that we are able to consider a different class of functions as compared to those considered in the theorems of [47, 51] (in the special case when F is odd) as mentioned in Section 3.4 of Chapter 3.

In the present chapter, we extend the Lienard theorem further for a class of non-symmetric Lienard system. It appears that the study of non-symmetric problems considered here have yet to receive a proper attention in the literature. The present work aims at filling up this gap. By extending the techniques of [55, 56] we are now able to prove

the existence of *at least one* (respectively, multiple) limit cycle (cycles), (Theorem 4.4.1−4.4.3) even when $F(x)$ is not necessarily an odd function. An upper estimate of the amplitude of the limit cycles is obtained as in [55] in case of symmetric odd function F. We apply this result to a class of deformed (non-symmetric) Van der Pol equation and derive upper/lower estimates of the amplitude of the deformed limit cycle. In Example 4.5.1 we construct a non-symmetric system with two limit cycles satisfying conditions of Theorem 4.4.2. In Example 4.5.2 we give another construction of a Lienard system with three limit cycles, that satisfies the conditions of Theorem 4.4.3, but, nevertheless, violates those of Theorem 7.12 (Chapter 4 of [51]) and Theorem 3 of [47]. All the numerical examples along with corresponding diagrams are calculated using Mathematica with machine level precision. No artificial truncation of numerical digits have been allowed. As a consequence we display in the tabulated values all the digits generated by Mathematica.

Let us remark that Zhifen [65] proved a number of theorems ensuring the existence of *at most one* limit cycle for Lienard systems with a class of functions not satisfying the classical Lienard theorems. However, our theorems ensure the existence of *at least* N number of limit cycles for a class of non-symmetric Lienard systems thereby extending the studies available in the current literature. We also remark that the results reported in [62,63] appear to cover a wider class of problems. However, most of the theorems in the above references can guarantee at most one limit cycle under some general analytic conditions on the functions f, g, F and G. For uniqueness in [63], however, a very special set of conditions relating $G(x)$ and $F(x)$ are required. In our approach, on the other hand, the stated sufficient conditions can ensure the existence of a minimum number of (i.e., at least N) limit cycles, though perhaps in a limited set of problems involving non-symmetric system as defined above. The novelty of our approach is, of course, its simplicity. Moreover, it comes as a bit of a surprise to realize that the simple technique of potential (energy) integral method can still yield interesting new results even for a class of non-symmetric Lienard systems. However, we are still unable to state a sufficient condition for exact number of limit cycles. A suitable amalgamation of the above two complementary ap-

proaches might guarantee the existence of exact number of limit cycles. However, at this level, we leave this problem for a future investigation.

The chapter is arranged as follows. Section 4.2 introduces preliminary results and notions that will be used subsequently. New formulation of the problem is presented in Section 4.3 and the extensions of the Lienard theorem are proved in Section 4.4. We also present the example of a deformed Van der Pol equation in this section. In Section 4.5, we give two examples in support of our theorems on multiple limit cycles. Finally, Section 4.6 contains some concluding remarks.

4.2 Recollection of Preliminaries

We recall, Theorem 2.3.1 in Chapter 2 following [55], the weaker version of the Lienard theorem [3] thereby introducing notations that will be necessary for subsequent applications.

It can be shown that [3] by symmetry of paths, a typical phase path YQY' (c.f. Figure 2.1) of the system (4.2) becomes a limit cycle iff $OY = OY'$. We defined $V_{YQY'}$ and $v\,(x, y)$ for the path YQY' in Figure 2.1 given by Equations (2.8) and (2.9) respectively for the system (4.2). We recall Remark 2.2.1 that if Γ denotes a curve joining more (or less) than three successive points, the potential V_Γ will have more (or less) than three indices. For example, if we consider the curve $\Gamma = Y_+Q_+Q_-Y'_-$ (see Figure 4.1) as used in the proof of Proposition 4.3.2 then

$$V_{Y_+Q_+Q_-Y'_-} = \int\limits_{Y_+Q_+Q_-Y'_-} dv.$$

It follows that

$$dv = y\ dy + g\ dx = F\ dy \tag{4.3}$$

so that

$$OY = OY' \Leftrightarrow V_{YQY'} = 0. \tag{4.4}$$

We defined $\bar{\alpha}$ given by Equation (2.17) and proved that $V_{YQY'}$ has a simple zero at an $\alpha \leq \bar{\alpha}$ [55] for the system (4.2) in Lienard theorem. So, $\bar{\alpha}$ provides an efficient upper estimate of the amplitude of the unique limit cycle of Lienard equations [55]. We also generalized

Lienard theorem [3] for exactly N limit cycles [56].

In this Chapter we consider a function F which is not necessarily odd. So, to apply the above method of potential function on such system some modifications of previous formulation is required as discussed in the following section.

4.3 New Formulation

In the Lienard plane the symmetry of the paths as in the classical Lienard system is lost here because of more general nature of F. In this and subsequent sections we shall always consider the function g as an odd function. The key feature of this new technique is given as the following proposition which is proved by the help of very simple geometric transformation. Analogous transformations ware originally considered by Filipov [51, 66].

Proposition 4.3.1 *The Lienard system (4.2) is equivalent to the systems*

$$\dot{x} = y - F_p(x), \qquad \dot{y} = -g(x), \quad x > 0 \tag{4.5a}$$

$$\dot{x} = y - F_n(x), \qquad \dot{y} = -g(x), \quad x > 0 \tag{4.5b}$$

where $F_p(x) = F(x)$ *and* $F_n(x) = -F(-x)$ *with* $x > 0$.

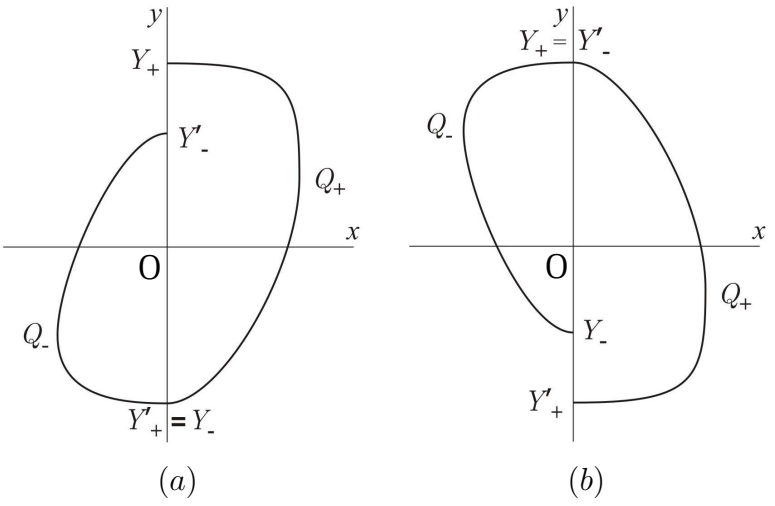

Figure 4.1: Typical paths for the Lienard theorem

Proof. Here we shall consider the Lienard plane, as shown in Figure 4.1. We shall first consider the plane when $x < 0$. Replacing x by $-x$ and y by $-y$ and using the odd nature of g the Lienard system (4.2) for $x < 0$ reduces to

$$\dot{x} = y - F_n(x), \qquad \dot{y} = -g(x), \quad x > 0$$

where $F_n(x) = -F(-x)$ with $x > 0$. However, if $x > 0$ in the phase plane of (4.2) then keep the original system intact and represent it, for convenience, in the new form

$$\dot{x} = y - F_p(x), \qquad \dot{y} = -g(x), \quad x > 0$$

where $F_p(x) = F(x)$. Thus the positive and negative half planes with respect to y-axis in the phase plane of (4.2) are equivalent to the systems (4.5a) and (4.5b) respectively. Hence, the result follows. ■

We must note that the present transformation differs from Filipov's in the sense that the original Lienard equation in the Lienard plane, is transformed into two same systems for $x > 0$ whereas Filipov's transformation gives two first order nonlinear equations in a transformed plane. Further, our method appears to generate the intended results in a much more simpler manner as compared to the results available in the literature.

Replacing x by $-x$ and y by $-y$ in the Lienard system (4.2) when $x < 0$, the phase paths undergo a reflection about the origin and assumes the form of the system (4.5b) for $x > 0$. Typical paths of the system (4.2) are shown in Figures 4.1(a) and 4.1(b) which on similar reflection reduce to the Figure 4.2(a) with $OY_- = OY'_+$ and the Figure 4.2(b) with $OY_+ = OY'_-$ respectively. The phase planes of both the systems (4.5a) and (4.5b) are shown together in each of the last two figures. In Figure 4.1(a) (or 4.1 (b)) the path $Y_+Q_+Y_-Q_-Y'_-$ (or $Y_-Q_-Y_+Q_+Y'_+$) with $OY_- = OY'_+$ (or $OY_+ = OY'_-$) becomes a closed path if and only if $OY_+ = OY'_-$ (or $OY_- = OY'_+$). Now we have the following proposition.

Proposition 4.3.2 *The system (4.2) has a closed path if and only if the system (4.5) has paths with $OY_- = OY'_+$ (or $OY_+ = OY'_-$) as shown in Figure 4.2(a) (or 4.2(b)) for which $OY_+ = OY'_-$ (or $OY_- = OY'_+$)*

holds.

Proof. We define the line integrals (similar to the integral $V_{YQY'}$ de-

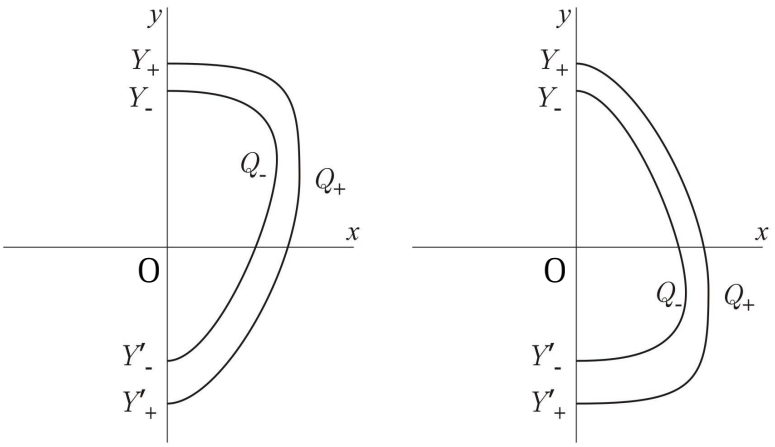

Figure 4.2: Typical paths for the system (4.5)

fined by Equation (2.8) in Chapter 2)

$$V^{+}_{Y_+Q_+Y'_+} = v^{+}_{Y'_+} - v^{+}_{Y_+} = \int\limits_{Y_+Q_+Y'_+} dv^{+},$$

$$V^{-}_{Y_-Q_-Y'_-} = v^{-}_{Y'_-} - v^{-}_{Y_-} = \int\limits_{Y_-Q_-Y'_-} dv^{-},$$

where

$$v^{+}(x,y) = \int_0^x g(u)\,du + \frac{1}{2}y^2, \tag{4.6a}$$

$y = y(x)$ being the solutions of (4.5a) and

$$v^{-}(x,y) = \int_0^x g(u)\,du + \frac{1}{2}y^2, \tag{4.6b}$$

$y = y(x)$ being the solutions of (4.5b). We must note that we shall use V^{+} and V^{-} with more (or less) than three indices as mentioned in Remark 2.2.1 of Chapter 2.

We shall first prove that $V_{Y_+Q_+Q_-Y'_-} = V^{+}_{Y_+Q_+Y'_+} + V^{-}_{Y_-Q_-Y'_-}$. We have

$$V_{Y_+Q_+Q_-Y'_-} = V_{Y_+Q_+Y'_+} + V_{Y_-Q_-Y'_-}.$$

If $x > 0$ then the systems (4.2) and (4.5a) are same systems and so it is obvious that

$$V_{Y_+Q_+Y'_+} = V^+_{Y_+Q_+Y'_+}.$$

We now assume that $(x_1, y_1) = (x_1(t), y_1(t))$ is a solution of the system (4.2) when $x < 0$ and $(x_2, y_2) = (x_2(t), y_2(t))$ be that of the system (4.5b). Then clearly we have

$$x_2 = -x_1, \quad y_2 = -y_1.$$

Since, g is an odd function we have

$$\begin{aligned} g(x_2) &= g(-x_1) \\ &= -g(x_1) \end{aligned}$$

so that

$$\dot{y}_2 = -\dot{y}_1,$$

which obviously follows from the result that $y_2 = -y_1$ establishing the consistency of the transformation. Again, since $F_n(x_2) = -F(-x_2) = -F(x_1)$ from Equations (2.9), (2.8) and (4.3) it follows that

$$\begin{aligned} V_{Y_-Q_-Y'_-} &= \int\limits_{Y_-Q_-Y'_-} F(x_1)\, dy_1 \\ &= \int\limits_{Y_-Q_-Y'_-} F(x_1)\, \dot{y}_1 dt \\ &= \int\limits_{Y_-Q_-Y'_-} F(x_1)\, (-\dot{y}_2)\, dt \\ &= \int\limits_{Y_-Q_-Y'_-} F_n(x_2)\, \dot{y}_2 dt \\ &= V^-_{Y_-Q_-Y'_-}. \end{aligned}$$

Thus,

$$\begin{aligned} V_{Y_+Q_+Q_-Y'_-} &= V_{Y_+Q_+Y'_+} + V_{Y_-Q_-Y'_-} \\ &= V^+_{Y_+Q_+Y'_+} + V^-_{Y_-Q_-Y'_-}. \end{aligned}$$

It follows, therefore, from a slight variation of (4.4), that a phase path is a limit cycle of the system (4.2) (where $F(x)$ may not be an odd function)

$$\begin{aligned} &\text{iff} \quad V_{Y_+Q_+Q_-Y'_-} = V^+_{Y_+Q_+Y'_+} + V^-_{Y_-Q_-Y'_-} = 0 \\ &\Leftrightarrow \quad \left(v^+_{Y_+} - v^+_{Y'_+}\right) + \left(v^-_{Y_-} - v^-_{Y'_-}\right) = 0 \\ &\Leftrightarrow \quad \{v(0, OY_+) - v(0, OY'_+)\} + \{v(0, OY_-) - v(0, OY'_-)\} = 0. \end{aligned}$$

Since $v(0, OY_+) = \dfrac{1}{2} OY_+^2$ etc. so we have

$$\left\{OY_+^2 - OY_+'^2\right\} + \left\{OY_-^2 - OY_-'^2\right\} = 0.$$

As a consequence, a path $Y_+Q_+Y_-Q_-Y'_-$ (or $Y_-Q_-Y_+Q_+Y'_+$) with $OY_- = OY'_+$ (or $OY_+ = OY'_-$) in the Figure 4.1(a) (or 4.1 (b)) becomes a closed path if and only if

$$OY_+ = OY'_- \,(\text{or } OY_- = OY'_+)\,.$$

This completes the proof. ■

Remark 4.3.1 *The system (4.5a) (or (4.5b)) passes through the point $Q_+(\alpha, F_p(\alpha))$ (or $Q_-(\alpha, F_n(\alpha))$). So, their solutions are also dependent on α. Therefore, we can conclude that the potentials V^+ and V^- are implicitly dependent upon α, though from their definitions it seem that they are only time integrals of dv^+ and dv^- respectively. We shall use this observation in the proof of the theorems in section 4.4.*

Remark 4.3.2 *When $F(x)$ is odd, Q_+ and Q_- become image of each other under reflection about origin and hence would coincide. Moreover, over the full cycle Σ in the phase plane of (4.2)*

$$\begin{aligned} &V_\Sigma = 0 \\ \Leftrightarrow\ &V_{\Sigma_+} = V_{\Sigma_-} = 0, \end{aligned}$$

where

$$\Sigma = \Sigma_+ + \Sigma_-,$$

Σ_+ (or Σ_-) being the half cycle for $x > 0$ (or $x < 0$) in the phase plane of (4.5a) (or (4.5b)) respectively. In the present more general

case $V_{\Sigma_+} = V^+_{Y_+Q_+Y'_+}$ *and* $V_{\Sigma_-} = V^-_{Y_-Q_-Y'_-}$ *need not vanish individually. This splitting of* Σ *into* Σ_+ *and* Σ_- *(for a general* $F(x)$*) is utilized in the proof of the following theorems.*

4.4 New Theorems

We now extend the classical Lienard theorem as follows by removing the odd nature of the function F.

Theorem 4.4.1 *The equation (4.1) has at least one periodic solution if*

- *(i)* f *and* g *are continuous;*
- *(ii)* $g(x)$ *is odd function with* $g(x) > 0$ *for* $x > 0$*;*
- *(iii)* F *has zeroes only at* $x = 0$, $x = a_1$, $x = -a_{-1}$ *for some* $a_1, a_{-1} > 0$;
- *(iv)* $F(x) \to \infty$ $(or\ -\infty)$ *as* $x \to \infty$ $(or\ -\infty)$ *monotonically for* $x > a_1$ $(or\ x < -a_{-1})$.

Remark 4.4.1 *Since* f *is continuous everywhere, so its primitive* F *is differentiable everywhere. Thus,* $F'(0+0) = F'(0-0)$*. Therefore, it follows that* $F'_p(0+0) = F'_n(0+0)$*, i.e.,* F_p *and* F_n *are both simultaneously monotonic increasing or decreasing at the origin.*

Proof. The Lienard equation (4.1) is reduced to the system (4.5). The proof can be achieved through the following steps, the detail deduction of which are analogous to those for the Lienard theorem (for details see [3]) and so omitted.

Step (A) : As Q_+ (or Q_-) moves out of the point $A_1(a_1, 0)$ (or $A_{-1}(a_{-1}, 0)$) along the curve A_1C_+ (or $A_{-1}C_-$), the potential $V^+_{Y_+B_+} + V^+_{B'_+Y'_+}$ $\left(\text{or } V^-_{Y_-B_-} + V^-_{B'_-Y'_-}\right)$ is positive and monotone decreasing.

Step (B) : As Q_+ (or Q_-) moves out of the point $A_1(a_1, 0)$ (or $A_{-1}(a_{-1}, 0)$) along the curve A_1C_+ (or $A_{-1}C_-$), $V^+_{B_+Q_+B'_+}$ $\left(\text{or } V^-_{B_-Q_-B'_-}\right)$ is monotone decreasing.

Step (C) : From (A) and (B) it follows that $V^+_{Y_+Q_+Y'_+} = V^+_{Y_+B_+} + V^+_{B'_+Y'_+} + V^+_{B_+Q_+B'_+}$ $\left(\text{or } V^-_{Y_-Q_-Y'_-} = V^-_{Y_-B_-} + V^-_{B'_-Y'_-} + V^-_{B_-Q_-B'_-}\right)$ is monotone decreasing to the right of the point A_1 (or A_{-1}), (Figure 4.3).

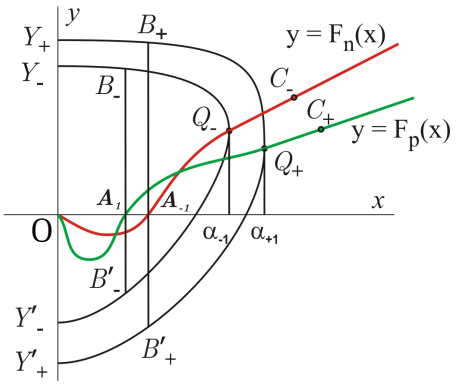

Figure 4.3: Phase path for the system (4.5)

Step (D) : The quantity $V^+_{B_+Q_+B'_+}$ $\left(\text{or } V^-_{B_-Q_-B'_-}\right)$ tends to $-\infty$ as the paths moves away to infinity.

Step (E) : From steps (A) and (B) it follows that the quantity $V^+_{Y_+B_+} + V^+_{B'_+Y'_+}$ $\left(\text{or } V^-_{Y_-B_-} + V^-_{B'_-Y'_-}\right)$ is bounded quantity. Therefore as Q_+ (or Q_-) moves to infinity from the right of A_1 (or A_{-1}) ultimately the quantity $V^+_{B_+Q_+B'_+}$ $\left(\text{or } V^-_{B_-Q_-B'_-}\right)$ dominates and hence $V^+_{Y_+Q_+Y'_+}$ $\left(\text{or } V^-_{Y_-Q_-Y'_-}\right)$ monotonically decreases to $-\infty$ to the right of A_1 (or A_{-1}). In other words, the monotone decreasing nature of $V^+_{B_+Q_+B'_+}$ $\left(\text{or } V^-_{B_-Q_-B'_-}\right)$ is inherited by $V^+_{Y_+Q_+Y'_+}$ $\left(\text{or } V^-_{Y_-Q_-Y'_-}\right)$ as Q_+ (or Q_-) moves out of A_1 (or A_{-1}) along the curve $y = F_p(x)$ (or $y = F_n(x)$).

Step (F) : $V^+_{Y_+Q_+Y'_+} > 0$ $\left(\text{or } V^-_{Y_-Q_-Y'_-} > 0\right)$ when the point Q_+ (or Q_-) is at A_1 (or A_{-1}) or to the left of the point A_1 (or A_{-1}).

It thus follows from (E) and (F) that $V^+_{Y_+Q_+Y'_+}$ $\left(\text{or } V^-_{Y_-Q_-Y'_-}\right)$ is monotone decreasing continuous function which changes its sign from positive to negative as the point Q_+ (or Q_-) moves out of $A_1(a_1, 0)$ (or $A_{-1}(a_{-1}, 0)$) along the curve. As a result, both $V^+_{Y_+Q_+Y'_+}$ and $V^-_{Y_-Q_-Y'_-}$ must vanish once and only once at $x = x_0^+$ and $x = x_0^-$ (say) respectively and remain negative as $x \to \infty$ from either of these points. By continuity, it then also follows that the integrated potential over the full path $V_{Y_+Q_+Q_-Y'_-}$ must also vanish at least once as $x \to \infty$.

Let us make a remark to clarify why $V_{Y_+Q_+Q_-Y'_-}$ vanishes at least once and not exactly once. To answer this question we need to emphasis on the fact that due to asymmetry of the function F the monotonicity of

$V^+_{Y_+Q_+Y'_+} = V^+$ (say) and $V^-_{Y_-Q_-Y'_-} = V^-$ (say) may start for different values of the argument α (c.f. Remark 4.3.1), which varies over x-axis in the Lienard plane. As a result the domain of monotonicity of V^+ and V^- may differ and consequently we may get certain region when $x > \min\{a_1, a_{-1}\}$ in which V^+ is negative and decreasing but V^- is positive and increasing so that $V^+ = -V^- \Rightarrow V^+ + V^- = 0$ holds for the first time as shown in the Figure 4.4. Since the potential V^-

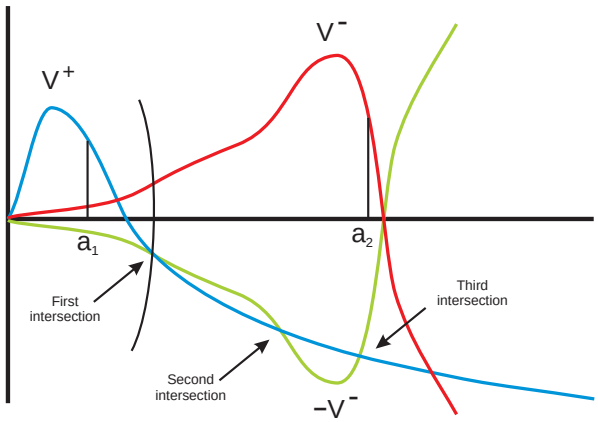

Figure 4.4: Possible intersections of V^+ and V^- for odd number of times.

ultimately decreases, so $-V^-$ ultimately increases. As a result if the curve of $-V^-$ intersects that of V^+ for the second time it must intersect V^+ again for one more time. Thus, after first intersection of the curves of V^+ and $-V^-$, the subsequent intersections of these two curves occur in pairs. Hence V^+ and $-V^-$ can intersect each other odd number of times as $x \to \infty$ when $x > \min\{a_1, a_{-1}\}$. Thus, there is at least one closed path and the proof is complete. ■

Remark 4.4.2 *We define*

$$y_{p+}(0) = OY_+ > 0, \quad y_{p-}(0) = -OY'_+ < 0$$
$$y_{n+}(0) = OY_- > 0, \quad y_{n-}(0) = -OY'_- < 0$$

and consider the positive roots α'_+, α''_+, α'_- *and* α''_- *of the equations*

$$G(\alpha) = \frac{1}{2}y_{p+}^2(0) - \frac{1}{2}F_p^2(\alpha)$$
$$G(\alpha) = \frac{1}{2}y_{p-}^2(0) - \frac{1}{2}F_p^2(\alpha)$$
$$G(\alpha) = \frac{1}{2}y_{n+}^2(0) - \frac{1}{2}F_n^2(\alpha)$$
$$G(\alpha) = \frac{1}{2}y_{n-}^2(0) - \frac{1}{2}F_n^2(\alpha)$$

respectively. Let,

$$\bar{\alpha}_+ = \max\{\alpha'_+, \alpha''_+\}, \ \underline{\alpha}_+ = \min\{\alpha'_+, \alpha''_+\} \tag{4.7}$$
$$\bar{\alpha}_- = \max\{\alpha'_-, \alpha''_-\}, \ \underline{\alpha}_- = \min\{\alpha'_-, \alpha''_-\} \tag{4.8}$$

and

$$\bar{\alpha}_{S1} = \min\{\bar{\alpha}_+, \bar{\alpha}_-\}, \ \underline{\alpha}_{S1} = \min\{\underline{\alpha}_+, \underline{\alpha}_-\} \tag{4.9}$$
$$\bar{\alpha}_{G1} = \max\{\bar{\alpha}_+, \bar{\alpha}_-\}, \ \underline{\alpha}_{G1} = \max\{\underline{\alpha}_+, \underline{\alpha}_-\}. \tag{4.10}$$

By an argument as in [55] *we can conclude that* $V^+_{Y_+Q_+Y'_+}$ $\left(or\ V^-_{Y_-Q_-Y'_-}\right)$ *vanishes when* Q_+ $(or\ Q_-)$ *lies at the point* $(\bar{\alpha}_+, 0)$ $(or\ (\bar{\alpha}_-, 0))$ *or to the left of the point. Since, in the system (4.5) we have* $\dot{x} = y - F_p(x)$ $(or\ \dot{x} = y - F_n(x))$ *so* $\dot{x}$ *changes its sign as the path* $Y_+Q_+Y'_+$ $(or\ Y_-Q_-Y'_-)$ *crosses the curve* $y = F_p(x)$ $(or\ y = F_n(x))$*. Therefore, it follows that*

$$\underline{\alpha}_{S1} = \min\{\underline{\alpha}_+, \underline{\alpha}_-\} = \min\{\alpha'_+, \alpha''_+, \alpha'_-, \alpha''_-\}$$

and

$$\bar{\alpha}_{G1} = \max\{\bar{\alpha}_+, \bar{\alpha}_-\} = \max\{\alpha'_+, \alpha''_+, \alpha'_-, \alpha''_-\}$$

are respectively the lower *and* upper *estimates of the exact amplitude* $\hat{\alpha}$ *of the limit cycle so that* $\underline{\alpha}_{S1} \leq \hat{\alpha} \leq \bar{\alpha}_{G1}$*. This may be considered to be an advantage over our previous estimate of the amplitude of the limit cycle for a symmetric Lienard system. Notice that in the symmetric case* $\alpha'_+ = \alpha'_-$, $\alpha''_+ = \alpha''_-$ *and so* $\bar{\alpha}_+ = \bar{\alpha}_-$*. Ascertaining the relationship between* $\hat{\alpha}$ *and* $\bar{\alpha}_{S1}$*, i.e., if* $\hat{\alpha} \leq \bar{\alpha}_{S1}$ *or* $\bar{\alpha}_{S1} \leq \hat{\alpha}$ *is still an open problem.*

(*c.f. Example 4.5.1, Figure 4.7(d)*).

Remark 4.4.3 *The problem of unique limit cycle is still open. However, in the following example we consider a class of deformed non-symmetric Van der Pol equation admitting one and only one limit cycle.*

Example 4.4.1 *Let us consider the function* $F_p(x) = \mu\left(\frac{\lambda_p x^3}{3} - x\right)$ *and the function* $F_n(x) = \mu\left(\frac{\lambda_n x^3}{3} - x\right)$ *for the system (4.5) with* $\mu = 1$ *and* $g(x) = x$. *If we take* $\lambda_p = \lambda_n = 1$ *then we get the Van der Pol equation. However, if we take* λ_p *and* λ_n *in such a manner that the function* F *becomes non-symmetric then we get a new equation. Let us call it a* ***deformed Van der Pol equation****. The values of* $y_{p+}(0)$, $y_{p-}(0)$, $y_{n+}(0)$, $y_{n-}(0)$ *along with* $\bar{\alpha}_{S1}$ *and* $\bar{\alpha}_{G1}$ *are given in the Table 4.1 for different values of* λ_p *and* λ_n *with* $\mu = 1$. *Here* $y_{p+}(0)$ *and* $y_{p-}(0)$ *are used as initial conditions for the limit cycle solution of the systems (4.5a) and (4.5b) respectively.*

For the Van der Pol equation $\lambda_p = \lambda_n = 1$ *and we have* $\bar{\alpha}_{S1} = \bar{\alpha}_{G1} = 2.0327736318429275$ *is an upper estimate of the amplitude of the limit cycle. As noted already in* [55] *this happens to be a much better estimate of the Van der Pol amplitude in comparison to those available in the literature* [52, 53, 67]. *Clearly, our estimate is quite close to the exact value of the amplitude. Moreover, it transpires that the estimate* $\bar{\alpha}_{S1}$ *is closer to the actual amplitude of the symmetric Van der Pol equation. If on the other hand we consider the functions* F_p *and* F_n *with nonlinearity parameter* μ ***sufficiently small*** *we expect that any limit cycle of system (4.5) or the system (4.2) will be close to the solution of the same system with* $\mu = 0$ *and approach to it as* $\mu \to 0$. *Without any loss of generality, the general solution of the system (4.2) with* $\mu = 0$ *is written as*

$$x = r\cos t$$

and then

$$y = \dot{x} = -r\sin t$$

which generate circular paths in phase plane. Since for sufficiently small μ *we expect that any limit cycle of system (4.2) will approach the above*

λ_p	1.02	1.04	1.06
λ_n	0.98	0.96	0.94
$y_{p+}(0) = -y_{n-}(0)$	2.193478695	2.21481198	2.236740625
$y_{n+}(0) = -y_{p-}(0)$	2.1524918885	2.132789532	2.113584485
α'_+	2.0329457261190154	2.032806950683748	2.0324218480280547
α''_+	2.013325874544811	1.994408426015775	1.9759975761321324
α'_-	2.0322161536454377	2.031185439877457	2.0295787875286386
α''_-	2.052777479244506	2.07336427136114	2.0945632942167314
$\bar{\alpha}_+$	2.0329457261190154	2.032806950683748	2.0324218480280547
$\bar{\alpha}_-$	2.052777479244506	2.07336427136114	2.0945632942167314
$\bar{\alpha}_{S1}$	2.0329457261190154	2.032806950683748	2.0324218480280547
$\bar{\alpha}_{G1}$	2.052777479244506	2.07336427136114	2.0945632942167314

λ_p	1.08	1.1
λ_n	0.92	0.9
$y_{p+}(0) = -y_{n-}(0)$	2.25929348	2.2825016
$y_{n+}(0) = -y_{p-}(0)$	2.09485594	2.076584397
α'_+	2.031846119344476	2.0311282977516116
α''_+	1.958071002088851	1.9406077845053018
α'_-	2.0272748520378485	2.0241298592842316
α''_-	2.116405787425522	2.1389253649204987
$\bar{\alpha}_+$	2.031846119344476	2.0311282977516116
$\bar{\alpha}_-$	2.116405787425522	2.1389253649204987
$\bar{\alpha}_{S1}$	2.031846119344476	2.0311282977516116
$\bar{\alpha}_{G1}$	2.116405787425522	2.1389253649204987

Table 4.1: Computed values of different parameters corresponding to the system (4.5) with $\mu = 1$ and $g(x) = x$ for different values of λ_p and λ_n.

solution as $\mu \to 0$, *so* $\exists$ *some value of* r *for which*

$$x(t) \approx r\cos t,\ \ y(t) \approx -r\sin t \tag{4.11}$$

on the limit cycle and the period T *is close to* 2π *i.e.,*

$$T \approx 2\pi. \tag{4.12}$$

Now, Equation (2.9) gives

$$\mathcal{E}(t) = v(x(t), y(t)) = \int_0^x g(u)\,du + \frac{1}{2}y^2 = \frac{1}{2}x^2(t) + \frac{1}{2}y^2(t)$$

which is nothing but the energy function of the system (4.2). It follows from (4.2)

$$\frac{d\mathcal{E}}{dt} = y\cdot\dot{y} + x\cdot\dot{x} = y(-x) + x(y - F(x)) = -xF(x)$$

By the energy balance method [3] *the change in total energy over one*

period of a limit cycle must vanish so that

$$\mathcal{E}(T) - \mathcal{E}(0) = \int_0^T \frac{d\mathcal{E}}{dt} = 0$$
$$\Rightarrow -\int_0^T x(t) F(x(t)) dt = 0.$$

Using the approximations (4.11) and (4.12), one finally obtains

$$\int_0^{2\pi} r\cos t \cdot F(r\cos t)\, dt = 0$$
$$\Rightarrow \int_0^{\frac{\pi}{2}} r\cos t \cdot F_p(r\cos t)\, dt + \int_{\frac{\pi}{2}}^{\frac{3\pi}{2}} r\cos t \cdot F_n(r\cos t)\, dt + \int_{\frac{3\pi}{2}}^{2\pi} r\cos t \cdot F_p(r\cos t)\, dt = 0$$
$$\Rightarrow \mu\left(\tfrac{1}{16}\pi r^2\left(r^2\lambda_p - 4\right)\right) + \mu\left(\tfrac{1}{8}\pi r^2\left(r^2\lambda_n - 4\right)\right) + \mu\left(\tfrac{1}{16}\pi r^2\left(r^2\lambda_p - 4\right)\right) = 0$$
$$\Rightarrow r^2(\lambda_p + \lambda_n) = 8.$$

Since amplitude is a positive quantity, so we have

$$r = \sqrt{\frac{8}{\lambda_p + \lambda_n}} = 2\sqrt{\frac{2}{\lambda_p + \lambda_n}}. \tag{4.13}$$

We now compute the values of $\bar{\alpha}_{S1}$ and $\bar{\alpha}_{G1}$ for different values of $\mu \approx 0$, λ_p and λ_n in the Table 4.2 and compare them with the perturbative values of r obtained from (4.13).

$\mu = 0.02$			
λ_p	1.5	1.4	1.3
λ_n	0.5	0.6	0.7
$y_{p+}(0) = -y_{n-}(0)$	2.0159185	2.0127257	2.0095448
$y_{n+}(0) = -y_{p-}(0)$	1.98450657	1.98759717	1.99069878
$\bar{\alpha}_{S1}$	2.0154899850306016	2.012406992632671	2.009319051135225
$\underline{\alpha}_{S1}$	1.9841344652092088	1.9873146915393793	1.990494191786599
$\bar{\alpha}_{G1}$	2.0158765138438426	2.0127111990491855	2.009543460158207
$\underline{\alpha}_{G1}$	1.984459698576056	1.9875796554113698	1.9906965207333664

λ_p	1.2	1.1
λ_n	0.8	0.9
$y_{p+}(0) = -y_{n-}(0)$	2.0063746	2.003212
$y_{n+}(0) = -y_{p-}(0)$	1.9938110155	1.996930448
$\bar{\alpha}_{S1}$	2.0062253140125708	2.003123032379586
$\underline{\alpha}_{S1}$	1.9936722718384052	1.9968451909296463
$\bar{\alpha}_{G1}$	2.0063724337047733	2.0031953536274405
$\underline{\alpha}_{G1}$	1.993809576425588	1.996915058213116

$\mu = 0.01$			
λ_p	1.5	1.4	1.3
λ_n	0.5	0.6	0.7
$y_{p+}(0) = -y_{n-}(0)$	2.00790308	2.006321	2.004733
$y_{n+}(0) = -y_{p-}(0)$	1.99219571	1.993753892	1.99530803
$\bar{\alpha}_{S1}$	2.0077995300848532	2.0062436126056222	2.0046778971897528
$\underline{\alpha}_{S1}$	1.9920992242115783	1.9936810405617162	1.9952555756028734
$\bar{\alpha}_{G1}$	2.0078922751285107	2.0063171879078263	2.0047326116475053
$\underline{\alpha}_{G1}$	1.992184294317276	1.9937497029474607	1.9953075264993791

λ_p	1.2	1.1
λ_n	0.8	0.9
$y_{p+}(0) = -y_{n-}(0)$	2.00316	2.001584
$y_{n+}(0) = -y_{p-}(0)$	1.99687719	1.99844259
$\bar{\alpha}_{S1}$	2.0031233405233038	2.001561990739505
$\underline{\alpha}_{S1}$	1.996841849543573	1.998421044881503
$\bar{\alpha}_{G1}$	2.003159508672354	2.0015799205582305
$\underline{\alpha}_{G1}$	1.9968767894582675	1.9984386676322419

Table 4.2: Computed values of different parameters corresponding to the system (4.5) with $\mu \approx 0$ and $g(x) = x$ for different values of λ_p and λ_n such that $\lambda_p + \lambda_n = 2$.

In Table 4.2, $\lambda_p + \lambda_n = 2$ for all the cases. We see that $\bar{\alpha}_{S1} \to 2 + 0$, $\bar{\alpha}_{G1} \to 2 + 0$ and $\underline{\alpha}_{S1} \to 2 - 0$, $\underline{\alpha}_{G1} \to 2 - 0$ as $\lambda_p - \lambda_n \to 0$ and $\mu \to 0$ corresponding to the case of symmetric Van der Pol equation with the amplitude $\hat{\alpha} = r = 2$ given by (4.13). This clearly justifies the fact that the results obtained by our formulation is very close to results obtained by energy balance method establishing the efficiency of the new formulation at least when $\mu \to 0$. Estimates of the amplitudes for symmetric and non-symmetric Van der Pol equations following our approach when the nonlinearity parameter $\mu \to \infty$ is still under investigation and will

be reported elsewhere. We remark that the values of the parameters in Table 4.1 correspond to a non-perturbative value of μ*, i.e.* $\mu = 1$ *and those of Table 4.2 correspond to the perturbative region* $\mu \to 0$. Finally, this example presents us a non-symmetric model having unique limit cycle at the level of perturbative analysis i.e., when μ is small i.e., $\mu << 1$. However, an important fact to notice is that this class of deformed non-symmetric Van der Pol equation is still quite robust because the non-symmetric parameters λ_p and λ_n are of order $O(1)$.

Remark 4.4.4 *When the functions* F_p *and* F_n*, on the other hand, become monotone decreasing for* $x > \bar{\alpha}_+$ *and* $x > \bar{\alpha}_-$ *respectively (and thus violating the condition (iv) of Theorem 4.4.1) then the quantities* $V^+_{Y_+Q_+Y'_+}$ *and* $V^-_{Y_-Q_-Y'_-}$ *can change their signs again from negative to positive and then we may get at least one more limit cycle surrounding the previous limit cycles. A result for the existence of such limit cycles have been proved in Theorem 4.4.2 in which we need the existence of second roots* a_2 *and* a_{-2} *of the functions* F_p *and* F_n *respectively satisfying the inequalities* $a_1 < \bar{\alpha}_+ < a_2$ *and* $a_{-1} < \bar{\alpha}_- < a_{-2}$*. The relative positions of* $\bar{\alpha}_+$ *and* $\bar{\alpha}_-$ *may be classified in the following four distinct cases, each having several subcases.*

Case 1 :	$a_{-1} < a_1$ *and* $a_2 < a_{-2}$
Case 2 :	$a_1 < a_{-1}$ *and* $a_{-2} < a_2$
Case 3 :	$a_1 < a_{-1}$ *and* $a_2 < a_{-2}$
Case 4 :	$a_{-1} < a_1$ *and* $a_{-2} < a_2$

In case 1 *we have* $a_{-1} < a_1 < \bar{\alpha}_+ < a_2 < a_{-2}$*. Now,* $\bar{\alpha}_-$ *may be placed in either of the four subintervals* (a_2, a_{-2}), $(\bar{\alpha}_+, a_2)$, $(a_1, \bar{\alpha}_+)$ *or* (a_{-1}, a_1) *leading to the four subcases* $1.1 - 1.4$.

Case 1.1 :	$a_{-1} < a_1 < \bar{\alpha}_+ < a_2 < \bar{\alpha}_- < a_{-2}$
Case 1.2 :	$a_{-1} < a_1 < \bar{\alpha}_+ < \bar{\alpha}_- < a_2 < a_{-2}$
Case 1.3 :	$a_{-1} < a_1 < \bar{\alpha}_- < \bar{\alpha}_+ < a_2 < a_{-2}$
Case 1.4 :	$a_{-1} < \bar{\alpha}_- < a_1 < \bar{\alpha}_+ < a_2 < a_{-2}$

Similarly, cases $2, 3, 4$ *can be classified in the following several subcases.*

Case 2.1 :	$a_1 < a_{-1} < \bar{\alpha}_- < a_{-2} < \bar{\alpha}_+ < a_2$
Case 2.2 :	$a_1 < a_{-1} < \bar{\alpha}_- < \bar{\alpha}_+ < a_{-2} < a_2$
Case 2.3 :	$a_1 < a_{-1} < \bar{\alpha}_+ < \bar{\alpha}_- < a_{-2} < a_2$
Case 2.4 :	$a_1 < \bar{\alpha}_+ < a_{-1} < \bar{\alpha}_- < a_{-2} < a_2$
Case 3.1 :	$a_1 < a_{-1} < \bar{\alpha}_+ < a_2 < \bar{\alpha}_- < a_{-2}$
Case 3.2 :	$a_1 < a_{-1} < \bar{\alpha}_+ < \bar{\alpha}_- < a_2 < a_{-2}$
Case 3.3 :	$a_1 < a_{-1} < \bar{\alpha}_- < \bar{\alpha}_+ < a_2 < a_{-2}$
Case 3.4 :	$a_1 < \bar{\alpha}_+ < a_{-1} < a_2 < \bar{\alpha}_- < a_{-2}$
Case 3.5 :	$a_1 < \bar{\alpha}_+ < a_{-1} < \bar{\alpha}_- < a_2 < a_{-2}$
Case 3.6 :	$a_1 < \bar{\alpha}_+ < a_2 < a_{-1} < \bar{\alpha}_- < a_{-2}$
Case 4.1 :	$a_{-1} < a_1 < \bar{\alpha}_- < a_{-2} < \bar{\alpha}_+ < a_2$
Case 4.2 :	$a_{-1} < a_1 < \bar{\alpha}_- < \bar{\alpha}_+ < a_{-2} < a_2$
Case 4.3 :	$a_{-1} < a_1 < \bar{\alpha}_+ < \bar{\alpha}_- < a_{-2} < a_2$
Case 4.4 :	$a_{-1} < \bar{\alpha}_- < a_1 < a_{-2} < \bar{\alpha}_+ < a_2$
Case 4.5 :	$a_{-1} < \bar{\alpha}_- < a_1 < \bar{\alpha}_+ < a_{-2} < a_2$
Case 4.6 :	$a_{-1} < \bar{\alpha}_- < a_{-2} < a_1 < \bar{\alpha}_+ < a_2$

If we consider Case 1.1 *in which* $a_{-1} < a_1 < \bar{\alpha}_+ < a_2 < \bar{\alpha}_- < a_{-2}$ *it is quite possible that* $V^+_{Y_+Q_+Y'_+} > 0$ *and* $V^-_{Y_-Q_-Y'_-} < 0$ *but* $V^+_{Y_+Q_+Y'_+} + V^-_{Y_-Q_-Y'_-} = 0$, *at certain point in the interval* (a_{-1}, a_1) (*see Figure 4.5(a)*) *and in that case by Theorem 4.4.1 we will have a limit cycle*

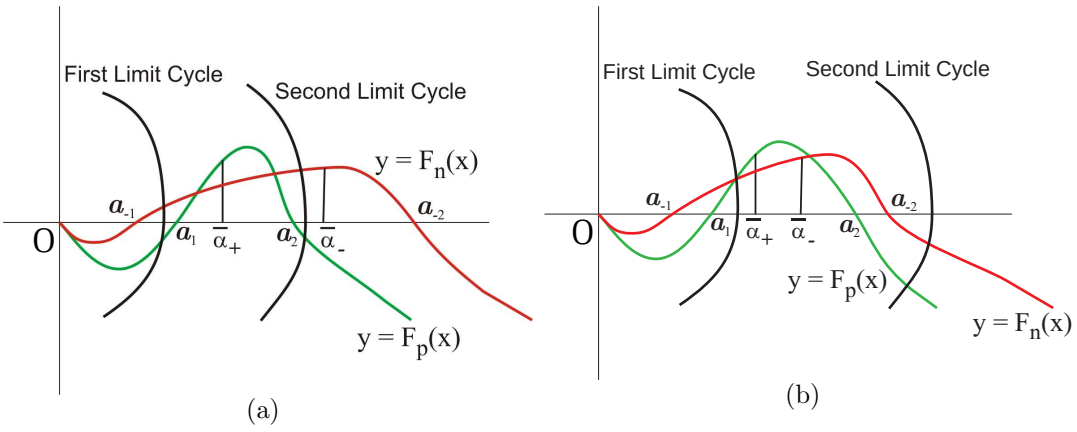

Figure 4.5: (*a*) A possible relative positions of limit cycles in Case 1.1.
(*b*) A possible relative positions of limit cycles expected in Theorem 4.4.2.

passing through the interval (a_{-1}, a_1) *on the* x*-axis. Next,* $V^+_{Y_+Q_+Y'_+}$ *and* $V^-_{Y_-Q_-Y'_-}$ *both become negative at the points right to the point* $(a_1, 0)$. *If further, the function* F_p *becomes monotone decreasing, then in the*

Theorem 4.4.2 it is shown that $V^{+}_{Y_+Q_+Y'_+}$ *again changes its sign from positive to negative and as a result it may so happen that* $V^{+}_{Y_+Q_+Y'_+} < 0$ *and* $V^{-}_{Y_-Q_-Y'_-} > 0$ *but* $V^{+}_{Y_+Q_+Y'_+} + V^{-}_{Y_-Q_-Y'_-}$ *vanishes again on a point situated at the left to the point* $(\bar{\alpha}_-, 0)$*. In that case we will have one more limit cycle passing through the interval* $(a_2, \bar{\alpha}_-)$ *(c.f. Figure 4.5(a)). However, we don't consider such a possibility here.* Instead, we restrict to the class of functions F_p and F_n so that a second class of limit cycles might arise at the right of the point $(\bar{\alpha}_-, 0)$. *The reason for this choice is that the existence of the second class of limit cycles could be proved easily with a minimal modification of the methods of* [55]*. As a consequence, the present study is limited to the following eight cases*

Case 1.2*, Case* 1.3*, Case* 2.2*, Case* 2.3
Case 3.2*, Case* 3.3*, Case* 4.2*, Case* 4.3

which can be represented more succinctly as

$$\max\{a_{-1}, a_1\} < \bar{\alpha}_{S1} \leq \bar{\alpha}_{G1} < \min\{a_{-2}, a_2\}\,.$$

Keeping this condition in mind we construct the condition (iv) *in Theorem 4.4.2 and expect the second class of limit cycles around the origin in a position as shown in Figure 4.5(b). This condition also helps us to keep the previous group of limit cycles in such a manner that they pass through the interval* $(\underline{\alpha}_{S1}, \bar{\alpha}_{G1})$ *and remain separate from the second group of limit cycles confirmed by Theorem 4.4.2 below. Although this condition does not always ensure the exactness of the number of limit cycles, but it helps us to ascertain a number of the limit cycles along with lower and upper estimates of their amplitudes. The study of the remaining cases will be taken up separately.*

We now extend Theorem 4.4.1 for the existence of at least two limit cycles.

Theorem 4.4.2 *Let* f *and* g *be two functions satisfying the following properties.*

(*i*) *f and g are continuous;*

(*ii*) *g is odd function and $g(x) > 0$ for $x > 0$.;*

(*iii*) *F has zeroes only at $x = 0$, $x = a_i$, $x = -a_{-i}$ for $a_i, a_{-i} > 0$, $i = 1, 2$. Moreover, $\exists\ \bar{\alpha}_+$, $\bar{\alpha}_-$ satisfying $a_2 > \bar{\alpha}_+$ and $a_{-2} > \bar{\alpha}_-$ and defined by (4.7) & (4.8).*

(*iv*) *Further, $\max\{a_1, a_{-1}\} < \bar{\alpha}_{S1} \leq \bar{\alpha}_{G1} < \min\{L_1, L_{-1}\}$, where L_1 & L_{-1} are the first local maxima of $F_p(x)$ and $F_n(x)$ from origin in $[a_1, a_2]$ and $[a_{-1}, a_{-2}]$ respectively, $\bar{\alpha}_{S1}$ & $\bar{\alpha}_{G1}$ being defined by (4.9) & (4.10) respectively ;*

(*v*) *F_p and F_n are monotonic increasing in $a_1 < x \leq \bar{\alpha}_{G1}$ & $a_{-1} < x \leq \bar{\alpha}_{G1}$ respectively and $F_p(x)$ & $F_n(x) \to -\infty$ as $x \to \infty$ monotonically for $x > a_2$ & $x > a_{-2}$ respectively;*

Then the equation (4.1) has at least two limit cycles around the origin.

Proof. The slope of a phase path of the system (4.5a) is given by

$$\frac{dy}{dx} = \frac{-g(x)}{y - F_p(x)}. \tag{4.14}$$

Thus, a phase path is horizontal if $\dfrac{dy}{dx} = 0$, i.e. if $g(x) = 0$, i.e. if $x = 0$ (by (ii) above). Similarly, a phase path is vertical on the curve $y = F_p(x)$. Above the curve $y = F_p(x)$ we have $\dot{x} > 0$ and below $\dot{x} < 0$. Moreover, $\dot{y} < 0$ for $x > 0$ and $\dot{y} > 0$ for $x < 0$. We get similar observations for the system (4.5b).

By observations in Section 4.3 the existence of at least one inner limit cycle is ensured. We shall prove the existence of at least one more limit cycle by showing that $V^+_{Y_+Q_+Y'_+} + V^-_{Y_-Q_-Y'_-}$ vanishes at least once more in the interval $x > \bar{\alpha}_{G1}$. Now,

$$V^+_{Y_+Q_+Y'_+} = V^+_{Y_+X_+} + V^+_{X_+B_+} + V^+_{B_+Q_+B'_+} + V^+_{B'_+X'_+} + V^+_{X'_+Y'_+} \tag{4.15}$$

where, $X_+X'_+$ is a line parallel to y-axis passing through the point $A_1(a_1, 0)$ where the function F changes its sign from negative to positive and $B_+B'_+$ is a line parallel to y-axis passing through the point $A_2(a_2, 0)$ where the function F changes its sign from positive to negative. The proof is carried out in brief through the steps (A) to (F) below. The detail calculations are analogous to those in [55] and so are omitted to

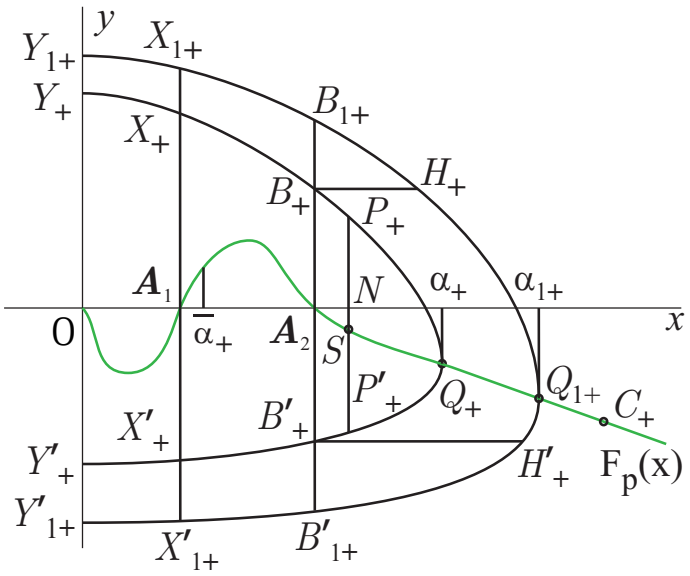

Figure 4.6:

avoid repetitions. Here we refer to the Figure 4.6.

Step (A) : As Q_+ moves out from A_2 along A_2C_+, $V^+_{Y_+X_+} + V^+_{X'_+Y'_+}$ is positive and monotonic decreasing.

Step (B) : As Q_+ moves out from A_2 along A_2C_+, $V^+_{X_+B_+} + V^+_{B'_+X'_+}$ is negative and monotonic increasing.

Step (C) : As Q_+ moves out from A_2 along A_2C_+, $V^+_{B_+Q_+B'_+}$ is positive and monotonic increasing and tends to $+\infty$ as the path recedes to infinity.

Step (D) :

From steps (A) and (B) it follows that the quantities $V^+_{Y_+X_+} + V^+_{X'_+Y'_+}$ and $V^+_{X_+B_+} + V^+_{B'_+X'_+}$ are bounded quantities. Thus by (4.15) and by step (C) it follows that $V^+_{Y_+Q_+Y'_+}$ is monotonic increasing to $+\infty$ to the right of A_2.

Step (E) :

By the construction of $\bar{\alpha}_+$ it is clear that $V^+_{Y_+Q_+Y'_+} < 0$ in $\bar{\alpha}_+ \leq x < a_2$ i.e., to the left of A_2. Again from step (D) we conclude that $V^+_{Y_+Q_+Y'_+}$ ultimately becomes positive as Q_+ moves out of A_2 along the curve of $F_p(x)$. Therefore, by the same reason given in conclusion of the Theorem 4.4.1, it follows that there is one and only one path in the region $x > \bar{\alpha}_+$ such that

$$V^+_{Y_+Q_+Y'_+} = 0.$$

We get a similar result for the system (4.5b) and prove that $V^{-}_{Y_-Q_-Y'_-} = 0$ once and only once in the region $x > \bar{\alpha}_-$. Therefore, we can conclude, again by continuity, that $V^{+}_{Y_+Q_+Y'_+} + V^{-}_{Y_-Q_-Y'_-}$ vanishes *at least* once in the interval $x > \bar{\alpha}_{G1}$.

Step (F) :

By the construction of $\bar{\alpha}_{G1}$ and by step (E) it is clear that equation (4.1) has at least two limit cycles around the origin, the second group of limit cycles surround the first one. This completes the proof of the theorem. ■

The existence of at least N limit cycles can now be established by a straight forward extension of the above proof (See [56] for an equivalent theorem when $F(x)$ is odd). We state the theorem as follows without its proof.

Theorem 4.4.3 *Let f and g be two functions satisfying the following properties.*

- (i) *f and g are continuous;*
- (ii) *g is odd function and $g(x) > 0$ for $x > 0$;*
- (iii) *F has $2N+1$ zeroes at $x = 0$, $x = a_i$, $x = -a_{-i}$, $i = 1, 2, ..., N$ where $0 < a_1 < a_2 < ... < a_N$, $0 < a_{-1} < a_{-2} < ... < a_{-N}$ such that in each intervals $I_i = [a_i, a_{i+1}]$ and $J_i = [a_{-i}, a_{-i-1}]$, $i = 1, 2, \ldots N-1$, there exists $\bar{\alpha}_{+i}, \bar{\alpha}_{-i}$ satisfying properties given by (4.7) & (4.8) for which*
$$\max\{a_i, a_{-i}\} < \bar{\alpha}_{Si} \leq \bar{\alpha}_{Gi} < \min\{L_i, L_{-i}\},$$
where $\bar{\alpha}_{Si} = \min\{\bar{\alpha}_{-i}, \bar{\alpha}_{+i}\}$ and $\bar{\alpha}_{Gi} = \max\{\bar{\alpha}_{-i}, \bar{\alpha}_{+i}\}$ and L_i, L_{-i} are the unique extremum of F_p & F_n in I_i and J_i respectively, $i = 1, 2, \ldots, N-2$ and L_{N-1} & L_{-N+1} are the first local extremum of F_p & F_n in I_{N-1} and J_{N-1} respectively;
- (iv) *F_p and F_n are monotonic increasing in $a_1 < x \leq \bar{\alpha}_{G1}$ & $a_{-1} < x \leq \bar{\alpha}_{G1}$ respectively and $F_p(x)$ & $F_n(x) \to -\infty$ as $x \to \infty$ monotonically for $x > a_2$ & $x > a_{-2}$ respectively;*

Then the equation (4.1) has at least N limit cycles around the origin.

4.5 Examples

Example 4.5.1 *Let us consider the system (4.2) with* $g(x) = x$ *and*

$$F_p(x) = \begin{cases} 0.06 - 0.075\sqrt{1 - \left(\frac{x - 0.075}{0.125}\right)^2}, & 0 \le x < 0.15; \\ -0.072 + 0.09\sqrt{1 - \left(\frac{x - 0.24}{0.15}\right)^2}, & 0.15 \le x < 0.33; \\ 0.0027242514970059716 - 0.014565337147451757\sqrt{1 - \left(\frac{x - 0.497}{0.17}\right)^2}, & 0.33 \le x < 0.4; \\ -0.008913399920006166 - 0.01624207423758168\,(x - 0.4), & x \ge 0.4; \end{cases}$$

$$F_n(x) = \begin{cases} 0.0384 - 0.048\sqrt{1 - \left(\frac{x - 0.048}{0.08}\right)^2}, & 0 \le x < 0.096; \\ -0.06 + 0.075\sqrt{1 - \left(\frac{x - 0.186}{0.15}\right)^2}, & 0.096 \le x < 0.276; \\ 0.0015379153986609972 - 0.010773623289007252\sqrt{1 - \left(\frac{x - 0.4403}{0.166}\right)^2}, & 0.276 \le x < 0.4; \\ -0.007243734864895105 - 0.04960723806394788\,(x - 0.4), & x \ge 0.4; \end{cases}$$

Here, the function F *is not an odd function and the zeros of* F_p *and* F_n *are*

$$a_0 = 0,\ a_1 = 0.15,\ a_2 = 0.33,\ a_{-1} = 0.096,\ a_{-2} = 0.276$$

and

$$L_1 = 0.24,\ L_{-1} = 0.186.$$

For the first limit cycle we have

$$y_{p+}(0) = -y_{n-}(0) = 0.147417407$$
$$\text{and } y_{n+}(0) = -y_{p-}(0) = 0.16039063131.$$

Therefore,

$$\alpha'_+ = 0.1474125964844939,\ \alpha''_+ = 0.16033411486109234,$$
$$\alpha'_- = 0.1597918435191034,\ \alpha''_- = 0.14689442746154402$$

and so,

$$\max\{a_1, a_{-1}\} < \bar{\alpha}_{S1} = 0.1597918435191034$$
$$< \bar{\alpha}_{G1} = 0.16033411486109234 < \min\{L_1, L_{-1}\}$$

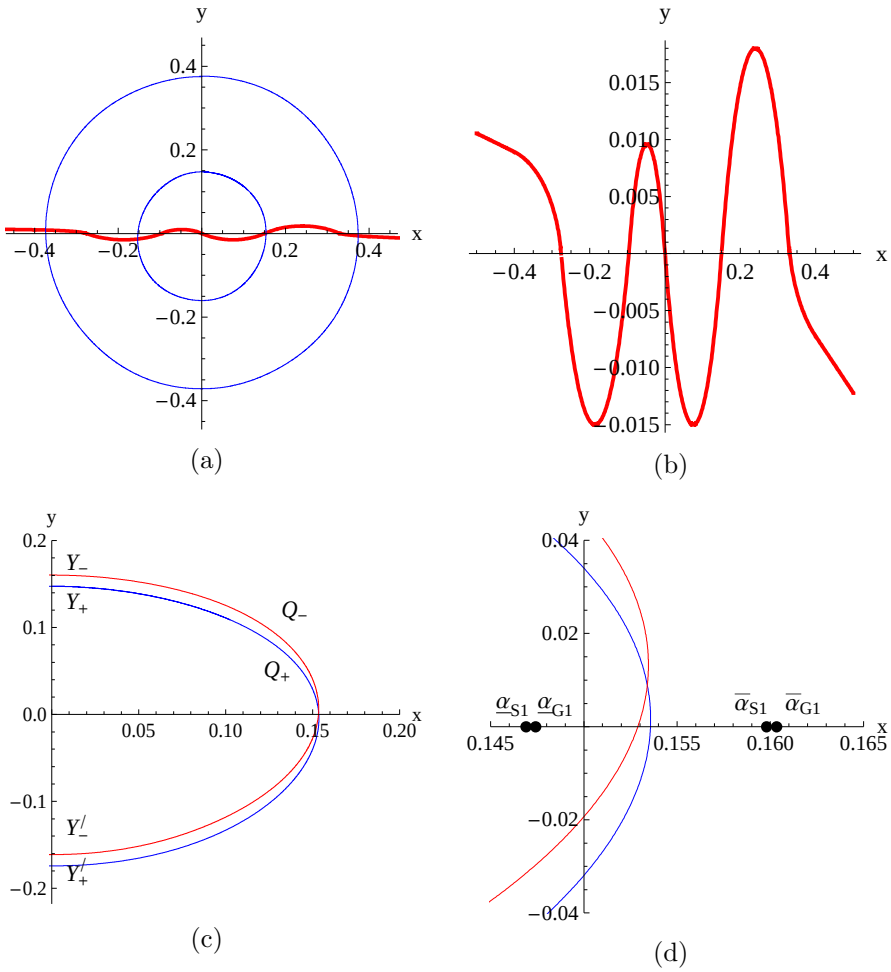

Figure 4.7: (a) Two limit cycles of the system (4.2) in Example 4.5.1
(b) The function F in Example 4.5.1
(c) The segments of the inner limit cycle for the system (4.5) in Example 4.5.1. The assymmetry of the cycles is revealed in the enlarged figure.
(d) The region $\{0.145 \leq x \leq 0.165, \ -0.04 \leq y \leq 0.04\}$ in subfigure (c) is enlarged in this figure.

satisfying Theorem 4.4.2, which ensures the existence of at least two limit cycles for the system (4.2). Numerically, however we get exactly two limit cycles in the present problem. We note that for the second limit cycle

$$y_{p+}(0) = -y_{n-}(0) = 0.375387338$$
$$\text{and } y_{n+}(0) = -y_{p-}(0) = 0.37168865577.$$

The limit cycles are shown in the Subfigure 4.7(a) along with the graph of F in Subfigure 4.7(b). The right half and the left half reflected about

the origin of the inner limit cycle are plotted in the same Subfigure 4.7(c) revealing the asymmetry in the limit cycle. A part of this subfigure is enlarged in Subfigure 4.7(d) along with the positions of $\bar{\alpha}_{S1}$ *and* $\bar{\alpha}_{G1}$*. The inequality* $\underline{\alpha}_{S1} \leq \hat{\alpha} \leq \bar{\alpha}_{S1} \leq \bar{\alpha}_{G1}$ *holds in this case. However, the possibility of* $\underline{\alpha}_{S1} \leq \bar{\alpha}_{S1} \leq \hat{\alpha} \leq \bar{\alpha}_{G1}$ *cannot be ruled out.*

We now present an example in support of Theorem 4.4.3.

Example 4.5.2 *We now consider the system (4.2) with* $g(x) = x$ *and the functions* F_p *and* F_n *are changed in their forth segments defined as*

$$F_p(x) = \begin{cases} 0.06 - 0.075\sqrt{1 - \left(\frac{x - 0.075}{0.125}\right)^2}, & 0 \leq x < 0.15; \\ -0.072 + 0.09\sqrt{1 - \left(\frac{x - 0.24}{0.15}\right)^2}, & 0.15 \leq x < 0.33; \\ 0.0027242514970059716 - 0.014565337147451757\sqrt{1 - \left(\frac{x - 0.497}{0.17}\right)^2}, & 0.33 \leq x < 0.664; \\ 0.45\,(x - 0.664), & x \geq 0.664; \end{cases}$$

$$F_n(x) = \begin{cases} 0.0384 - 0.048\sqrt{1 - \left(\frac{x - 0.048}{0.08}\right)^2}, & 0 \leq x < 0.096; \\ -0.06 + 0.075\sqrt{1 - \left(\frac{x - 0.186}{0.15}\right)^2}, & 0.096 \leq x < 0.276; \\ 0.0015379153986609972 - 0.010773623289007252\sqrt{1 - \left(\frac{x - 0.4403}{0.166}\right)^2}, & 0.276 \leq x < 0.6046; \\ 0.45\,(x - 0.6046), & x \geq 0.6046; \end{cases}.$$

Clearly, the function F *is not odd. Here the zeros of* F_p *and* F_n *are*

$$a_0 = 0,\ a_1 = 0.15,\ a_2 = 0.33,\ a_3 = 0.664,$$
$$a_{-1} = 0.096,\ a_{-2} = 0.276,\ a_{-3} = 0.6046.$$

Here,

$$L_1 = 0.24,\ L_2 = 0.497,\ L_{-1} = 0.186,\ L_{-2} = 0.4403.$$

For the first limit cycle we have

$$y_{p+}(0) = -y_{n-}(0) = 0.147417407$$
$$\text{and } y_{n+}(0) = -y_{p-}(0) = 0.16039063131.$$

which are same as the results in Example 4.5.1. Therefore,

$$\alpha'_+ = 0.1474125964844939,\ \alpha''_+ = 0.16033411486109234,$$
$$\alpha'_- = 0.1597918435191034,\ \alpha''_- = 0.14689442746154402$$

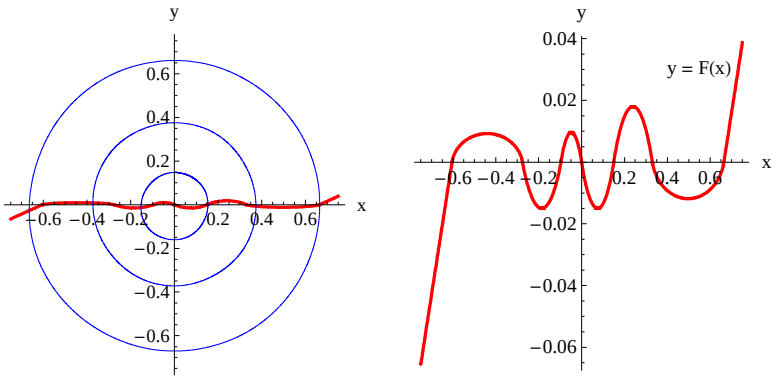

(a) (b)

Figure 4.8: (a) Three limit cycles of the system (4.2) in Example 4.5.2
(b) The function F in Example 4.5.2, plotted with a smaller scale along y-axis in the interval $[-0.06, 0.04]$.

and so,

$$\begin{aligned}\max\{a_1, a_{-1}\} &< \bar{\alpha}_{S1} = 0.1597918435191034 \\ &< \bar{\alpha}_{G1} = 0.16033411486109234 < \min\{L_1, L_{-1}\}\end{aligned}$$

satisfying Theorem 4.4.3.
For the second limit cycle

$$\begin{aligned}y_{p+}(0) &= -y_{n-}(0) = 0.375387338 \\ \text{and } y_{n+}(0) &= -y_{p-}(0) = 0.37168865577,\end{aligned}$$

which are again same as the results in Example 4.5.1. Therefore,

$$\begin{aligned}\alpha'_+ &= 0.3753134681519253,\ \alpha''_+ = 0.37162060806354147, \\ \alpha'_- &= 0.3715966486889184,\ \alpha''_- = 0.37529389613310704\end{aligned}$$

and so,

$$\begin{aligned}\max\{a_2, a_{-2}\} &< \bar{\alpha}_{S2} = 0.37529389613310704 \\ &< \bar{\alpha}_{G2} = 0.3753134681519253 < \min\{L_2, L_{-2}\}\end{aligned}$$

satisfying Theorem 4.4.3. This justifies the existence of at least three limit cycles for the system (4.2). The limit cycles are shown in the Figure 4.8. However, the model again admits exactly three limit cycles, as in Examples 4.4.1 and 4.5.1.

Remark 4.5.1 *If in Example 4.5.2,* L_{+0} *represents the unique local extremum of the function* F_p *in* $(0, a_1)$ *then we have* $L_{+0} = 0.075$ *and* $L_2 = 0.497$*, so that* $|F(L_{+0})| = 0.015 > |F(L_2)| = 0.011841085650445785$ *implying that* β_2 *mentioned in Theorem* 3 *of* [47] *or in Theorem* 7.12*, chapter* 4 *of the book* [51] *does not exist and hence these theorems are not applicable for the corresponding Lienard system showing an advantage of Theorem 4.4.3 over these theorems.*

Remark 4.5.2 *The quantities* $y_{p+}(0) = -y_{n-}(0)$ *and* $y_{n+}(0) = -y_{p-}(0)$ *for the first and second limit cycle around origin in the Examples 4.5.1 and 4.5.2 are same. This is because of the fact that the functions* F_p *and* F_n *in these two examples are same in the common domain* $[0, 0.4]$ *and thereby establishes a previous observation of* [55] *that the amplitude of a limit cycle does not depend on the asymptotic behaviour of the function* F *as* $x \to \infty$*. Moreover, in all the three numerical examples we do get exact number of limit cycles. One may therefore, infer that the above class of non-symmetric problems admit exact number of limit cycles because of the fact that the actual variation in the forms of* F_p *and* F_n *is rather small. However, we are still unable to quantify the degree of their smallness analytically.*

4.6 Concluding Remarks

An extension of the classical Lienard theorem is presented to ensure at least one or multiple limit cycles for a class of non-symmetric Lienard systems when the function $F(x)$ need not be an odd function. Upper and lower estimates of the amplitude of a limit cycle are also computed. A class of non-symmetric deformed Van der Pol equation is studied in detail. An exact formula for the perturbative amplitude is derived for this class of equations. The estimated upper and lower bounds of the amplitudes are shown to agree quite well with the perturbative value. The problem of exactly N limit cycles for the non-symmetric Lienard equation is still open. The example of deformed Van der Pol equation might offer an interesting approach in elucidating a set of sufficient conditions for exact number of limit cycles.

Part II

Approximate Limit Cycle: Amplitude and Shape

Chapter 5

Analytic Approximation of Amplitude of Limit Cycles by Homotopy Analysis Method

5.1 Introduction

We have extended the results available in literature in search of sufficient condition for existence of exactly one or multiple limit cycles in case of symmetric Lienard systems and for existence of at least N limit cycles in case of nonsymmetric Lienard systems in the previous chapters. In the current and subsequent chapter we shall study some results on the characteristics such as size, amplitude etc. of limit cycles in the case of a special class of Lienard systems. Indeed, we shall restrict our study in case of Rayleigh equation

$$\ddot{y} + \varepsilon \left(\frac{1}{3}\dot{y}^3 - \dot{y} \right) + y = 0 \tag{5.1}$$

and Van der Pol (VdP) equation

$$\ddot{x} + \varepsilon \, \dot{x} \left(x^2 - 1 \right) + x = 0, \tag{5.2}$$

which arise very frequently in modeling the dynamics of different nonlinear systems in the fields of Physics, Biology, Acoustics, Robotics, Engineering etc. [10,11]. Here the dots are used to designate the derivative with respect to time t. Many nonlinear systems can be converted to the above systems by suitable transformations. Although a lot of research have been done on these systems using analytical and numerical techniques, determination of analytic formula for shape, size etc.

of limit cycles have been quite a challenging task for a long time, specially in nonperturbative regime. Mostly, perturbation techniques are used based on the existence of small or large parameters. These techniques use perturbation parameters to convert a nonlinear problem into infinite number of linear subproblems. The solution of the original nonlinear problem is then approximated by the solution of first few finite number of these linear subproblems. However, the presence of these parameters in these techniques impose some significant restrictions on the approximate solution in long time scale. As a result the asymptotic phenomena cannot be properly described by perturbative techniques. We know that limit cycle is an isolated closed curve that arise only in nonlinear system. This is an isolated closed curve Γ (say) in the phase plane so that any path in its suitable small neighbourhood starting from a point, specified by some given initial condition, ultimately converges to (or diverge from) Γ in long asymptotic time. As a result perturbation techniques do not give good approximations of different characteristics of limit cycles such as its size, shape etc.

In recent past some new techniques have been introduced such as multiple scale analysis, method of boundary layers, WKB method and so on [1,3] in order to find good, uniformly valid approximate solutions to a nonlinear problem, specially in nonperturbative regime. The recently developed homotopy analysis method (HAM) [18,68] helps us to find good analytic approximation to the exact solution. The aim of this new improved method is to derive in an unified manner uniformly valid asymptotic quantities of interest for a given nonlinear dynamical problem, i.e., the approximate analytic formulae for different asymptotic quantities remains valid uniformly for all values of the perturbative (or nonlinearity) parameters involved in the problem [41].

The Rayleigh and the Van der Pol (VdP) equations represent two closely related nonlinear systems and it is easy to observe that differentiating (5.1) with respect to time t and putting $\dot{y}(t) = x(t)$ we obtain (5.2). Both these systems have unique isolated periodic orbit (limit cycle). The amplitude of a periodic oscillation $y(t)$ (or $x(t)$) is generally defined by $\max|y(t)|$ (or $\max|x(t)|$) over the entire cycle. It is well known that the naive perturbative solutions of these equations are use-

ful when $0 < \varepsilon \ll 1$ and yields the asymptotic value $a(\varepsilon) \approx 2$ of the amplitude for the limit cycle correctly. For $\varepsilon \gg 1$, simple analysis based on singular perturbation theory also yields the asymptotic amplitude for the relaxation oscillation as $a(\varepsilon) \approx 2$ for the VdP equation. However, the conventional perturbative approaches fail when ε is finite. One of the aim of this chapter is to determine efficient approximate formulae for the amplitude of the limit cycle for the Rayleigh systems by HAM. Lopez et al. [18] have reported an efficient formula for the amplitude of the VdP limit cycle by HAM. We note here that a key difference in Rayleigh and VdP oscillators is the fact that with increase in input energy (voltage), the amplitude of the Rayleigh periodic oscillation increases, when that of the VdP oscillator remains almost constant at the value 2, with possible increase in the corresponding frequency only. For large ε (≥ 1) relaxation oscillations, on the other hand, the Rayleigh system shows up a rather fast building up and slow subsequent release of internal energy, when the VdP models the reverse behaviour, with slow rise and fast drop in the accumulated energy.

As remarked above, HAM is formulated to determine the uniformly valid global asymptotic behaviours of relevant dynamical quantities like amplitude, period, frequency etc. related to periodic solutions of these equations for finite values of ε, by devising efficient methods in eliminating divergent secular terms of the naive perturbation theory. HAM seems to have the advantage of yielding uniformly convergent solutions of very high order in the nonlinearity parameter ε utilizing a freedom in the choice of a free parameter h. The computation of higher order term could be facilitated by symbolic computational algorithms. This method is used to obtain good approximate solutions for the VdP equation by a number of authors [18, 69]. Lopez et al. [18] derived efficient formulae for estimating the amplitude of the limit cycle of the VdP equation for all values of $\varepsilon > 0$. Although, HAM is now considered to be an efficient method in the study of non-perturbative asymptotic analysis, it is recently pointed out [19] that this method might fail even in some innocent looking nonlinear problems.

Here we compute an analytic expressions of the amplitude of the periodic solutions of the Rayleigh equation (5.1) as functions of ε. Same

has been already reported by Lopez et al. [18] for the VdP equation (5.2). The HAM contains a control parameter $h = h(\varepsilon)$ which controls the convergence of the approximation to the numerically computed exact value of the amplitude for all values of ε. Suitable choice of h can control the relative percentage error. In the Section 5.2 we have deduced the solution to the Rayleigh equation (5.1) by HAM.

5.2 Computation of Amplitude by HAM

The Homotopy Analysis method proposed by Liao [68, 69] is used to obtain the solution of non-linear equation even if the problem does not contain a small or large parameter. HAM always gives a family of functions at any given order of approximation. An auxiliary parameter h is introduced in HAM to control the convergence region of approximating series involved in this method to the exact solution. HAM is based on the idea of homotopy in topology. In simple language, it involves continuous deformation of the solution of a linear ordinary differential equation (ODE) to that of desired nonlinear ODE. The solution of linear ODE gives a set of functions called *base functions*. One advantage of HAM is that it can be used to approximate a nonlinear problem by efficient choice of different sets of base functions. A suitable choice of the set of base functions and the convergence control parameter can speed up the convergence process.

In this paper we consider the self-excited system (5.1), which can be written as the ODE

$$\ddot{U}(t) + \varepsilon\left(\frac{1}{3}\dot{U}^3(t) - \dot{U}(t)\right) + U(t) = 0, \quad t \geq 0, \tag{5.3}$$

where the dot denotes the derivative with respect to the time t. We know that a limit cycle represents an isolated periodic motion of a self-excited system. We have mentioned earlier that it is an isolated closed curve Γ (say) in the phase plane so that any path in its suitable small neighbourhood starting from a point, specified by some given initial condition, ultimately converges to (or diverge from) Γ. Consequently, this periodic motion represented by limit cycle is independent of initial conditions. It, however, involves the frequency ω and the amplitude a

of the oscillation. Therefore, without loss of generality, we consider an initial condition

$$U(0) = a, \qquad \dot{U}(0) = 0. \tag{5.4}$$

In [31], an alternative initial condition i.e. $U(0) = 0,\ \dot{U}(0) = a$ was considered. Let,

$$\tau = \omega t \text{ and } U(t) = a\ u(\tau)$$

so that (5.3) and (5.4) respectively become

$$\omega^2 u''(\tau) + \varepsilon\left(\frac{1}{3}a^2\omega^2 u'^2(\tau) - 1\right)\omega u'(\tau) + u(\tau) = 0 \tag{5.5}$$

and

$$u(0) = 1, \quad u'(0) = 0. \tag{5.6}$$

Since the limit cycle represents a periodic motion, so we suppose that the initial approximation to the solution $u(\tau)$ to (5.5) can be taken as

$$u_0(\tau) = \cos\tau.$$

Let, ω_0 and a_0 respectively denote the initial approximations of the frequency ω and the amplitude a.

We consider a linear operator

$$\mathcal{L}[\phi(\tau, p)] = \omega_0^2\left[\frac{\partial^2\phi(\tau, p)}{\partial\tau^2} + \phi(\tau, p)\right] \tag{5.7}$$

so that for the coefficients C_1 and C_2

$$\mathcal{L}(C_1\sin\tau + C_2\cos\tau) = 0. \tag{5.8}$$

We further consider a nonlinear operator

$$\begin{aligned}
&\mathcal{N}[\phi(\tau, p), \Omega(p), A(p)] \\
&= \Omega^2(p)\frac{\partial^2\phi(\tau, p)}{\partial\tau^2} \\
&+ \varepsilon\left[\frac{1}{3}A^2(p)\Omega^3(p)\left(\frac{\partial\phi(\tau, p)}{\partial\tau}\right)^3 - \Omega(p)\left(\frac{\partial\phi(\tau, p)}{\partial\tau}\right)\right] + \phi(\tau, p).
\end{aligned} \tag{5.9}$$

Next, we construct a homotopy as

$$\mathcal{H}\left[\phi\left(\tau,p\right),h,p\right]=\left(1-p\right)\mathcal{L}\left[\phi\left(\tau,p\right)-u_{0}\left(\tau\right)\right]\\-h\ p\ \mathcal{N}\left[\phi\left(\tau,p\right),\Omega\left(p\right),A\left(p\right)\right],\tag{5.10}$$

where $p\in[0,1]$ is the embedding parameter and h a non-zero auxiliary (control) parameter used to improve the convergence of series expansions. Setting $\mathcal{H}\left[\phi\left(\tau,p\right),h,p\right]=0$ we obtain zero-th order deformation equation

$$\left(1-p\right)\mathcal{L}\left[\phi\left(\tau,p\right)-u_{0}\left(\tau\right)\right]-h\ p\ \mathcal{N}\left[\phi\left(\tau,p\right),\Omega\left(p\right),A\left(p\right)\right]=0\tag{5.11}$$

subject to the initial conditions

$$\phi\left(0,p\right)=1,\quad\left.\frac{\partial\phi\left(\tau,p\right)}{\partial\tau}\right|_{\tau=0}=0.\tag{5.12}$$

Clearly, as p increases from $p=0$ to $p=1$, (5.11) changes from $\mathcal{L}\left[\phi\left(\tau,p\right)-u_{0}\left(\tau\right)\right]=0$ to $\mathcal{N}\left[\phi\left(\tau,p\right),\Omega\left(p\right),A\left(p\right)\right]=0$ and as a consequence $\phi\left(\tau,p\right)$ varies from the initial guess $\phi\left(\tau,0\right)=u_{0}\left(\tau\right)=\cos\tau$ to the exact solution $\phi\left(\tau,1\right)=u\left(\tau\right)$, so does $\Omega\left(p\right)$ from ω_{0} to exact frequency ω and $A\left(p\right)$ from a_{0} to the exact amplitude a. It can be shown that assuming $\phi\left(\tau,p\right)$, $\Omega\left(p\right)$, $A\left(p\right)$ analytic in $p\in[0,1]$ so that

$$u_{k}\left(\tau\right)=\left.\frac{1}{k!}\ \frac{\partial^{k}}{\partial p^{k}}\phi\left(\tau,p\right)\right|_{p=0},\ \omega_{k}=\left.\frac{1}{k!}\ \frac{\partial^{k}}{\partial p^{k}}\Omega\left(p\right)\right|_{p=0},\ a_{k}=\left.\frac{1}{k!}\ \frac{\partial^{k}}{\partial p^{k}}A\left(p\right)\right|_{p=0}\tag{5.13}$$

we have,

$$u\left(\tau\right)=\sum_{k=0}^{\infty}u_{k}\left(\tau\right),\tag{5.14}$$

$$\omega=\sum_{k=0}^{\infty}\omega_{k},\tag{5.15}$$

$$a=\sum_{k=0}^{\infty}a_{k},\tag{5.16}$$

where $u_{k}\left(\tau\right)$ are solutions of the k-th order deformation equation

$$\mathcal{L}\left[u_{k}\left(\tau\right)-\chi_{k}u_{k-1}\left(\tau\right)\right]=h\ R_{k}\left(\tau\right)\tag{5.17}$$

subject to the initial conditions

$$u_k(0) = 0, \qquad u_k'(0) = 0 \tag{5.18}$$

in which

$$\begin{aligned} R_k(\tau) &= \frac{1}{(k-1)!}\frac{\partial^{k-1}}{\partial p^{k-1}}\mathcal{N}\left[\phi(\tau,p), \Omega(p), A(p)\right]\Big|_{p=0} \\ &= \sum_{n=0}^{k-1} u''_{k-1-n}(\tau)\sum_{j=0}^{n}\omega_j\omega_{n-j} + u_{k-1}(\tau) \\ &+ \frac{\varepsilon}{3}\sum_{n=0}^{k-1}\sum_{i=0}^{n}\left(\sum_{r=0}^{i} a_r a_{i-r}\right)\times\left(\sum_{s=0}^{n-i}\omega_s\sum_{h=0}^{n-i-s}\omega_h\omega_{n-i-s-h}\right) \\ &\times\left(\sum_{j=0}^{k-1-n} u'_j(\tau)\sum_{m=0}^{k-1-n-j} u'_m(\tau)\, u'_{k-1-n-j-m}(\tau)\right) - \varepsilon\sum_{n=0}^{k-1}\omega_n u'_{k-1-n}(\tau) \end{aligned} \tag{5.19}$$

and

$$\chi_k = \begin{cases} 0, & k \le 1, \\ 1, & k > 1. \end{cases} . \tag{5.20}$$

To ensure that the solution to the k-th order deformation equation (5.17) do not contain the secular terms $\tau\sin\tau$ and $\tau\cos\tau$ the coefficients of $\sin\tau$ and $\cos\tau$ in the expressions of R_k in (5.19) must vanish giving successive values of ω_k and a_k.

The linear equation $\mathcal{L}(\phi(\tau,p)) = 0$ represents a simple harmonic motion with frequency 1. So, we choose the initial guess of ω as $\omega_0 = 1$. Again, by perturbation method [3] we find $a \to 2$ as $\varepsilon \to 0$. So, we choose the initial guess of a as $a_0 = 2$. Solving the differential equations given by (5.11), (5.12), (5.17), (5.18) and avoiding the generation of secular terms in each iteration we obtain

$$u_1(\tau) = -\frac{1}{24}h\varepsilon\sin 3\tau + \frac{1}{8}h\varepsilon\sin\tau,\ \omega_1 = -\frac{1}{16}h\varepsilon^2,\ a_1 = \frac{1}{8}h\varepsilon^2,$$

$$\begin{aligned} u_2(\tau) = &\left(\frac{1}{384}h^2\varepsilon^3 - \frac{1}{24}h^2\varepsilon - \frac{1}{24}h\varepsilon\right)\sin 3\tau - \frac{1}{64}h^2\varepsilon^2\cos 3\tau \\ &+ \frac{1}{64}h^2\varepsilon^2\cos\tau + \left(\frac{1}{8}h^2\varepsilon - \frac{1}{128}h^2\varepsilon^3 + \frac{1}{8}h\varepsilon\right)\sin\tau \end{aligned}$$

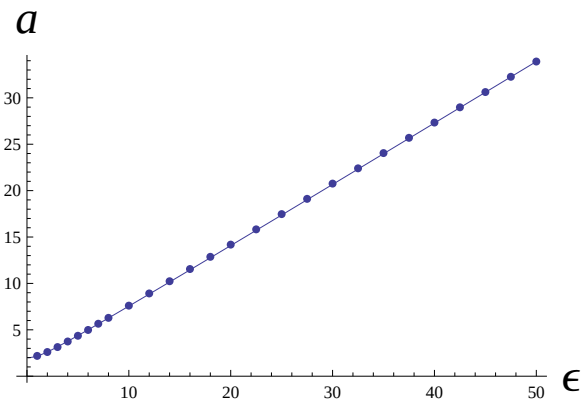

Figure 5.1: The exact amplitude of Rayleigh Equation (by solid line) and its approximation $a_E(\varepsilon)$ given by (5.24) (by bold points) for $0 < \varepsilon \leq 50$.

so that

$$R_1 = \frac{1}{3}\varepsilon \sin 3\tau,$$
$$R_2 = \frac{1}{24}\left[3h\varepsilon^2 \cos 3\tau + \left(8h\varepsilon - \frac{1}{2}h\varepsilon^3\right)\sin 3\tau\right].$$

Computing R_k successively, we can find the successive expressions of $u_k(\tau)$, ω_k and a_k. The first order approximation to the amplitude in (5.16) is

$$a \approx a_0 + a_1 = 2 + \frac{1}{8}h\varepsilon^2 = a_E(\varepsilon) \quad \text{(say)}. \tag{5.21}$$

The above first order expression for the amplitude involves as yet arbitrary control parameter h. Lopez et. al. [18] proposed specific ε-dependent expressions for h to obtain an efficient formula for the VdP limit cycle amplitude. They made the proposal that h, besides being continuous, must also vanish in the limits of $\varepsilon \to 0$ and $\varepsilon \to \infty$ to reproduce the zeroth order perturbative solutions. In our application of HAM for the Rayleigh limit cycle amplitude, we have chosen a different set of base functions and so can weaken the condition considerably, both on the continuity and the asymptotic limit $\varepsilon \to \infty$. From careful inspections of the graph of the exact amplitude (Figure 5.1), it turns

out that an appropriate ansatz for the control parameter h is given by

$$h = \frac{1}{0.5 + \varepsilon\ b(\varepsilon)}, \tag{5.22}$$

where, $b(\varepsilon)$ is taken as the step function in the domain $0 < \varepsilon \leq 50$ as follows:

ε :	$0 < \varepsilon \leq 4$	$4 < \varepsilon \leq 5$	$5 < \varepsilon \leq 7$	$7 < \varepsilon \leq 8$	$8 < \varepsilon \leq 9$
$b(\varepsilon)$:	0.162	0.165	0.168	0.171	0.174
ε :	$9 < \varepsilon \leq 11$	$11 < \varepsilon \leq 15$	$15 < \varepsilon \leq 20$	$20 < \varepsilon \leq 30$	$30 < \varepsilon \leq 50$
$b(\varepsilon)$:	0.176	0.179	0.181	0.183	0.185

With this particular form of h, we are able to find an analytic approximation $a_E(\varepsilon)$ to the numerically computed exact value $a = a(\varepsilon)$ in the domain $0 < \varepsilon \leq 50$ with maximum relative percentage error $\left|\frac{a_E(\varepsilon) - a(\varepsilon)}{a(\varepsilon)} \times 100\right|$ less than 1%. Obviously, better accuracy fit can be obtained by considering finer subdivisions in the definition of $b(\varepsilon)$. We remark that a piece-wise continuous ε dependence of h as above is admissible in the framework of HAM.

Since the exact graph of $a(\varepsilon)$ is almost a straight line for sufficiently large ε $(7 < \varepsilon \leq 50)$, we can reduce the number of steps to 4 only. Let us choose

$$h = \frac{8m}{\varepsilon} - \frac{56m}{\varepsilon^2} + \frac{8c}{\varepsilon^2} - \frac{16}{\varepsilon^2}, \qquad 7 < \varepsilon \leq 50 \tag{5.23}$$

so that (5.21) becomes

$$a_E(\varepsilon) = \begin{cases} 2 + \frac{1}{8}\left(\frac{1}{0.5+0.162\ \varepsilon}\right)\varepsilon^2, & 0 < \varepsilon \leq 4; \\ 2 + \frac{1}{8}\left(\frac{1}{0.5+0.165\ \varepsilon}\right)\varepsilon^2, & 4 < \varepsilon \leq 5; \\ 2 + \frac{1}{8}\left(\frac{1}{0.5+0.168\ \varepsilon}\right)\varepsilon^2, & 5 < \varepsilon \leq 7; \\ m(\varepsilon - 7) + c, & 7 < \varepsilon \leq 50; \end{cases}, \tag{5.24}$$

where m and c are computed from the exact solution as

$$m = \frac{a(50) - a(7)}{50 - 7} = 0.657692 \text{ and } c = a(7) = 5.63108$$

keeping the maximum relative percentage error $\left|\frac{a_E(\varepsilon) - a(\varepsilon)}{a(\varepsilon)} \times 100\right|$ less than 1%. The plot of $a_E(\varepsilon)$ given by (5.24) is shown by bold

points in Figure 5.1 (explicit discontinuities of h at $\varepsilon = 4, 5$ and 7 are not visible at the resolution of the plotted figure) . As remarked above,

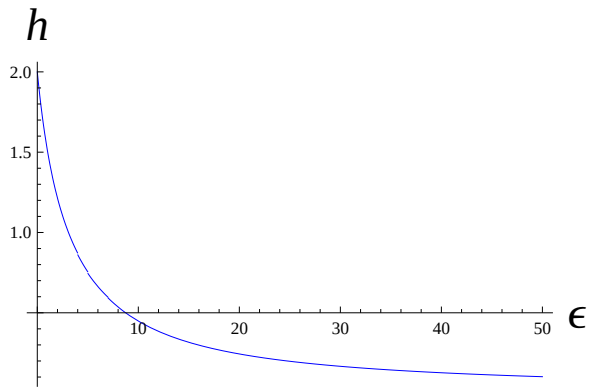

Figure 5.2: The graph of $h(\varepsilon)$ used for approximation of the amplitude by HAM given by (5.24) for $0 < \varepsilon \leq 50$.

Lopez et. al. [18] proposed that a reasonable property for h would be to vanish in the limits as $\varepsilon \to 0$ and $\varepsilon \to \infty$. However, from (5.22) and (5.23) we observe that a suitable approximation to the amplitude of Rayleigh equation can be obtained even if h do not follow this property. The graph of $h(\varepsilon)$ is given in Figure 5.2 for $0 < \varepsilon \leq 50$ (discontinuity in h is not visible at the level of resolution in the figure).

5.3 Concluding Remarks

In Section 5.2 we find that one can obtain more accurate approximate formula by suitable choices of the control parameter $h(\varepsilon)$ upto any desired level of accuracy. We also note that a piecewise continuous control parameter h enables us to obtain good approximation by solving only the first order deformation equation. However, 5.21 shows that the first order HAM estimated amplitude $a(\varepsilon)$ is $O\left(\varepsilon^2\right)$. We do not undertake the computation of the VdP amplitude by HAM separately, as that was already reported by Lopez et al. [18]. We shall use these results in the subsequent chapters and compare them with our newly developed *Improved Renormalization Group Method* for estimation of different characteristics of limit cycles in the context of Rayleigh and Van der Pol equations [41].

Chapter 6

Analytic Approximation of Amplitude of Limit Cycles by Renormalization Group Method

6.1 Introduction

We have discussed Homotopy Analysis Method (HAM) in Chapter 5 by which one can obtain analytic approximation of different characteristics of limit cycles, such as amplitude, frequency etc., for a nonlinear system. We found sufficiently good analytic expression for amplitude of Rayleigh limit cycle as a function of the nonlinearity parameter ε. In this chapter we shall discuss Renormalization Group Method (RGM) which is another useful technique to obtain uniformly valid analytic approximation of different aspects of limit cycles as mentioned above for nonlinear systems. We shall restrict our discussion for the Rayleigh equation

$$\ddot{y} + \varepsilon \left(\frac{1}{3}\dot{y}^3 - \dot{y} \right) + y = 0 \tag{6.1}$$

and the Van der Pol equation

$$\ddot{x} + \varepsilon \, \dot{x} \left(x^2 - 1 \right) + x = 0, \tag{6.2}$$

where the dots are used to designate the derivative with respect to time t. The importance of these two closely related systems are already mentioned in Chapter 5. RGM has wide variety of applications including singular and reductive perturbation problems in a unified way. The objective of RGM is to improve local solution obtained by Neive pertur-

bation technique into a global solution by eliminating divergent secular terms. The RGM was originally formulated for managing divergences in the quantum field theory [70]. Later, this method had seen deep applications [27, 71, 72] in phase transitions and critical phenomena in statistical mechanics. Subsequently, Chen et al. [31, 73] successfully translated the RG formalism into the study of nonlinear differential equations. It is noted that RGM is more efficient and accurate than conventional singular perturbative approaches in obtaining global informations from a naive perturbation series in ε. It is also recognized that RGM generated expansions yield ε-dependent space/time scales naturally, when conventional approaches normally require invoking such scales in an ad hoc manner.

Here we report analytic expressions of the amplitude of the periodic solution of the Rayleigh equation (6.1) as functions of ε. We report here the RG solution upto order 3. To the author's knowledge this seems to be the first higher order computation other than second order computations reported so far by various authors [31, 36]. In this chapter we compute the classical RG solution upto $O(\varepsilon^3)$ order and compare estimated values of the limit cycle amplitude with the exact values. The pertubative RGM, however, appears to have the limitation that the computation of higher order renormalized solutions could be quite involved and tedious. More serious is the inability of assuring the convergence of the renormalized expansions for large nonlinearity parameter. Further, there is still no evidence in the literature that RGM could be employed successfully to asymptotic estimation of the amplitude of an isolated periodic orbit for all values of ε.

6.2 Basic Idea of RGM

The basic idea in RGM is to eliminate the divergent secular term of the form $(t - t_0)\sin t$, where t_0 is the initial time, of the naive perturbation series for the solution of the nonlinear problem, by exploiting the arbitrariness in fixing the initial moment t_0. The original prescription rests on introducing new initial time τ in the form $(t - \tau + \tau - t_0)\sin t$ and to allow the renormalized amplitude $R = R(\tau)$ and phase $\theta = \theta(\tau)$ of

the renormalized solution to depend on the new parameter, viz., $\tau - t_0$ so that the original naive perturbative, constant values of amplitude R_0 and phase θ_0 $(= 0)$ (say) 'flow' following the RG flow equations of the form

$$\frac{dR}{d\tau} = f(R, \varepsilon), \ \frac{d\theta}{d\tau} = g(R, \varepsilon). \tag{6.3}$$

The functions in the right hand sides of the RG flow equations, in general, should depend both on R and θ, besides the explicit ε dependence. We suppress the θ dependence for simplicity that should suffice for our present analysis of the Rayleigh and Van der Pol (VdP) equations (c.f. equations (6.6), (6.7)). The flow equations are derived from the consistency condition that the actual renormalized solution $y(t, \tau)$ should be independent of the arbitrary initial adjustment τ:

$$\frac{\partial y}{\partial \tau} = 0.$$

The final form of the uniformly valid RG solution $y_R(t)$ is obtained by setting $\tau = t$ that eliminates the secular terms. Let us remark here that the actual convergence of the RG expansions is not well addressed and should require further investigations. Moreover, estimation of asymptotic amplitude for a limit cycle as $t \to \infty$, for instance, from the perturbation expansion of f is expected to fail for $\varepsilon > \approx O(1)$.

6.3 Computation of Amplitude by RG Method

The Renormalization Group method (RGM) introduced by Chen, Goldenfeld and Oono (CGO) [31, 73] gives a unified formal approach to derive asymptotic expansions for the solutions of a large class of nonlinear ODEs. The RG method is used in solid state physics [74, 75], quantum field theory [70] and other areas of physics [27, 71, 72]. One advantage of RGM is that it starts from naive perturbation expansion of a problem and is expected to yield automatically the gauge functions such as fractional powers of ε and logarithmic terms in ε in the renormalized expansion. One does not require to have any prior knowledge to prescribe these unexpected gauge functions in an ad hoc manner. DeVille et al. [35] have introduced an algorithmic approach for RGM which we adopt for the following application. As it will transpire the RGM ap-

pears to be deficient in estimating amplitude of a periodic orbit because of the absence of any free control parameter. In Chapter 7 we have improved this RGM to incorporate a control parameter similar to HAM and derive efficient estimations of amplitudes of both the Rayleigh and VdP equations. However, before the introduction of the Improved RG Method (IRGM), we first discuss the *conventional* RG method, given by DeVille et al. and use it to obtain amplitude and phase equations for the Rayleigh equation (6.1). These equations are already obtained in [31,35] to the order $O\left(\varepsilon^3\right)$ which agree with the experimental values as $\varepsilon \to 0$ only. We have extended these results to the order $O\left(\varepsilon^4\right)$ and notice that higher order perturbative computations of the RG flow equations would fail to obtain good estimation of the amplitude of the periodic cycle for all values of ε.

Substituting the naive expansion

$$y(t) = y_0(t) + \varepsilon y_1(t) + \varepsilon^2 y_2(t) + \varepsilon^3 y_3(t) + \cdots$$

in (6.1), we find at each order

$$\begin{aligned}
O(1) &: \ddot{y}_0 + y_0 = 0; \\
O(\varepsilon) &: \ddot{y}_1 + y_1 = \dot{y}_0 - \frac{1}{3}\dot{y}_0^3; \\
O\left(\varepsilon^2\right) &: \ddot{y}_2 + y_2 = \dot{y}_1 - \dot{y}_0^2\dot{y}_1; \\
O\left(\varepsilon^3\right) &: \ddot{y}_3 + y_3 = \dot{y}_2 - \dot{y}_0^2\dot{y}_2 - \dot{y}_1^2\dot{y}_0.
\end{aligned}$$

The solutions are

$y_0(t) = Ae^{i(t-t_0)} + c.c.$;

$y_1(t) = \frac{1}{24}iA^3e^{i(t-t_0)} + \frac{1}{2}A\left(1 - AA^*\right)(t-t_0)\,e^{i(t-t_0)} - \frac{1}{24}iA^3e^{3i(t-t_0)} + c.c$;

$$\begin{aligned}
y_2(t) = {} & \left(\tfrac{1}{32}A^3 - \tfrac{3}{64}A^4A^*\right)e^{i(t-t_0)} \\
& + \begin{pmatrix} -\frac{1}{24}iA^4A^* + \frac{1}{16}iA^3(A^*)^2 + \frac{1}{48}iA^3 \\ +\frac{1}{48}iA^2(A^*)^3 - \frac{1}{8}iA \end{pmatrix}(t-t_0)\,e^{i(t-t_0)} \\
& + \left(\tfrac{3}{8}A^3(A^*)^2 - \tfrac{1}{2}A^2A^* + \tfrac{1}{8}A\right)(t-t_0)^2\,e^{i(t-t_0)} \\
& + \left(\tfrac{3}{64}A^4A^* - \tfrac{1}{32}A^3 + \tfrac{1}{192}A^5\right)e^{3i(t-t_0)}
\end{aligned}$$

$$
\begin{aligned}
&- \tfrac{1}{16} i A^3 \left(1 - A A^*\right) \left(t - t_0\right) e^{3i(t-t_0)} - \tfrac{1}{192} A^5 e^{5i(t-t_0)} + c.c. \ ; \\
y_3\left(t\right) = &\begin{pmatrix} -\frac{1}{384} i A^6 A^* + \frac{37}{1536} i A^5 (A^*)^2 + \frac{1}{2304} i A^5 \\ +\frac{1}{512} i A^4 (A^*)^3 - \frac{7}{256} i A^4 A^* - \frac{1}{128} i A^3 \end{pmatrix} e^{i(t-t_0)} \\
&+ \begin{pmatrix} +\frac{1}{1152} A^6 A^* + \frac{5}{128} A^5 (A^*)^2 - \frac{119}{1152} A^4 (A^*)^3 \\ +\frac{11}{384} A^3 (A^*)^4 - \frac{7}{128} A^4 A^* + \frac{1}{48} A^3 \\ +\frac{11}{64} A^3 (A^*)^2 - \frac{1}{64} A^2 (A^*)^3 \end{pmatrix} \left(t - t_0\right) e^{i(t-t_0)} \\
&+ \begin{pmatrix} +\frac{3}{64} i A^5 (A^*)^2 - \frac{3}{32} i A^4 (A^*)^3 - \frac{1}{24} i A^4 A^* \\ -\frac{1}{32} i A^3 (A^*)^4 + \frac{3}{32} i A^3 (A^*)^2 + \frac{1}{192} i A^3 \\ +\frac{1}{16} i A^2 A^* + \frac{1}{48} i A^2 (A^*)^3 - \frac{1}{16} i A \end{pmatrix} \left(t - t_0\right)^2 e^{i(t-t_0)} \\
&+ \left(-\tfrac{5}{16} A^4 (A^*)^3 + \tfrac{9}{16} A^3 (A^*)^2 - \tfrac{13}{48} A^2 A^* + \tfrac{1}{48} A\right) \left(t - t_0\right)^3 e^{i(t-t_0)} \\
&+ \begin{pmatrix} +\frac{1}{4608} i A^7 + \frac{7}{512} i A^6 A^* - \frac{37}{1536} i A^5 (A^*)^2 \\ -\frac{1}{128} i A^5 - \frac{1}{512} i A^4 (A^*)^3 + \frac{1}{128} i A^3 + \frac{7}{256} i A^4 A^* \end{pmatrix} e^{3i(t-t_0)} \\
&+ \begin{pmatrix} -\frac{1}{96} A^6 A^* - \frac{7}{64} A^5 (A^*)^2 + \frac{1}{128} A^5 \\ +\frac{1}{384} A^4 (A^*)^3 + \frac{21}{128} A^4 A^* - \frac{1}{16} A^3 \end{pmatrix} \left(t - t_0\right) e^{3i(t-t_0)} \\
&+ \left(-\tfrac{5}{64} i A^5 (A^*)^2 + \tfrac{1}{8} i A^4 A^* - \tfrac{3}{64} i A^3\right) \left(t - t_0\right)^2 e^{3i(t-t_0)} \\
&+ \left(\tfrac{17}{2304} i A^5 - \tfrac{17}{1536} i A^6 A^* - \tfrac{5}{4608} i A^7\right) e^{5i(t-t_0)} \\
&+ \left(\tfrac{5}{384} A^6 A^* - \tfrac{5}{384} A^5\right) \left(t - t_0\right) e^{5i(t-t_0)} + \tfrac{1}{1152} i A^7 e^{7i(t-t_0)} + c.c.
\end{aligned}
$$

We choose the homogeneous parts to the solutions y_1, y_2 and y_3 in such a manner that the solutions vanish at the initial time t_0, i.e. $y_1\left(t_0\right) = y_2\left(t_0\right) = y_3\left(t_0\right) = 0$. Next, we renormalize the integration constant A and create a new renormalized quantity $\mathcal{A}$ as

$$
A = \mathcal{A} + a_1 \varepsilon + a_2 \varepsilon^2 + a_3 \varepsilon^3 + O\left(\varepsilon^4\right)
$$

where the coefficients $a_1, a_2, a_3, \ldots$ are chosen to absorb the homogeneous parts of the solutions $y_1, y_2, \ldots$. Choosing

$$a_1 = -\frac{i}{24}\mathcal{A}^3,\ a_2 = -\frac{\mathcal{A}^3}{32}\left(1 - \frac{3}{2}\mathcal{A}\mathcal{A}^* + \frac{1}{6}\mathcal{A}^2\right),$$
$$a_3 = \frac{1}{1152}i\mathcal{A}^7 - \frac{17}{1536}i\mathcal{A}^6\mathcal{A}^* + \frac{17}{2304}i\mathcal{A}^5 - \frac{37}{1536}i\mathcal{A}^5(\mathcal{A}^*)^2 + \frac{7}{256}i\mathcal{A}^4\mathcal{A}^* + \frac{1}{128}i\mathcal{A}^3$$

we obtain

$$y_0(t) = \mathcal{A}e^{i(t-t_0)} + c.c.\ ;$$

$$y_1(t) = \left(\tfrac{1}{2}\mathcal{A}\left(1 - \mathcal{A}\mathcal{A}^*\right)(t-t_0)\,e^{i(t-t_0)} - \tfrac{1}{24}i\mathcal{A}^3e^{3i(t-t_0)}\right) + c.c.\ ;$$

$$\begin{aligned} y_2(t) = {} & \left(\tfrac{1}{16}i\mathcal{A}^3(\mathcal{A}^*)^2 - \tfrac{1}{8}i\mathcal{A}\right)(t-t_0)\,e^{i(t-t_0)} \\ & + \tfrac{1}{8}\mathcal{A}\left(\mathcal{A}\mathcal{A}^* - 1\right)\left(3\mathcal{A}\mathcal{A}^* - 1\right)\ \ (t-t_0)^2\ \ e^{i(t-t_0)} \\ & + \left(\tfrac{3}{64}\mathcal{A}^4\mathcal{A}^* - \tfrac{1}{32}\mathcal{A}^3\right)e^{3i(t-t_0)} + \tfrac{1}{16}i\mathcal{A}^3\left(\mathcal{A}\mathcal{A}^* - 1\right)\ \ (t-t_0)\ \ e^{3i(t-t_0)} \\ & - \tfrac{1}{192}\mathcal{A}^5e^{5i(t-t_0)} + c.c.\ ; \end{aligned}$$

$$\begin{aligned} y_3(t) = {} & \left(-\tfrac{13}{128}\mathcal{A}^4(\mathcal{A}^*)^3 + \tfrac{11}{64}\mathcal{A}^3(\mathcal{A}^*)^2\right)(t-t_0)\,e^{i(t-t_0)} \\ & + \left(-\tfrac{3}{32}i\mathcal{A}^4(\mathcal{A}^*)^3 + \tfrac{3}{32}i\mathcal{A}^3(\mathcal{A}^*)^2 + \tfrac{1}{16}i\mathcal{A}^2\mathcal{A}^* - \tfrac{1}{16}i\mathcal{A}\right)(t-t_0)^2\,e^{i(t-t_0)} \\ & + \left(-\tfrac{5}{16}\mathcal{A}^4(\mathcal{A}^*)^3 + \tfrac{9}{16}\mathcal{A}^3(\mathcal{A}^*)^2 - \tfrac{13}{48}\mathcal{A}^2\mathcal{A}^* + \tfrac{1}{48}\mathcal{A}\right)(t-t_0)^3\,e^{i(t-t_0)} \\ & + \left(-\tfrac{37}{1536}i\mathcal{A}^5(\mathcal{A}^*)^2 + \tfrac{1}{128}i\mathcal{A}^3 + \tfrac{7}{256}i\mathcal{A}^4\mathcal{A}^*\right)e^{3i(t-t_0)} \\ & + \left(-\tfrac{7}{64}\mathcal{A}^5(\mathcal{A}^*)^2 + \tfrac{21}{128}\mathcal{A}^4\mathcal{A}^* - \tfrac{1}{16}\mathcal{A}^3\right)(t-t_0)\,e^{3i(t-t_0)} \\ & + \left(-\tfrac{5}{64}i\mathcal{A}^5(\mathcal{A}^*)^2 + \tfrac{1}{8}i\mathcal{A}^4\mathcal{A}^* - \tfrac{3}{64}i\mathcal{A}^3\right)(t-t_0)^2\,e^{3i(t-t_0)} \\ & + \left(\tfrac{17}{2304}i\mathcal{A}^5 - \tfrac{17}{1536}i\mathcal{A}^6\mathcal{A}^*\right)e^{5i(t-t_0)} \\ & + \left(\tfrac{5}{384}\mathcal{A}^6\mathcal{A}^* - \tfrac{5}{384}\mathcal{A}^5\right)(t-t_0)\,e^{5i(t-t_0)} \\ & + \tfrac{1}{1152}i\mathcal{A}^7e^{7i(t-t_0)} + c.c. \end{aligned}$$

Remark 6.3.1 *DeVille et al.* [35] *have obtained same result correct upto* $O\left(\varepsilon^3\right)$. *However, their computed expression of* a_2 *is not correct. We have made the correction in the expression of* a_2.

We observe that each of $y_1(t)$, $y_2(t)$, $y_3(t)$ contains secular terms. As a consequence the solution

$$y(t) = y_0(t) + y_1(t)\,\varepsilon + y_2(t)\,\varepsilon^2 + y_3(t)\,\varepsilon^3 + O\left(\varepsilon^4\right)$$

becomes divergent as $t \to \infty$. To regularize the perturbation series using RGM an arbitrary time τ is introduced and $t - t_0$ is split as $(t-\tau)+(\tau - t_0)$. The terms containing $\tau - t_0$ is absorbed in the renormalized counterpart $\mathcal{A}$ of the constant of integration A. Since the final solution should not depend upon the choice of the arbitrary time τ, so

$$\left.\frac{\partial y}{\partial \tau}\right|_{\tau=t} = 0 \tag{6.4}$$

for any t. However, DeVille et al. [35] have simplified this condition and proposed an equivalent condition as

$$\left.\frac{\partial y}{\partial t_0}\right|_{t_0=t} = 0. \tag{6.5}$$

We note that renormalized counterpart $\mathcal{A}$ is no longer a constant of motion in RGM. The RG condition (6.5) is developed in such a manner that one need to differentiate the terms containing $e^{i(t-t_0)}$, $e^{-i(t-t_0)}$, $(t-t_0)\,e^{i(t-t_0)}$ and $(t-t_0)\,e^{-i(t-t_0)}$ and thereafter substituting $t_0 = t$ the resultant expression is equated to zero. The other terms related to higher harmonics are not involved in RG condition. Simplifying RG condition (6.5) we get

$$\begin{aligned}\frac{\partial \mathcal{A}}{\partial t_0} = \mathcal{A}i - \frac{1}{2}\mathcal{A}\left(\mathcal{A}\mathcal{A}^* - 1\right)\varepsilon - \frac{1}{8}i\mathcal{A}\left(1 - \frac{1}{2}\mathcal{A}^2(\mathcal{A}^*)^2\right)\varepsilon^2 \\ - \frac{1}{64}\mathcal{A}^3(\mathcal{A}^*)^2\left(\frac{13}{2}\mathcal{A}\mathcal{A}^* - 11\right)\varepsilon^3\end{aligned}$$

to the order $O\left(\varepsilon^4\right)$. Taking $\mathcal{A} = \frac{R}{2}e^{i(t+\theta)}$ we obtain corresponding am-

plitude and phase flow equations to the order $O\left(\varepsilon^4\right)$ as

$$\frac{dR}{dt} = \frac{1}{2}R\left(1-\frac{R^2}{4}\right)\varepsilon + \frac{1}{1024}R^5\left(11-\frac{13}{8}R^2\right)\varepsilon^3 + O\left(\varepsilon^4\right) \tag{6.6}$$

$$\frac{d\theta}{dt} = -\frac{1}{8}\left(1-\frac{R^4}{32}\right)\varepsilon^2 + O\left(\varepsilon^4\right). \tag{6.7}$$

To the author's knowledge these higher order flow equations are reported for the first time in the literature. We remark that above flow equations match exactly with $O(\varepsilon^3)$ flow equations of the Van der Pol equation [36]. Although not done explicitly, we expect that the $O\left(\varepsilon^4\right)$ VdP flow equations would also have the equivalent forms. For latter reference, we also write down the order $O(\varepsilon^2)$ renormalized solution of the Rayleigh equation [31]

$$y(t) = R(t)\cos(t+\theta) + \frac{\varepsilon}{96}R(t)^3(\sin 3(t+\theta) - \sin(t+\theta)). \tag{6.8}$$

Solving the amplitude equation (6.6) by numerical method and taking the limit as $t \to \infty$ so that for a fixed value of ε we have $R \to a_{RG}(\varepsilon)$, the approximation of the amplitude of limit cycle of Rayleigh equation (6.1) by RGM, we obtain Figure 6.1 representing ε dependence of the amplitude a_{RG} by solid lines.

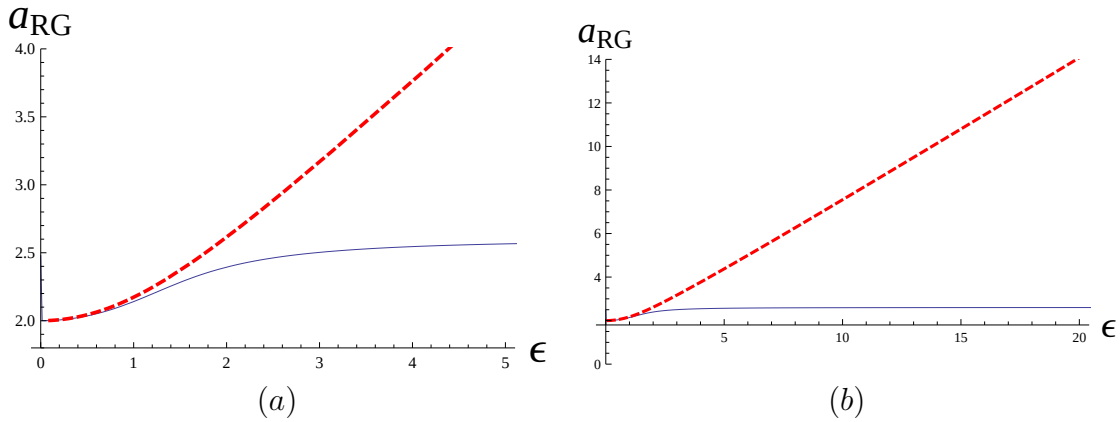

(a) (b)

Figure 6.1: Graph of $a_{RG}(\varepsilon)$ (by solid lines) correct upto $O(\varepsilon^4)$ and compared with exact graph of $a(\varepsilon)$ (by dotted lines) for $0 < \varepsilon \leq 5$ in (a) and for $0 < \varepsilon \leq 20$ in (b).

Thus we observe that the RG flow equation to the order $O\left(\varepsilon^4\right)$ for the amplitude does not give good approximation to the exact solution for moderate and large values of ε.

6.4 Concluding Remarks

The basic idea of RGM has been presented in this chapter and applied on Rayleigh Equation (6.1) to find RG flow equations for amplitude and phase of the limit cycle solution. We found in Figure 6.1 that the numerical solution of the RG amplitude equation (6.6) fail to give good approximation of the exact amplitude for nonperturbative values of the nonlinearity parameter ε. Therefore, we required to modify this classical RGM in such a manner that one can control the convergence of the renormalized solution to the exact solution for all values of ε in order to generate uniformly valid analytic solution of a given differential equation.

Chapter 7

Improved Renormalization Group Method

7.1 Introduction

We have discussed Homotopy Analysis Method (HAM) and Renormalization Group Method (RGM) in the previous two chapters. Both of these two methods have the objective to derive global solutions to nonlinear differential equations. HAM involves a convergence control parameter h by which one can control the convergence of an approximate solution to any level of precision. It helps us to evaluate analytic approximation to different quantities such as amplitude, frequency etc. related to a limit cycle. However, we found in Chapter 6 that classical RG solution fails to give good approximation to the amplitude of the limit cycle for Rayleigh equation

$$\ddot{y} + \varepsilon \left(\frac{1}{3}\dot{y}^3 - \dot{y} \right) + y = 0 \tag{7.1}$$

with moderately large values of $\varepsilon > \approx O(1)$, where the dots are used to designate the derivatives with respect to time t (c.f. Figure 6.1 in Chapter 6). Let us recall that there are some limitations in the conventional form of RGM (c.f. Chapter 6). The actual convergence of the RG expansions is not well addressed and should require further investigations. We observe that in RGM we do not have any control parameter h as we have in case of HAM. In this Chapter we shall improve the classical RGM by introducing similar control parameters which will help us to control the convergence of the approximate solution to the exact one for

a given nonlinear ordinary differential equation (ODE) to any desired degree of precision. In this chapter, along with the Rayleigh equation we shall also study the Van der Pol equation

$$\ddot{x} + \varepsilon\, \dot{x}\left(x^2 - 1\right) + x = 0. \tag{7.2}$$

In IRGM, we advocate the concept of *nonlinear time* [40,76,77] that extends the original RG idea of eliminating the divergent secular term of the form $(t - t_0)\sin t$, where t_0 is the initial time, in the naive perturbation series for the solution of the nonlinear problem, by exploiting the arbitrariness in fixing the initial moment t_0. In the framework of nonlinear time, we suppose the arbitrary initial time τ to depend explicitly on the nonlinearity parameter (coupling strength) ε of the nonlinear equation, so that one can write $\tau/\varepsilon = \varepsilon^h$ where $h = h\left(\varepsilon t\right),\ \varepsilon t > 1$ is a slowly varying (almost constant), free (asymptotic) control parameter for $t \to \infty$ and $\varepsilon \ \to$ either to 0 or ∞, to be utilized judiciously to improve the convergence and non-perturbative global asymptotic behaviour of the original RG proposal ($h < 0$ for $0 < \varepsilon < 1$). We note that there is a slight abuse of the notation τ as discussed in Chapter 5. In Section 7.2, we give an overview, in brief, of an extended analytic framework that naturally supports nontrivial existence of such an asymptotic scaling parameter $h(\tilde{\tau})$ as a function of the rescaled $O(1)$ variable $\tilde{\tau} = \varepsilon t \sim O(1)$, satisfying what we call the *principle of duality structure*. The secular terms in the naive perturbation series would now be altered instead as $(t - \tau/\varepsilon + \tau/\varepsilon - t_0)\sin t$ and we obtain the new RG flow equations in the form

$$\frac{dR}{d\tau} = f_0\left(R\right)\left(1 + O\left(\varepsilon^2\right)\right),\ \frac{d\theta}{d\tau} = \varepsilon g_1\left(R\right)\left(1 + O\left(\varepsilon^3\right)\right), \tag{7.3}$$

where $f_0(R)$ and $g_1(R)$ are nonzero, minimal order R dependent terms in the respective perturbation series. Following the analogy of RG prescription in annulling secular divergence through corresponding 'flowing' of the renormalized perturbative amplitude and phase, we next make *the key assumption that there exists, for a given nonlinear oscillation, a set of right control parameters h^i that would absorb any possible secular or other kind of divergence in the higher order pertur-*

bation series, so that in the asymptotic limit $t \to \infty$, one obtains the finite, non-perturbative flow equations directly for the periodic orbit of the nonlinear system

$$\frac{da}{d\tau_1} = f_0(a), \ \frac{d\theta}{d\tau_2} = g_1(a), \tag{7.4}$$

where

$$\tau_i = \varepsilon^{i \times h^i_{RG}(\tilde{\tau})},$$

and $h^i_{RG}(\tilde{\tau})$ is a finite *scale* independent control parameter in the rescaled variable $\tilde{\tau} \sim O(1)$ and $a(\varepsilon) = \lim_{t\to\infty} R(\varepsilon, t)$ is the ε- dependent amplitude of the limit cycle. A simple quadrature formula should then relate the control parameter $h_{RG} := h^1_{RG}$ with the amplitude $a(\varepsilon)$. As a consequence, adjusting the control parameter h_{RG} suitably, one can generate an efficient algorithm to estimate the amplitude $a(\varepsilon)$ that would compare well with the exact values, upto any desired accuracy. It will transpire that the control parameter $h_{RG}(\varepsilon)$ must respect some asymptotic conditions depending on the characteristic features of a particular relaxation oscillation (c.f. Section 7.3).

Exploiting the rescaling symmetry, one may as well rewrite the above non-perturbative flow equations (7.4) in the equivalent $\tilde{\tau} \sim O(1)$ dependent scaling variable $\tau = \tilde{\tau}^{H_{RG}(\tilde{\tau})}$, $\left(H_{RG}(\tilde{\tau}) = h_{RG}(\tilde{\tau})\frac{\log\tilde{\tau}}{\log\varepsilon}\right)$, for each fixed value of the nonlinearity parameter ε that should expose small scale $\tilde{\tau} \sim O(1)$ dependent variation of the amplitude. As a by-product that would allow one to retrieve an efficient approximation of the limit cycle orbit for the nonlinear oscillator. It turns out that the general framework of IRGM is quite successful in obtaining excellent fits for the limit cycle orbit even for relaxation oscillation corresponding to nonlinearity parameters $\varepsilon \geq 1$.

It follows that the application of the idea of nonlinear time in RG formalism offers one with a robust formalism for global asymptotic analysis for a general nonlinear system that might even be advantageous in many respects compared to HAM. The application of nonlinear time in HAM will be considered separately.

The chapter is organized as follows. In Section 7.2 we give a brief overview of the *novel* analytic framework extending the standard clas-

sical analysis to one that supports naturally the above stated *duality structure* and the emergent nonlinear scaling patterns typical for a given nonlinear system. The IRGM is proposed using the idea of nonlinear time in Section 7.3. Approximate formulae for the amplitude of limit cycle solution have been deduced there in the context of Rayleigh and VdP equations. The application of nonlinear time on limit cycles of the Rayleigh and Van der Pol equations is included in Section 7.4. Finally, some concluding remarks are included in Section 7.5.

7.2 Nonlinear Time: Formal Structure

The idea of nonlinear time can be given a rigorous meaning in a non-classical extension of the ordinary analysis [42,78]. Recall that the real number system $\mathbb{R}$ is generally constructed as the metric completion of the rational field $\mathbb{Q}$ under the Euclidean metric $|x-y|\,,\ x,y\in\mathbb{Q}$. More specifically, let S be the set of all Cauchy sequences $\{x_n\}$ of rational numbers $x_n\in\mathbb{Q}$. Then S is a ring under standard component-wise addition and multiplication of two rational sequences. Then the real number field $\mathbb{R}$ is the quotient space S/S_0, where the set S_0 is the set of all Cauchy sequences converging to $0\in\mathbb{Q}$ and is a maximal ideal in the ring S. Alternatively, $\mathbb{R}$ can be considered as the set $[S]$ of equivalence classes, when two sequences in S are said to be equivalent if their difference belongs to S_0.

The nonclassical extension $\mathbb{R}^*$ of $\mathbb{R}$ is based on a *finer* equivalence relation that is defined in S_0 as follows: let $\{a_n\}\in S_0$. Consider an associated family of Cauchy sequences of the form

$$S_{0a}:=\left\{A^{\pm}\mid A^{\pm}=\{a_n\times a_n^{\pm a^{\pm}_{m_n}}\}\right\},$$

where $a^{\pm}_{m_n}\neq 0$ is Cauchy for $m_n>N$ and N sufficiently large. Clearly, $S_{0a}\subset S_0$, and sequences of S_{0a} also converges to 0 in the metric $|\cdot|$. As a parametrizes sequences in S, it follows that $\bigcup\limits_{\{a\}}S_{0a}=S$. Assume further that $a^{\pm}_{m_n}$ respect the *duality structure* defined by $\left(a^{-}_{m_n}\right)^{-1}\propto a^{+}_{m_n}$ for $m_n>N$. The duality structure extends also over the limit elements: viz., $\mathbb{R}\ni\ (a^{-})^{-1}\propto a^{+}$ where $a^{\pm}_{m_n}\to a^{\pm}$ as $m_n\to\infty$ such that $a^{\pm}$ are

close to 1 in $\mathbb{R}$.

Next define an equivalence relation in S_{0a} declaring two sequences $A_1,\ A_2$ in the set S_{0a} equivalent if the associated exponentiated sequences $a^1_{m_n}$ and $a^2_{m_n}$ differ by an element of S_0 for $m_n > N$. In particular, one may impose the condition that $A_1 \equiv A_2$ if and only if $\exists\ M$ such that $a^1_{m_n} = a^2_{m_n}\ \forall\ m_n > M$. Clearly, the usual metric $|\cdot|$ fails to distinguish elements belonging to two distinct such finer equivalent classes. However, the metric defined as the natural logarithmic extension of the Euclidean norm, generically called the *asymptotically visibility metric* is introduced by

$$h\left(A_1, A_2\right) = \lim_{n\to\infty} \left|\log_{|A_0|^{-1}} \left|\frac{A_1}{A_2}\right|\right|,$$

where $A_0 = \{a_n\} \in S_0$. The sequence A_0 is said to define a natural scale relative to which elements in S_0 gets nontrivial values and hence become distinguishable. The limit exists because of concerned sequences $a^{\pm}_{m_n}$ being Cauchy. Note that the mapping $h : S_0 \to \mathbb{R}^+$ defined by

$$h(A) = \lim_{n\to\infty} \left|\log_{|A_0|^{-1}} \left|\frac{A}{A_0}\right|\right|$$

is actually a nontrivial norm [42, 78] (for simplicity of notation, we use same symbol to denote both the norm and metric).

The extended real number system $\mathbb{R}^*$ admitting duality induced *fine structure* is given, by definition, as the equivalence class under this finer equivalence relation viz., $\mathbb{R}^* := S/S_0$ when convergence is induced naturally by the asymptotically visibility metric $h\left(x, y\right)$. Clearly, under the usual norm $|\cdot|$, $\mathbb{R}^*$ reduces to $\mathbb{R}$ as the exponentiated elements $a^{\pm}$ are essentially invisible. The natural application of the visibility norm on $\mathbb{R}^*$ is activated in the following steps. For any two distinct elements $x,\ y \in \mathbb{R} \subset \mathbb{R}^*$, *set*, by definition, $h\left(x, y\right) = 0,\ x \neq y$; $h\left(x, y\right)$ being nontrivial only for $y \in x + S_0$. This choice is natural as for any element $x \in \mathbb{R}$, the corresponding limiting h norm viz.,

$$h\left(x\right) = \lim_{n\to\infty} \log_{|A_0|^{-1}} \left|\frac{x}{A_0}\right| = 1 \text{ and } h\left(x, y\right) = 0,\ \forall\ x, y \in \mathbb{R}.$$

For nontrivial values of $h\left(x, y\right),\ x,\ y \in \mathbb{R}^*$, the definition of the visibil-

ity metric extends over to $h(x,y) = \lim_{n\to\infty} \left|\log_{\varepsilon^{-n}} \left|\frac{x-y}{\varepsilon^n}\right|\right|$, which exists by construction, where $A_0 = \{\varepsilon^n\},\ 0 < \varepsilon < 1$.

Next, consider the metric $d : \mathbb{R}^* \to R^+$ by $d(x,y) = |x-y| + h(x,y)$. Clearly, $d(x,y) = |x-y|$ for any $x,\ y \in \mathbb{R}$ and $d(x,y) = h(x,y)$ for $x,\ y \in \mathbb{R}^* - \mathbb{R}$ and hence $(\mathbb{R}^*, d)$ is a complete metric space. The metric $h(x,y)$ acting nontrivially on S_0 is essentially an ultrametric: $h(x,y) \leq \max\{h(x,y), h(x,y)\}$. This follows immediately from the observation that h maps $\mathbb{R}$ to the singleton set $\{1\}$. Further, the ultrametric h must be discretely valued [78] and hence the nontrivial value set of h viz., $h(S_0)$ is countable. As a consequence, the set S_0 is totally disconnected and perfect in the induced topology.

More detailed analytic aspects (including the idea of smooth jump differentiability and jump derivative) of the extended system $\mathbb{R}^*$ equipped with the metric d will be reported elsewhere [42]. Here, we make a few relevant remarks.

Remark 7.2.1 *Even as the size of a $\delta-$ neighbourhood of a point $x \in \mathbb{R}$ vanishes linearly, the same for $x^* \in \mathbb{R}^*$ need not vanish at the same rate and may only vanish at a slower rate $\delta h(\delta)$. The real number model $\mathbb{R}$ is called the hard or string model when the space $\mathbb{R}^*$ is called the soft or fluid model of real numbers* [40]*. The ordinary differential measure dx gets extended in $\mathbb{R}^*$ as $d(h(x)\,x)$.*

Remark 7.2.2 *Consider the open interval $(\delta, \delta^{-1}) \subset \mathbb{R}^*$. In the asymptotic limit $\delta \to 0^+$, the duality structure identifies the right neighbourhood of δ with the left neighbourhood of δ^{-1} in a nontrivial manner. As a consequence, the linear (translation) group action on $\mathbb{R}$ is extended to a nonlinear $SL(2,R)$ group on $\mathbb{R}^*$. In fact, the translation subgroup acts on $\mathbb{R}$, when the inversion acts nontrivially only on $\mathbb{R}^*$ in the sense that the visibility norm h is invariant under inversion $\hat{\imath}$: $h(\hat{\imath}A) = \hat{\imath}(h(A))$ where $\hat{\imath}(A) = \left\{a_n^{-1} \times a_n^{(a^-_{m_n})^{-1}}\right\},\ A = \left\{a_n \times a_n^{-a^-_{m_n}}\right\}$. For a translation T_r by a shift r, on the other hand, $h(T_r(A)) = h(A)$ and hence $T_r(A) = A \ \Rightarrow r = 0$ (i.e. T acts trivially). Above two* salient *properties of the duality structure are expected to have significant application in nonlinear problems.*

Remark 7.2.3 *To give an example of the intricate nonlinear structure that can get encoded into a well behaved (smooth) function in* $\mathbb{R}$*, let us consider the simplest case of a real variable* x*. In* $\mathbb{R}^*$ *the variable* x *gets extended to, say,* $X = xe^{\phi(\log X)}$*. The function* ϕ *exposing the nonlinear dependence is also assumed to be differentiable. Differentiating* X *with respect to* x *one gets* $xX'(1-\phi') = X$*, where '' denotes derivation with the argument. We now assume that* $\phi(\log X)$ *is vanishingly small (i.e. less than accuracy level* δ *in any given application) for* $0 < x < \infty$ *and* $O(1)$ *when* $|\log X| \gg 1$ *i.e.* $x \to 0$ *or* ∞*. As a consequence, existence of* ϕ *is felt only in the asymptotic neighbourhoods (Remark 7.2.2) of* 0 *or* ∞*. We now make a further assumption that* $\phi' = 0$ *almost everywhere in an asymptotic neighbourhood, but every where in* $0 < x < \infty$*. Then* X *satisfies* $xX' = X$ *a.e. in* $\mathbb{R}^*$*. Thus ordinary variable* $x \in \mathbb{R}$ *gets extended in* $\mathbb{R}^*$ *as* X *which has the intermittent property of a Cantor devil's Staircase function in an asymptotic neighbourhood. Since, under duality structure, such a neighbourhood has ultrametric topology,* X *in fact satisfies the above scale invariant equation everywhere in* $\mathbb{R}^*$*, because ordinary non-differentiability at the points of the associated Cantor set is removed by inversion mediated jump increments* [42,78]*. This example tells that an ordinary function can have nonlinear and nonlocal functional dependence with itself, along with rhythmic (intermittent) variability that can have significant amplification in an asymptotic sector.*

Remark 7.2.4 *The asymptotic scaling variables* $h_0(\varepsilon)$ *and* $H_{RG}(\tilde{\tau})$ *introduced in Subsection 7.3.1 correspond to the associated visibility norm* $h(A)$ *defined above. A real variable* $t \in \mathbb{R}$ *approaching asymptotically either to* 0 *or* ∞ *has natural images in* $\mathbb{R}^*$ *in the form* $\tau_0 = t \times t^{-h^-(\varepsilon t)}$*,* $h^-(\varepsilon t) < 1$ *and* $\tau_\infty = t \times t^{h^+(\varepsilon t)}$*,* $h^+(\varepsilon t) > 1$ *respectively. The scaling exponents* $h^\pm$ *encode asymptotic scaling information of a given nonlinear system. Further,* $(h^-(\varepsilon t))^{-1} \propto h^+(\varepsilon t)$ *by duality. In Section 7.3.1, we discuss how such information can be systematically extracted in the case of a limit cycle for a nonlinear oscillator.*

Remark 7.2.5 *The fine structures in* $\mathbb{R}^*$ *remain inactive (passive/hidden) in absence of any stimulus, either intrinsic or exter-*

nal. In presence of an external input, say, the actions of the nontrivial component of the metric d and the associated duality structure become manifest. The RG analysis makes room for direct implementation of the intrinsically realized duality structure in the context of a nonlinear system in the soft model $\mathbb{R}^*$.

7.3 Improved RG Method: use of Nonlinear Time

In RGM an arbitrary time τ is introduced in between current time t and the initial time t_0 so that $t-t_0 = (t-\tau)+(\tau-t_0)$ in order to remove the divergent terms in the naive perturbation expansion for the solution of the given differential equation. The solution is renormalized by suitable choice of the constants of integration to remove the terms containing $(\tau - t_0)$ and keeping the terms having $(t-\tau)$. Since the solution should be independent of the arbitrary time τ, the RG condition

$$\left.\frac{\partial y}{\partial \tau}\right|_{\tau=t} = 0$$

is applied to the renormalized solution. However, in the previous section we have seen that the method fails to produce good approximations to the exact solution for $\varepsilon \sim O(1)$. Our target is not only to remove the divergent terms in the solution but also to introduce some control parameter $h(\varepsilon)$ which can control the RG solution in such a manner that this solution ultimately converges to the exact solution. Moreover, our another goal is to achieve this accuracy by merely solving the differential equation to a minimal order of the expansion parameter, viz., upto $O(\varepsilon^2)$ or less.

Since the basic idea is to split the time difference $t-t_0$ by introduction of an arbitrary time, so we can write $t - t_0 = \left(t - \frac{\tau}{\varepsilon}\right) + \left(\frac{\tau}{\varepsilon} - t_0\right)$. From now on let us assume that $0 \ll \varepsilon <\approx 1$. The case $\varepsilon >\approx 1$ will be commented upon later. The constants of integration can be renormalized in order to remove the terms containing $\left(\frac{\tau}{\varepsilon} - t_0\right)$ from the solution keeping the terms containing $\left(t - \frac{\tau}{\varepsilon}\right)$. Finally analogous

to the classical RG method we put $t = \frac{\tau}{\varepsilon}$, i.e. $\tau = \varepsilon t$, in

$$\frac{\partial y}{\partial \tau} = 0 \tag{7.5}$$

giving rise to an improved form of the RG flow equation to remove secular terms involving $\left(t - \frac{\tau}{\varepsilon}\right)$. So far the improved method does not produce any qualitative new result compared to the RGM and so we must get the same phase and amplitude equation as deduced in Section 6.3 in Chapter 6.

We next proceed one step further. As stated already in Section 7.1, we now exploit the possibility of extending the original linear t dependence of τ viz., $\tau = t$ of RGM in removing the explicit divergences by a *nonlinear dependence* $\tau = \varepsilon t$ along with the *additional condition* that $\tau \to \varepsilon^{-n}\phi(\tilde{\tau})$, where ϕ a slowly varying scaling function of the $O(1)$ rescaled variable $\tilde{\tau} = \varepsilon\tilde{t} \sim O(1)$, as the original linear time $t \to \infty$ following the *scales* $t \sim \varepsilon^{-n}\ \tilde{t},\ n = 1, 2, \ldots$. (Note that linear time flows with uniform rate 1 and τ is nonlinear since the rate $\dot{\phi}(\tilde{\tau}) < 1$). It follows that for a given nonlinear differential system, such a nonlinear time dependence always exists and nontrivial, provided one invokes a *duality principle* transferring nonlinear influences from the far asymptotic region into the finite observable sector in a cooperative manner [40, 42, 77].

In fact, as the linear time $t \to \infty$, following the above hierarchy of scales, there exists $\tilde{t}_n$ such that $1 \ll (\varepsilon t)^n < \varepsilon^{-n} < \tilde{t}_n$ and satisfying *the inversion law*

$$\frac{\tilde{t}_n}{\varepsilon^{-n}} \propto \frac{\varepsilon^{-n}}{(\varepsilon t)^n}. \tag{7.6}$$

This inversion law makes a room for transfer of effective influences, typical for the nonlinear system concerned, from nonobservable sector $t > \varepsilon^{-n}$ to the observable sector $t < \varepsilon^{-n}$ bypassing the dynamically generated singular points denoted by the scales ε^{-n}. Notice the nonlinear connection between scales of the form $\varepsilon^n\ \tilde{t}_n$ with the scale εt via duality structure (c.f. Section 7.2). Let $\tilde{t}(t) = \lim_{n\to\infty} \left(\tilde{t}_n\right)^{1/n}$ so that

$\varepsilon t < \varepsilon^{-1} < \tilde{t}\,(t)$ and $\dfrac{\tilde{t}_n}{\varepsilon^{-1}} \propto \dfrac{\varepsilon^{-1}}{(\varepsilon t)}$. Define

$$h_0\,(\tilde{\tau}) = \lim_{n\to\infty} \log_{\varepsilon^{-n}} \left(\frac{\tilde{t}_n}{\varepsilon^{-n}}\right). \tag{7.7}$$

Here, the scaling exponent h_0 corresponds to the visibility norm (c.f. Section 7.2), that can access (encode) the non-perturbative region (information) of the nonlinear system and $\tilde{\tau}$ is an $O\,(1)$ rescaled variable. The exponent h_0 is *scaling invariant* in the sense that it appears uniformly for every n as $t \to \infty$ through the scales $\tilde{t}_n = \varepsilon^{-n}\varepsilon^{-n\ h_0(\tilde{\tau})}$. As a consequence, a significant amount of asymptotic scaling information in the limit $t \to \infty$ could be simply retrieved by considering the scaling limit instead at $t = \varepsilon^{-1}$.

Exploiting the above insight, one now writes the nonperturbative scaling limit in the form

$$\tau = \lim \varepsilon t = \varepsilon^{-h_{RG}(\tilde{\tau})} > 1,\ \varepsilon < 1 \tag{7.8}$$

as $t \to \varepsilon^{-1}$. Moreover, $h_{RG}\,(\tilde{\tau}) = 1 - h_0\,(\tilde{\tau})$. As noted already, the scaling exponent $h_0\,(\tilde{\tau})$ here encodes the *effective* cooperative influence of far asymptotic sector $t > \varepsilon^{-n}$ into the observable sector $1 < t < \varepsilon^{-n}$ by the inversion mediated duality principle. As pointed out in Section 7.2, the duality principle *does* allow asymptotic limiting (non-perturbative) behaviour of the nonlinear system to be encoded into the scaling exponents of the nonlinear time τ that, in turn, offers an efficient handle in uncovering key dynamical information of the said system. Notice that, in the absence of the said duality the linear time t can in principle attain the scale ε^{-1} (say), and as a consequence $h_0 = 0$, retrieving the ordinary scaling of $\tau = \varepsilon t \sim \varepsilon^{-1}$ as $t \sim \varepsilon^{-2}$. This also establishes, in retrospect, that the scaling exponent $h_0\,(\varepsilon)$ is well defined and can exist nontrivially i.e. $h_0 \sim O\,(1)$ in a nonlinear problem. Further, the scaling variable τ is also positively directed with t. As a consequence, *the RG control parameter h_{RG} can be of both the signs, with relatively small numerical value in fully developed nonlinear systems $\varepsilon \gg 1$, but with a possible $O\,(1)$ variations for $\varepsilon \sim O\,(1)$ or less.*

The above construction actually tells somewhat more. Correspond-

ing to the first generation scales ε^{-n}, one can, in fact, have the *second generation* nonlinear scales

$$\tau_m = \lim \varepsilon^m t = \varepsilon^{-m\ h^m_{RG}(\tilde{\tau})} > 1,\ \varepsilon < 1 \tag{7.9}$$

as $t \to \varepsilon^{-m}$ with $h^1_{RG} = h_{RG}$. The *nonlinear time* τ now stands for these hierarchy of directed scales $\{\tau_m\}$. Consequently, as the linear time t approaches ∞ through the first generation linear scales, the slowly varying nonlinear time τ $\left(\text{or } \tau^{-1}\right)$ approaches to ∞ at slower and slower rates as represented by the numerically small RG scaling exponents $h^m_{RG}(\varepsilon)$, each of which remains almost constant over longer and longer intervals of ε^{-1} (as $\varepsilon^{-1} \to \infty$). In the present chapter we show how the first two scaling exponents $h_i(\tilde{\tau}),\ i = 1, 2$ relate to the nonperturbative properties of the limit cycle. We expect higher order scaling exponents h_m would have vital role in bifurcation of nonautonomous systems. This problem will be investigated elsewhere.

Let us remark that for $\varepsilon > 1$, we consider instead the first generation scales as ε^n, and the duality is invoked for variables satisfying $\frac{t}{\varepsilon} < \varepsilon < \tilde{t}(t)$ so that the asymptotic scaling variables are derived as $\tau_m = \varepsilon^{m\ h^m_{RG}(\tilde{\tau})},\ \varepsilon > 1$ where $h^m_{RG} = 1 - h^m_0$. Moreover, said proliferation of nonlinear scales (7.9) actually continues ad infinitum. In fact, interpreting each second generation scale τ_m, m fixed, as first generation scale, and iterating above steps one associates third generation scales $\tau_{m_k},\ k = 1, 2, \ldots$, and so on.

It now follows, from the above general remarks on the behaviour of h_{RG}, that the nonlinear time τ actually approaches 0 or ∞ as $\tau \sim (\log \varepsilon)^{-\alpha}$ or $\tau \sim (\log \varepsilon)^{\alpha}$, $\alpha > 0$ respectively as $\varepsilon \to \infty$. However, one must have $\tau = \varepsilon^{-h_{RG}(\varepsilon)} \to \infty$ as $\varepsilon \to 0$. An example of the asymptotic behaviours of h_{RG} is given by $\tau_m = \varepsilon^{\pm\alpha_m \frac{\log\log\varepsilon}{\log\varepsilon}}$ for $\varepsilon \to \infty$, which one expects to verify explicitly in evaluation of asymptotic quantities, such as amplitude of a periodic cycle, in a nonlinear system.

In the IRGM, we exploit this duality induced nontrivial scaling information to rewrite the lowest order perturbative flow equations (6.6) and (6.7) in Chapter 6 as the asymptotic RG flow equations in the limit

$t \to \infty$

$$\frac{da}{d\tau_1} = \frac{1}{2}a\left(1 - \frac{a^2}{4}\right) \tag{7.10}$$

$$\frac{d\psi}{d\tau_2} = -\frac{1}{8}\left(1 - \frac{a^4}{32}\right) \tag{7.11}$$

for the amplitude $a = a(\tilde{\tau})$ and the phase $\psi = \psi(\tilde{\tau})$ of the limit cycle of both the Rayleigh and Van der Pol equations, involving slowly varying nonlinear time scales $\tau_i,\ i = 1, 2$. The asymptotic scaling functions $\tau_1 = \phi_1(\varepsilon t) = \varepsilon^{h^1_{RG}}$ and $\tau_2 = \phi\left(\varepsilon^2 t\right) = \varepsilon^{2h^2_{RG}}$ are activated invoking nonlinear limits in (7.9) as $t \to \varepsilon^{-1}$ and $t \to \varepsilon^{-2}$ successively in the above equations. The slowly varying almost constant scaling functions ϕ_1 and ϕ_2, satisfying $|\ddot{\phi}_i| \ll |\dot{\phi}_i^2| \ll 1$, are assumed to have a rhythmic pattern over the cycle: when ϕ_1 varies slowly, ϕ_2 remains almost constant i.e. $\dot{\phi}_1 > 0,\ \dot{\phi}_2 \approx 0$ and vice versa successively on the cycle (c.f. Section 7.4). Nontrivial ultrametric neighbourhood structure induced asymptotically by duality principle (c.f. Section 7.2) can indeed support such *locally constant* nonlinear rhythmic behaviour. The above flow equations may therefore be considered *exact* and encode non-perturbative information of the limit cycle variables a and ψ respectively. The conventional perturbative RG flow equations in the linear time t is now extended into the non-perturbative flow equations in the nontrivial scaling variable $\tau_i = \varepsilon^{i\ h^i_{RG}(\tilde{\tau})},\ i = 1, 2$ involving the nonlinearity parameter $\varepsilon > 1$. The perturbative fixed point for the amplitude equation at $a = 2$ for $t \to \infty$ corresponding to the periodic oscillation with $\varepsilon \ll 1$ is extended to the by *small scale periodic* flow of amplitude $a(\tau_1)$ over the entire cycle. The associated phase $\psi(\tau_2)$ then flow at a slower rate *linearly with the higher order scale* τ_2 when $a(\tau_1)$ remains almost constant over a relatively small period of time.

The RG estimated approximate formulae for the amplitude $a(\varepsilon)$ for the Rayleigh and Van der Pol limit cycles are obtained from the equation (7.10) in the Subsection 7.3.1, when appropriate boundary condition, derived either from exact computation or from perturbative analysis, is used for a suitable finite value of ε. In Subsection 7.4.1, we present the efficient graph of the Rayleigh and VdP limit cycle parametrized

by the nonlinear scales $\tau_i = \phi_i(\tilde{\tau})\,,\ \tilde{\tau} \sim O(1)$ for fixed values of the nonlinearity parameter ε.

As it turns out, entire onus in the improved RG analysis essentially rests in proper estimation/identification of the scaling functions h^i_{RG} (i.e. $\phi_i(\tilde{\tau})$) which should yield correct dynamical properties of a nonlinear system. We hope to undertake more detailed and systematic analysis for determining h^i_{RG} elsewhere. In this work we limit ourselves only to show that IRGM can indeed yield correct amplitude and solution for the Rayleigh and VdP systems provided one makes appropriate choice of h^i_{RG} based on clues from exact computations and previously known approximate results (for instance the perturbative RGM). We remark finally that the perturbative RG method is known to extend the conventional multiple scale method [31]. Nonlinear time formalism introduces new set of nonlinear scales $\phi_n(\tilde{\tau})$ associated with ordinary scales ε^n. We study here the nontrivial applications of such nonlinear scaling functions.

7.3.1 Approximate Formula for Amplitude

We shall now use the above asymptotic amplitude flow equation (7.10) to find analytic approximations of the amplitudes of the limit cycle for both the Rayleigh and Van der Pol equations.

By a direct integration, one obtains from (7.10)

$$\ln\left(a^2-4\right) - 2\ln a = -\varepsilon^{h_{RG}} - 0.87953 \tag{7.12}$$

as the Rayleigh limit cycle amplitude where we use the boundary condition the value $a = 2.17271$ for $\varepsilon = 1$ (this choice simplifies calculation). It follows immediately that for suitable choices of the control parameter h_{RG} one can achieve efficient matching for the estimated amplitude $a_E(\varepsilon)$. For example, using the HAM generated approximate formula (5.24) in Chapter 5 for $a_E(\varepsilon)$, we can determine the control parameter $h_{RG}(\varepsilon)$ by the formula

$$h_{RG} = \frac{1}{\ln\varepsilon}\ln\left\{\left|\ln\left(\frac{a^2}{a^2-4}\right) - 0.87953\right|\right\} \tag{7.13}$$

In Figure 7.1, we display the typical piece-wise smooth form of $h_{RG}(\varepsilon)$

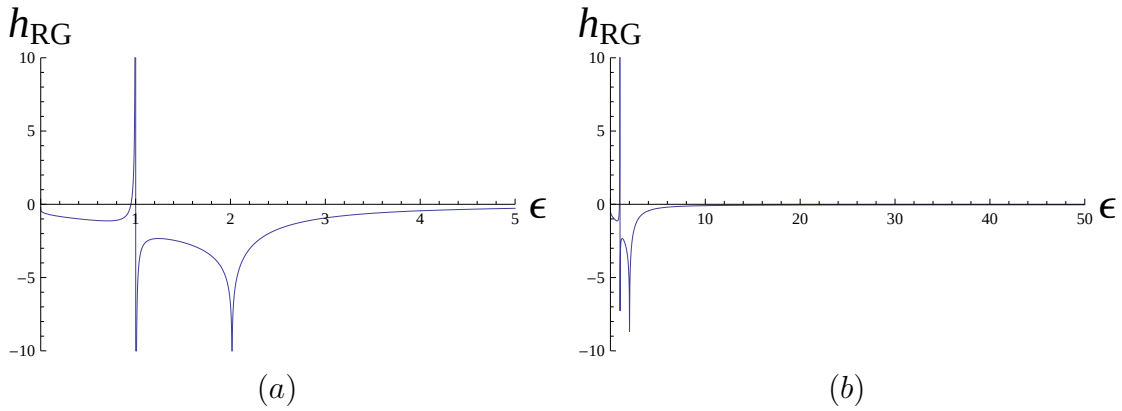

(a) (b)

Figure 7.1: The graph of $h_{RG}(\varepsilon)$ used for approximation of the amplitude of the Rayleigh equation (7.1) by HAM given by (7.13) for $0 < \varepsilon \leq 5$ in (a) and for $0 < \varepsilon \leq 50$ in (b).

given by (7.13) for the Rayleigh limit cycle amplitude that would reproduce the HAM generated amplitude with relative error less that 1%. Clearly, the graph reveals variability of h_{RG} for moderate values of ε, but the variability dies out fast for larger values ε, as expected.

We recall that the corresponding graph of the exact computed values of VdP amplitude $a(\varepsilon)$, on the other hand, has a hump like shape with a maximum roughly at $\varepsilon \approx 2.0235$ and having the asymptotic limits 2 as $\varepsilon \to 0$ and ∞. Lopez et al. [18] obtained HAM generated approximate formula for the VdP amplitude with relative error less than 0.05% at the order $O\left(\varepsilon^4\right)$. It is interesting to note that the RG generated formula (7.12) can reproduce the exact computed values of the VdP amplitude with error less than 0.05% directly from only the first order RG flow equation. To achieve this goal we first intuitively guess an estimated piecewise smooth formula for the estimated amplitude a_E by

$$a_E(\varepsilon) = \begin{cases} 1.998 + \dfrac{0.015}{8.121\ e^{-2.139\ \varepsilon} + 0.512\ e^{0.043\ \varepsilon}}, & 0 < \varepsilon < 3, \\ 2.0025 + \dfrac{0.031}{0.5\ e^{-2.033(\varepsilon - 2.183)} + 1.869\ e^{0.087(\varepsilon - 6.376)}}, & 3 \leq \varepsilon \leq 50, \end{cases} \tag{7.14}$$

keeping the maximum relative percentage error $\left|\dfrac{a_E(\varepsilon) - a(\varepsilon)}{a(\varepsilon)} \times 100\right|$ less than 0.05%. This shows that the approximation is quite accurate. The graph of $a_E(\varepsilon)$ is compared with the exact values in Figure 7.2. One may as well use a least square fit of the exact data instead of the above fit. We do not pursue this approach here.

Using this efficient formula for the VdP amplitude, we then obtain

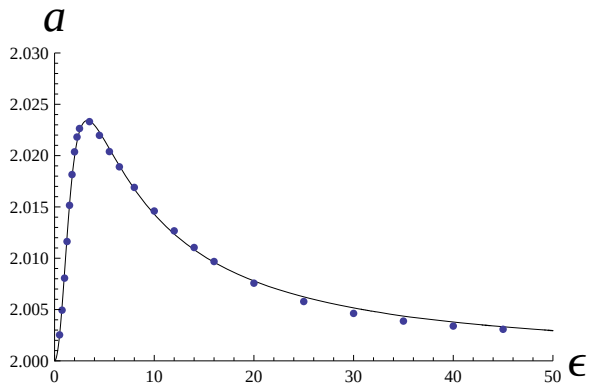

Figure 7.2: The exact amplitude of Van der Pol Equation (7.2) (by solid line) and its approximation $a_E(\varepsilon)$ given by (7.14) (by bold points) for $0 < \varepsilon \leq 50$.

the RG flow equation in the form

$$\ln\left(a^2-4\right)-2\ln a=-\varepsilon^{h_{RG}}-4.08785 \tag{7.15}$$

where we use the boundary condition $a = 2.0086$ for $\varepsilon = 1$ (for simplicity of calculation) for the VdP amplitude. Inverting this equation, we finally obtain the corresponding RG control parameter

$$h_{RG}=\frac{1}{\ln\varepsilon}\ln\left\{\left|\ln\left(\frac{a_E^2}{a_E^2-4}\right)-4.08785\right|\right\} \tag{7.16}$$

Figure 7.3 displays the piecewise smooth variation of h_{RG} with ε. The

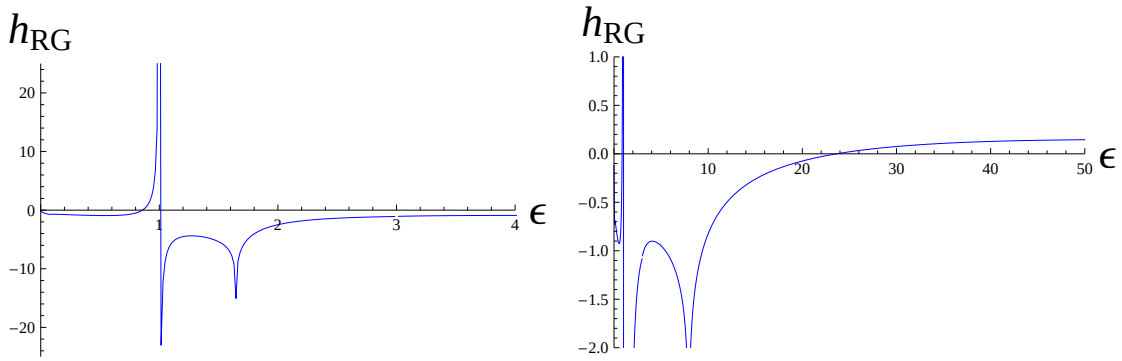

(a) (b)

Figure 7.3: The graph of $h_{RG}(\varepsilon)$ used for approximation (7.16) of the amplitude of the Van der Pol equation (7.2) for $0 < \varepsilon \leq 4$ in (a) and for $0 < \varepsilon \leq 50$ in (b).

rapid $O(1)$ variation for moderate values of ε is evident in Figure 7.3(a). As expected, h_{RG} dies out fast for larger values of ε. However, a change

in sign is noticed here already for $\varepsilon > 20$ (Figure 7.3 (b)). One expects many more such small scale sign variations as $\varepsilon \to \infty$. This particular form of the control parameter h_{RG}, in turn, would reproduce the VdP amplitude with relative error less than 0.05%. As this level of accuracy is achieved only at the order $O(\varepsilon)$, the improved RGM may be considered to be more efficient and advantageous compared to the HAM.

Alternatively, the amplitude equation (7.10) can be inverted as

$$a(\tilde{\tau}) = \frac{a_0}{\sqrt{e^{-\tilde{\tau}} + \frac{a_0^2}{4}(1 - e^{-\tilde{\tau}})}}, \tag{7.17}$$

where a_0 is estimated from the exact value of amplitude $a(\varepsilon_0)$ for a suitably chosen value of ε, for instance $\varepsilon = 1$. Recall that for the VdP equation $\tau \sim (\log \varepsilon)^{\alpha}$ and for the Rayleigh equation $\tau \sim (\log \varepsilon)^{-\alpha}$ for $\varepsilon \to \infty$ and $\alpha > 0$. By adjusting suitably the values of α over appropriate intervals on ε one should be able to obtain efficient matching with the exact values of $a(\varepsilon)$.

To summarize, the recipe for deriving approximate formula for limit cycle amplitude of a nonlinear system can be stated as follows: Determine the first order (perturbative) RG flow equation for amplitude in the nonlinear time τ. This will yield an explicit formula for amplitude a as a function of the nonlinearity parameter ε and the control parameter h_{RG}. Efficient match with the exact amplitude can be achieved by right choice of the control parameter h_{RG} or α. Alternatively, determine an efficient formula for $a(\varepsilon)$ by inspection (expert guess) or by appropriate curve fitting method. Then determine the control parameter h_{RG} by an inversion of the estimated amplitude $a_E(\varepsilon)$ as in equation (7.16) (and Figure 7.3). Since the equations concerned form a closed system, this already gives a proof of the unique existence of h_{RG} for a given nonlinear oscillation.

7.4 Application to Nonlinear Time: Limit Cycle

Consider a general nonlinear oscillator given by

$$\ddot{x} + x = \varepsilon f(x, \dot{x}) \tag{7.18}$$

We assume f such that the system admits a unique isolated cycle for $\varepsilon > 0$ and other relevant parameter values. For a finite nonlinearity $\varepsilon > 1$ (say), the usual linear time t is extended to one enjoying *right* asymptotic correction $t \to \ T_i = t\ \phi_i(\tilde{\tau}(t))$ as $t \to \infty$ through linear scales ε^i, where $\phi_i(\tilde{\tau})$ stands succinctly for the nontrivial intrinsically generated *slowly varying* scaling components arising from the associated visibility norm. Here, $\tilde{\tau}$, as usual denotes an $O(1)$ rescaled variable in the neighbourhood of linear scales ε^i. In the case of a nonlinear planar autonomous system the relevant dynamical quantities are only amplitude and phase of the nonlinear oscillation and so we have only two asymptotic scaling functions $\phi_i(\tilde{\tau})\,,\ i = 1, 2$ which get *selected* naturally so as to facilitate direct non-perturbative calculation of the asymptotic properties i.e. the amplitude and phase of the limit cycle of the system. An implementation of this non-pertubative scheme in the perturbative RG formalism is presented in Subsection 7.3.1 for computation of the amplitude of the concerned oscillators. In Subsection 7.4.1, we shall show that the computed plot (c.f. Figure 7.4) of the limit cycle for the Rayleigh and VdP oscillators could be matched arbitrarily closely for appropriate choices of the slowly varying nonlinear time when the amplitude and phase of the unperturbed periodic solution *flow linearly* in the appropriately chosen nonlinear scaling time variables.

Here, we give an alternative derivation of the nonperturbative *relaxation oscillation* flow equations ab-initio from the slowly varying nonlinear time in the context of the Rayleigh equation (7.1) with $\varepsilon \gg 1$. It will transpire that the new approach is free of any divergence problem because of its inbuilt RG cancellations via duality principle. Since we are interested in the planar limit cycle properties, we assume that all the relevant quantities e.g. the solution y, amplitude a and phase ψ are functions of asymptotic time variable $t \sim \varepsilon^n,\ n \gg 1$ and the associated nontrivial scaling variables $\tau_1 = \phi_1(\tilde{\tau})$ and $\tau_2 = \phi_2(\tilde{\tau})$ for a rescaled

$\tilde{\tau} \sim O(1)$. Higher order scaling variables $\tau_n,\ n > 2$ of the nonlinear structure of time variable may become relevant for a non-planar system. Accordingly, we write the ansatz $y(t, \tau_1, \tau_2) = y_0(t) + Y_1(\tau_1) + Y_2(\tau_2)$ for the limit cycle solution involving multiple time scales (only three for the planar system). Assuming slow variations of nonlinear scales $\tau_i = \phi_i,\ i = 1, 2$, viz. $|\phi_i''| \ll |\phi_i'^2| \ll 1,\ \phi_i' = \dfrac{d\phi_i}{d\tilde{\tau}}$, as $t \to \varepsilon^n,\ n \to \infty$ and noting that $\dfrac{dy}{dt} = \dfrac{\partial y_0}{\partial t} + \sum_i \dot{\tilde{\tau}}\phi_i' \dfrac{\partial Y_i}{\partial \tau_i}$ etc., the Rayleigh equation (7.1) simplifies to

$$\frac{\partial^2 y_0}{\partial t^2} + y_0 + \sum_i Y_i = \varepsilon \left(\frac{\partial y_0}{\partial t} + \sum_i \dot{\tilde{\tau}}\phi_i' \frac{\partial Y_i}{\partial \tau_i} \right) - \frac{\varepsilon}{3} \left(\left(\frac{\partial y_0}{\partial t} \right)^3 + 3 \left(\frac{\partial y_0}{\partial t} \right)^2 \sum_i \dot{\tilde{\tau}}\phi_i' \frac{\partial Y_i}{\partial \tau_i} \right) \tag{7.19}$$

where we drop all higher order terms involving ϕ_i'' and $\phi_i'^2$. Assuming $y_0(t) = a(\tau_1, \tau_2) \cos(t + \psi(\tau_1, \tau_2))$ with *flowing* amplitude and phase in scaling times τ_1 and τ_2 so that

$$\frac{\partial^2 y_0}{\partial t^2} + y_0 = 0 \tag{7.20}$$

we next get a simplified linearized evolution for the nonlinear components of the asymptotic limit cycle solution in the form

$$\left(1 - \left(\frac{\partial y_0}{\partial t} \right)^2 \right) \sum \dot{\phi}_i \frac{\partial Y_i}{\partial \tau_i} = \left\{ \frac{1}{3} \left(\frac{\partial y_0}{\partial t} \right)^3 - \frac{\partial y_0}{\partial t} \right\} + \varepsilon^{-1} \sum Y_i \tag{7.21}$$

where $\dot{\phi}_i = \dfrac{d\phi_i}{dt}$. As a consequence, under the assumption of slow varying nonlinear time scales, a second order nonlinear planar system (7.1) would decompose into a linear second order partial differential equation (7.20) for the zero level solution y_0 and an associated first order partial differential equation (7.21) for the nonlinear scale dependent components Y_i. Clearly, analogous decomposition holds actually for a larger class of planar autonomous systems (7.18) having a unique limit cycle solution. Extension of this result to multiple limit cycles would be considered separately.

We note here that since the system (7.20) and (7.21) is *under determined*, there is room for further restrictions to solve the system self-consistently. To re-derive the RG flow equations (7.10) and (7.11) from (7.21), we now make following assumptions: we write (i) $a(\tau_1, \tau_2) = a(\tau_1)$, $\psi(\tau_1, \tau_2) = \psi(\tau_2)$ so that amplitude varies slowly with first order scale τ_1 when the second order scale τ_2 and phase ψ remain almost constant. On the other hand as a stabilizes to an almost constant value, the phase begins to flow, though slowly with the second order scale τ_2. Such slow, almost constant, rhythmic cooperative variations of τ_1 and τ_2 are modeled, depending on the specific problem under consideration (see below and c.f. Subsection 7.4.1), to retrieve the RG flow equations correctly. As shown in the example (Remark 7.2.3) such a rhythmic nonlinear variation does exist in an ultrametric neighbourhood in $\mathbb{R}^*$. To further quantify the slow variation of dynamical variables, we next impose the condition that (ii) *the total variation of the exact solution* $y(t, \tau_1, \tau_2)$ *with respect to each slow variable* τ_i *along the full periodic cycle* C *must vanish viz.,* $\int\limits_C \frac{\partial y}{\partial \tau_i} dt = 0$ *for each* i. To avoid trivialities i.e. $\int\limits_C \cos(t + \psi) dt = 0$ etc., we, however, evaluate the concerned integrals only on the quarter cycle, with the understanding that phase shifts of $\frac{\pi}{2}$ are absorbed in the definition of ψ.

In the sufficiently large $\varepsilon > 1$ relaxation oscillation, one can further simplify (7.21) by dropping the ε^{-1} term to obtain

$$\sum \dot{\phi}_i \frac{\partial Y_i}{\partial \tau_i} = \frac{\frac{1}{3}\left(\frac{\partial y_0}{\partial t}\right)^3 - \frac{\partial y_0}{\partial t}}{1 - \left(\frac{\partial y_0}{\partial t}\right)^2} \equiv \Phi(y_{0t}),\ y_{0t} = \frac{\partial y_0}{\partial t}. \tag{7.22}$$

To make contact with RG flow equations (7.10) and (7.11) one now exploits *the freedom of right choice* in the functional forms of nonlinear scales. For the Rayleigh equation, we now set for slow, cooperatively active functional dependence (a) $\dot{\phi}_1 = \Phi(y_{0t}) S_1^{-1}(a, \psi, t)$, $\dot{\phi}_2 = 0$ and (b) $\dot{\phi}_1 = 0$, $\dot{\phi}_2 = \Phi(y_{0t}) S_2^{-1}(a, \psi, t)$ for successive slow variations, as described in (i), of the scales τ_1 and τ_2 respectively, where,

$S_1 = \frac{1}{2}a\left(\frac{a^2}{4} - 1\right)\cos(t+\psi)$ and $S_2 = \frac{1}{8}\left(1 - \frac{a^4}{32}\right)\sin(t+\psi)$ (recall the example in Remark 7.2.3 above highlighting wide possible choices and intricate functional dependence). These choices for S_1 and S_2 would yield the RG flow equations when condition (ii) is invoked.

Note that the relations in both (a) and (b) are truly nonlinear; the dynamical variables a and ψ in S_1 and S_2 depend implicitly in ϕ_1 and ϕ_2 respectively, which, in turn are *slowly varying* as the linear parameter t is assumed to vary in a neighbourhood of ε^n for a large but fixed n. Invoking the global slow variation condition (ii) for each i, in conjunction with the ansatz (a) and (b), one finally deduce the amplitude and phase flow equations (7.10) and (7.11) in slow variables τ_1 and τ_2 respectively.

In the present format, the flow equations, however, have got *new* interpretations: Amplitude and phase must flow in successive rhythmic manner; phase remains almost constant (i.e. $\frac{\partial\psi}{\partial\tau_i} = 0$ for each i) when amplitude varies slowly with τ_1 towards an almost constant value. Subsequently, the flowing of a is halted temporarily (i.e. $\frac{\partial a}{\partial\tau_i} = 0$), initiating flowing of ψ in next level variable τ_2. This rhythmic oscillation would obviously continue indefinitely over a cycle. The RG flow equations could be treated as non-perturbative because of *implicit* connections of nonlinear scaling time functions with amplitude and phase via intrinsically defined duality principle (c.f. Remark 7.2.3).

7.4.1 Approximating Limit Cycle

Here we calculate the approximate limit cycle orbit for the Rayleigh and VdP equations for a sufficiently large $\varepsilon > 1$. Perturbative RGM fails to give correct relaxation oscillation solution. The first order solution given in Section 5.2 in Chapter 5 by HAM is also found insufficient. In this work we do not undertake the problem of computing approximate limit cycle by HAM, which has been addressed by Lopez et al. [18] for the VdP equation. Our aim here is to highlight the strength of IRGM over perturbative RGM.

For a sufficiently large time $t \to \varepsilon^n$, n large, but fixed, the slowly

varying nonlinear scales τ_1 and τ_2 are activated in a successive rhythmic manner, as explained in Section 7.3, so that the perturbative solution given in (6.8) of Chapter 6 is extended to the asymptotic limit cycle (relaxation oscillation) solution

$$y(\tau_1, \tau_2) = a(\tau_1)\cos(\varepsilon^n + \psi(\tau_2)) + Y \tag{7.23}$$

where the amplitude a and phase ψ *flow* along the cycle following the nonperturbative flow equations (7.10) and (7.11) in the asymptotic scaling variables τ_1 and τ_2 respectively. Here, Y encodes all the renormalized perturbative terms depending on higher order, slowly varying nonlinear scales $\tau_i,\ i > 2$. The corresponding velocity component $\dot{y} = \dfrac{\partial y}{\partial t}$ at $t = \varepsilon^n$ has the form

$$\dot{y}(\tau_1, \tau_2) = -a(\tau_1)\sin(\varepsilon^n + \psi(\tau_2)) + \sum_i \dot{\tau}_i \frac{\partial Y}{\partial \tau_i}. \tag{7.24}$$

Equations (7.23) and (7.24) are the parametric equations of the limit cycle, parametrized by multiple nonlinear scales, when slowly varying amplitude a and phase ψ are computed from (7.10) and (7.11) respectively. An alternative derivation of (7.23) and (7.24) based purely on duality induced nonlinear scales is given in Section 7.4. We remark that (7.23) and (7.24) actually represent the general form of the limit cycle for a much large class of Lienard system having unique limit cycle. *Typical geometric shape of the periodic cycle of a given nonlinear system is controlled entirely by the rhythmic cooperative, almost constant variations of the nonlinear scales τ_i.* As explained in Section 7.3, scale invariance of the scaling functions $\tau_1 = \phi_1\left(\tilde{t}_1/\varepsilon\right)$ and $\tau_2 = \phi_1\left(\tilde{t}_2/\varepsilon^2\right)$ tells that as the linear time $t \to \varepsilon^n$, $\tau_1 \to \phi_1(1) = 1$ and $\tau_2 \to \phi_2(1) = 1$ with $\tilde{t}_1 \to \varepsilon$ and $\tilde{t}_2 \to \varepsilon^2$. We now set the initial conditions $a(1) = a_{\text{amp}}(\varepsilon),\ a'(1) = \dfrac{a(1)}{2}\left(1 - \dfrac{a(1)^2}{4}\right)$ and $\psi(1) = 0$, where $a_{\text{amp}}(\varepsilon)$ is the exact (experimental) value of the amplitude of the limit cycle. Setting further $\tau_1 = 1 + \eta_1$ and $\tau_2 = 1 + \eta_2$ as $t \to \varepsilon^n$, both amplitude and phase flow equations (7.10) and (7.11) now yield linear flow of amplitude and phase relative to the respective small scale slow, almost constant variables η_1 and η_2, satisfying

$|\eta_i^2| \ll 1$ and $|\ddot{\eta}_i| \ll |\dot{\eta}_i^2| \ll 1$, those vary in a rhythmic manner. The exact (experimental) limit cycle could now be approximated with any desired accuracy by smooth matching of the straight line segments of the form $(i)\ z - Z_0 = k\,(y - Y_0)$ and circular arcs of the form (ii) $(y - Y_0)^2 + (z - Z_0)^2 = a^2\,(\tau_1)$ over judiciously chosen intervals in y in the (y, z) plane, where $z = \dot{y}$, $k = -\tan\left(\varepsilon^n + \psi\,(\tau_2)\right)$, $Y_0 = Y$ and $Z_0 = \sum_i \dot{\tau}_i \frac{\partial Y}{\partial \tau_i}$. Because of the availability of cooperatively evolving resource of nonlinear scales, such a matching is always possible theoretically. In the alternative derivation of limit cycle equations in Section 7.4, we have outlined an approach to gain more analytic understanding of the rhythmic, cooperative variations of the nonlinear scaling functions. We hope to address the question of determining the precise analytic properties of the scaling functions $\phi_i\,(\tilde{\tau})$ corresponding to a given nonlinear system in future communications.

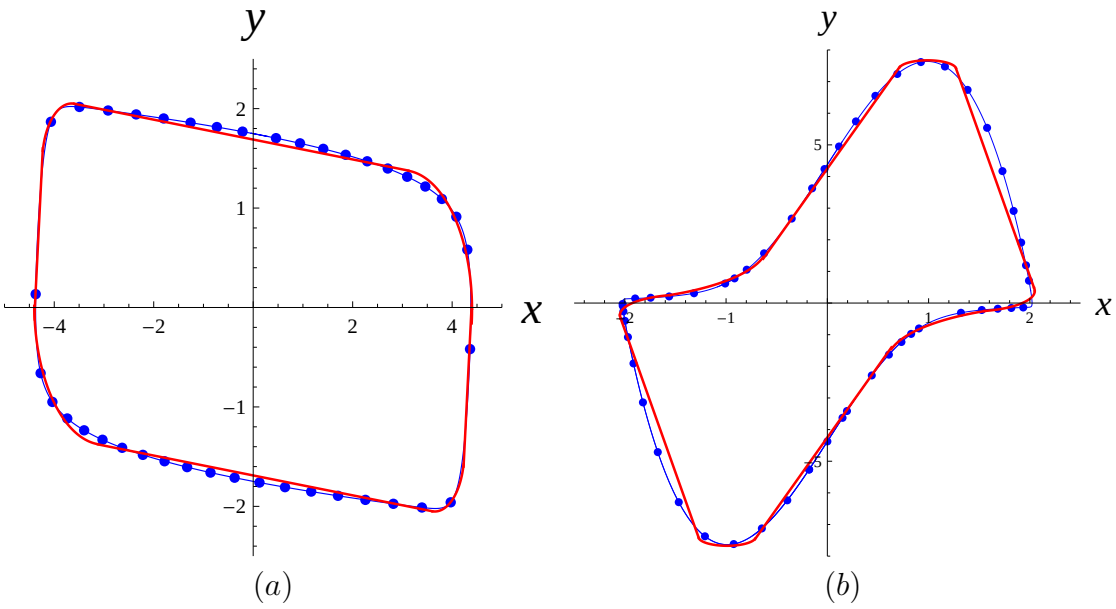

Figure 7.4: Approximate limit cycle for (a) Rayleigh equation and (b) Van der Pol equation; solid (red) line for approximate curve, dotted (blue) line for exact curve $(\varepsilon = 5)$.

In Figure 7.4(a) and Figure 7.4(b), we display the (y, z) phase plane relaxation oscillation for the Rayleigh and VdP equations with $\varepsilon = 5$. A piecewise smooth matching curve for upper half of the approximate

Rayleigh limit cycle for $\varepsilon = 5$ is

$$z(y) = \begin{cases} 0.02 - \sqrt{1.96 - (y+3)^2}, & -4.96 < y \leq -4.393, \\ 10y + 43.9, & -4.393 < y \leq -4.23, \\ 1.46 + \sqrt{0.35 - (y+3.65)^2}, & -4.23 < y \leq -3.6, \\ -0.1y + 1.689, & -3.6 < y \leq 3.12, \\ -0.02 + \sqrt{1.96 - (y-3)^2}, & 3.12 < y \leq 4.96; \end{cases}$$

given by solid (red) lines in Figure 7.4(a) and another such curve for upper half of the approximate VdP limit cycle for $\varepsilon = 5$ is

$$z(y) = \begin{cases} -0.388 + \sqrt{0.352 - (y+1.438)^2}, & -2.05 < y \leq -1.7, \\ 1.8 - \sqrt{3.2 - (y+2.38)^2}, & -1.7 < y \leq -0.633, \\ 4.5y + 4.25, & -0.633 < y \leq 0.6, \\ 6.5 + \sqrt{2.76 - (y-2.2)^2}, & 0.6 < y \leq 0.9, \\ 7.325 + \sqrt{0.063 - (y-1.04)^2}, & 0.90 < y \leq 1.28, \\ 0.38 + \sqrt{1530 - (y+37.2)^2}, & 1.28 < y \leq 1.8, \\ -13y + 26.8, & 1.8 < y \leq 2.033, \\ 0.388 + \sqrt{0.352 - (y-1.438)^2}, & 2.033 < y \leq 2.05; \end{cases}$$

shown as solid (red) lines in Figure 7.4(b).

Here, the piece-wise smooth matching curves approximating these cycles are presented in tabular forms. However, the smoothness at the joining points are achieved at the level of one decimal only. More accurate approximation may be achieved with smarter efforts. Judicious choice of slowly varying centres (Y_0, Z_0) and radii $a(\tau_1)$ of circular arcs of right sizes (a straight line segment being an arc with sufficiently large radius) should give better approximations with a given exact (experimental) cycle that can be obtained on a symbolic computation platform, Mathematica for instance. The phase plane dynamics of these slowly varying centres and radii is expected to reveal interesting new insights into asymptotic properties of the nonlinear oscillation.

It transpires from above discussion that radii, for instance, vary much faster in Rayleigh than that in VdP oscillator, in which case radii fluc-

tuate between small and large values through intermediate steps. This might be compared with fast and slow energy build ups in Rayleigh and VdP relaxation oscillations respectively. One would like to interpret this phase plane dynamics as cooperative evolution of multiple nonlinear scales driving amplitude and phase of the nonlinear oscillation to flow in such a fashion as to generate little circular arcs and linear segments which join smoothly together to form the complete orbit. Making an accurate plot then boils down to finding right kind of such arcs and line segments. Intricate dependence of the trajectory itself into the definition of the nonlinear scales (c.f. Remark 7.2.3) tells in retrospect that one needs to look for a novel iteration scheme that would allow one to extract the trajectory systematically as a limit process. This problem will be considered in detail elsewhere.

7.5 Concluding Remarks

In this chapter we have presented a comparative study of the homotopy analysis method and the Renormalization Group method. It turns out that the higher order perturbative calculations based on the conventional Renormalization group method would fail to give efficient formula for the limit cycle amplitudes for these nonlinear oscillators. However, an improved version of the Renormalization group analysis exploiting a novel concept of nonlinear time is shown to yield efficient amplitude formulae for all values of ε. Exploiting multiple nonlinear scales of the associated nonlinear time the improved RG method is also found to yield good plots for relaxation oscillation orbits for the Rayleigh and VdP systems.

We have presented brief review of the nonlinear time formalism and also given an alternative approach in deriving non-perturbative flow equations of amplitude and phase of a limit cycle problem. Non-perturbative information of asymptotic quantities get naturally encoded into nonlinear scales, that can be exploited judiciously to extract desired asymptotic properties of a relevant dynamical quantity. An algorithmic procedure of extracting such information is explained in estimating both the limit cycle amplitude and trajectory for Rayleigh and VdP

equations. More detailed analysis of the nonlinear time formalism in several other nonlinear systems will be considered in future.

Chapter 8

Future Scope

In the first part of this thesis, sufficient conditions for existence of the unique or multiple limit cycles for a class of Lienard systems are presented based on a simple extension of the classical Lienard theorem. The problem of developing powerful methods, leading to the proof of the exact number of limit cycles, for more wider class of Lienard systems is an active field of current research [47,51,52], with many authors, for instances, Lopez, Abbasbandy, Lopez-Ruiz [18, 67], Llibre [47] are making important new advances in this field. The limitation of our simple geometric approach becomes noticeable in our inability in obtaining a proof leading to exact number of limit cycles for the class of non-symmetric Lienard system. An extension of our approach in the light of current literature is necessary to achieve the goal. This is an important problem we would like to take up in near future.

Reconstruction of differential systems from incomplete information has been studied in Chapter 3 in the context of symmetric Lienard equation with a given number of limit cycles. Similar study for other kind of differential systems remains an open problem, especially with a given shape and size of a limit cycle. Another important class of problems in the Part I of the thesis is the possible extensions of the present approach to piece-wise smooth/continuous or even discontinuous (Lienard-like) systems [54, 79, 80], because non-smooth systems are more interesting, from the point of view of applications, rather than smooth systems.

In the second part of the thesis, a new Improved Renormalization Group Method is developed using new formalism of nonlinear time.

Use of multiple nonlinear scales enabled us to simulate cooperative behaviour among the asymptotic properties of different physical/dynamical parameters of a nonlinear system, viz. Rayleigh and Van der Pol systems in a much more efficient manner than that was possible in the context of conventional RGM. The formalism presented in the thesis, though appears to be novel and appealing, needs to be further substantiated by many more such applications in different classes of nonlinear systems, both autonomous as well as non-autonomous. One of our immediate goal in this area of research is to investigate non-autonomous VdP equation with a periodic forcing, in the context of nonlinear time formalism and to try to understand the period doubling bifurcation route to the chaotic attractor in the light of the associated hierarchy of nonlinear scales.

Bibliography

[1] C.M. Bender and S.A. Orszag. *Advanced Mathematical Methods for Scientists and Engineers I*. Springer Science & Business Media, 1999.

[2] S.L. Ross. *Introduction to Ordinary Differential Equations*. John Wiley & Sons, 1980.

[3] D.W. Jordan and P. Smith. *Nonlinear Ordinary Differential Equations: An Introduction to Dynamical Systems*, volume 2. Oxford University Press, 1999.

[4] S. Sastry. *Nonlinear Systems: Analysis, Stability, and Control*, volume 10. Springer Science & Business Media, 2013.

[5] H. Poincaré. *New Methods of Celestial Mechanics: Periodic Solutions, the Non-existence of Integral Invariants, Asymptotic Solutions*. National Aeronautics and Space Administration, 1967.

[6] B. Van der Pol. LXXXVIII. On relaxation-oscillations. *The London, Edinburgh, and Dublin Philosophical Magazine and Journal of Science*, 2(11):978–992, 1926.

[7] M.L. Cartwright and J.E. Littlewood. On Nonlinear Differential Equations of Second Order, I: The Equation $\ddot{y} + \kappa\left(1 - y^2\right)\dot{y} + y = b\lambda\kappa\cos\left(\lambda t + a\right)$, κ large. *J. Lond. Math. Soc.*, 20:180–189, 1945.

[8] N. Levinson. A Second Order Differential Equation with Singular Solutions. *Annals of Mathematics*, pages 127–153, 1949.

[9] Edward N E.N. Lorenz. Deterministic Nonperiodic Flow. *Journal of the Atmospheric Sciences*, 20(2):130–141, 1963.

[10] J.B. Keller and M. Miksis. Bubble Oscillations of Large Amplitude. *The Journal of the Acoustical Society of America*, 68(2):628–633, 1980.

[11] P. Veskos and Y. Demiris. Experimental Comparison of the Van der Pol and Rayleigh Nonlinear Oscillators for a Robotic Swinging Task. In *Adaptation in Artificial and Biological Systems*, pages 197–202. AISB, 2006.

[12] J. Guckenheimer, K. Hoffman and W. Weckesser. Numerical Computation of Canards. *International Journal of Bifurcation and Chaos*, 10(12):2669–2687, 2000.

[13] P.F. Rowat and A.I. Selverston. Modeling the Gastric Mill Central Pattern Generator of the Lobster with a Relaxation-oscillator Network. *Journal of neurophysiology*, 70(3):1030–1053, 1993.

[14] R. FitzHugh. Impulses and Physiological States in Theoretical Models of Nerve Membrane. *Biophysical journal*, 1(6):445, 1961.

[15] J. Nagumo, S. Arimoto and S. Yoshizawa. An Active Pulse Transmission Line Simulating Nerve Axon. *Proceedings of the IRE*, 50(10):2061–2070, 1962.

[16] S. Liao. *The Proposed Homotopy Analysis Technique for the Solution of Nonlinear Problems*. PhD thesis, Shanghai Jiao Tong University, 1992.

[17] S. Liao. *Homotopy Analysis Method in Nonlinear Differential Equations*. Springer, 2012.

[18] J.L. Lopez, S. Abbasbandy and R. Lopez-Ruiz. Formulas for the Amplitude of the Van der Pol Limit Cycle through the Homotopy Analysis Method. *Scholarly Research Exchange*, 2009.

[19] H.G.E. Meijer and T. Kalmár-Nagy. The Hopf-Van der Pol System: Failure of a Homotopy Method. *Differential Equations and Dynamical Systems*, 20(3):323–328, 2012.

[20] S. Liao. An Analytic Approximate Approach for Free Oscillations of Self-excited Systems. *International Journal of Non-Linear Mechanics*, 39(2):271–280, 2004.

[21] S. Liao. On the Homotopy Analysis Method for Nonlinear Problems. *Applied Mathematics and Computation*, 147(2):499–513, 2004.

[22] J. Cheng, S. Liao, R.N. Mohapatra and K. Vajravelu. Series Solutions of Nano Boundary Layer Flows by means of the Homotopy Analysis Method. *Journal of Mathematical Analysis and Applications*, 343(1):233–245, 2008.

[23] S. Liao. Comparison between the Homotopy Analysis Method and Homotopy Perturbation Method. *Applied Mathematics and Computation*, 169(2):1186–1194, 2005.

[24] W. Wu and S. Liao. Solving Solitary Waves with Discontinuity by means of the Homotopy Analysis Method. *Chaos, Solitons & Fractals*, 26(1):177–185, 2005.

[25] S. Liao. On the Homotopy Multiple-variable Method and its Applications in the Interactions of Nonlinear Gravity Waves. *Communications in Nonlinear Science and Numerical Simulation*, 16(3):1274–1303, 2011.

[26] N.N. Bogoliubov and D.V. Shirkov. *Introduction to the Theory of Quantized Fields*. New York, Interscience, 1959.

[27] K.G. Wilson. The Renormalization Group: Critical Phenomena and the Kondo Problem. *Reviews of Modern Physics*, 47(4):773, 1975.

[28] N. Goldenfeld. *Lectures on Phase Transitions and the Renormalization Group*. Addison-Wesley, 1993.

[29] G.I. Barenblatt. *Scaling*, volume 34. Cambridge University Press, 2003.

[30] E. Ott. *Chaos in Dynamical Systems*. Cambridge University Press, 2002.

[31] L.Y. Chen, N. Goldenfeld and Y. Oono. Renormalization Group and Singular Perturbations: Multiple Scales, Boundary Layers, and Reductive Perturbation Theory. *Physical Review E*, 54(1):376, 1996.

[32] E.E. Svanes. The Non-Perturbative Renormalization Group with Applications. Master Thesis, Norwegian University of Science and Technology, http://www.nt.ntnu.no/users/jensoa/svanes.pdf.

[33] L.Y. Chen, N. Goldenfeld and Y. Oono. Renormalization Group Theory for Global Asymptotic Analysis. *Physical review letters*, 73(10):1311, 1994.

[34] L.Y. Chen, N. Goldenfeld and Y. Oono. Renormalization Group and Singular Perturbations: Multiple Scales, Boundary Layers, and Reductive Perturbation Theory. *Physical Review E*, 54(1):376, 1996.

[35] R.E.L. DeVille, A. Harkin, M. Holzer, K. Josić and T.J. Kaper. Analysis of a Renormalization Group Method and Normal Form Theory for Perturbed Ordinary Differential Equations. *Physica D: Nonlinear Phenomena*, 237(8):1029–1052, 2008.

[36] A. Sarkar and J.K. Bhattacharjee. Renormalization Group as a Probe for Dynamical Systems. In *Journal of Physics: Conference Series*, volume 319, page 012017. IOP Publishing, 2011.

[37] V.F. Kovalev, V.V. Pustovalov and D.V. Shirkov. Group Analysis and Renormgroup Symmetries. *Journal of Mathematical Physics*, 39(2):1170–1188, 1998.

[38] V.F. Kovalev and D.V. Shirkov. Functional Self-similarity and Renormalization Group Symmetry in Mathematical Physics. *Theoretical and Mathematical Physics*, 121(1):1315–1332, 1999.

[39] V.F. Kovalev and D.V. Shirkov. Renormalization-group Symmetries for Solutions of Nonlinear Boundary Value Problems. *Physics-Uspekhi*, 51(8):815, 2008.

[40] D.P. Datta and S. Sen. Excitation of Flow Instabilities due to Nonlinear Scale Invariance. *Physics of Plasmas (1994-present)*, 21(5):052311, 2014.

[41] A. Palit and D.P. Datta. Comparative Study of Homotopy Analysis and Renormalization Group Methods on Rayleigh and Van der Pol Equations. *Differential Equations and Dynamical Systems*, 2015. Available first online 26 July 2015, Doi: 10.1007/s12591-015-0253-y.

[42] D.P. Datta and S. Sarkar. Duality Structure, Non-archimedean Extension of Real Number System and Emergent Fractal Sets. Submitted.

[43] A. Lins, C.C. Pugh and W. De Melo. On Liénard's Equation. In *Geometry and Topology*, pages 335–357. Springer, 1977.

[44] G.S. Rychkov. The Maximal Number of Limit Cycles of the System $\dot{y} = -x$, $\dot{x} = y - \left(a_1 x + a_3 x^3 + a_5 x^5\right)$ is Equal to Two. *Differential Equations*, 11:301, 1975.

[45] T. Holst and J. Sundberg. Number of Limit Cycles of a Certain Lienard Equation. Master's thesis, Matematiska Institutionen, Stockholms Universitet, 2006.

[46] H. Giacomini and S. Neukirch. Improving a Method for the Study of Limit Cycles of the Liénard Equation. *Physical Review E*, 57(6):6573, 1998.

[47] X. Chen, J. Llibre and Z. Zhang. Sufficient Conditions for the Existence of at least n or Exactly n Limit Cycles for the Liénard Differential Systems. *Journal of Differential Equations*, 242(1):11–23, 2007.

[48] K. Odani. Existence of Exactly N Periodic Solutions for Liénard Systems. *Funkcialaj Ekvacioj*, 39(2):217–234, 1996.

[49] X. Chen and Y. Chen. A Sufficient Condition for Liénard's Equation that has at most n Limit Cycles. In *J. Math. Res. Exposition*, volume 23, pages 333–338, 2003.

[50] F. Dumortier, D. Panazzolo and R. Roussarie. More Limit Cycles than Expected in Liénard Equations. *Proceedings of the American Mathematical Society*, 135(6):1895–1904, 2007.

[51] Z. Zhi-Fen, D. Tong-Ren, H. Wen-Zao and D. Zhen-Xi. *Qualitative Theory of Differential Equations*, volume 101. American Mathematical Soc., 2006.

[52] K. Odani. On the Limit Cycle of the Liénard Equation. *Archivum Mathematicum*, 36(1):25–31, 2000.

[53] J.S. López and R. López-Ruiz. Approximating the Amplitude and Form of Limit Cycles in the Weakly Nonlinear Regime of Liénard Systems. *Chaos, Solitons & Fractals*, 34(4):1307–1317, 2007.

[54] J. Llibre, E. Ponce and F. Torres. On the Existence and Uniqueness of Limit Cycles in Liénard Differential Equations Allowing Discontinuities. *Nonlinearity*, 21(9):2121–2142, 2008.

[55] A. Palit and D.P. Datta. On the Determination of Exact Number of Limit Cycles in Lienard Systems. *Bull. Cal. Math. Soc.*, 104:35–56, 2012.

[56] A. Palit and D.P. Datta. On a Finite Number of Limit Cycles in a Lienard System. *International Journal of Pure and Applied Mathematics*, 59:469–488, 2010.

[57] A.L. Goldberger. Is the Normal Heartbeat Chaotic or Homeostatic? *Physiology*, 6(2):87–91, 1991.

[58] D.L. Donoho. Nonlinear Wavelet Methods for Recovery of Signals, Densities, and Spectra from Indirect and Noisy Data. In *In Proceedings of Symposia in Applied Mathematics*, pages 173–205. American Mathematical Society, 1993.

[59] B. Zduniak, M. Bodnar and U. Foryś. A Modified Van der Pol Equation with Delay in a Description of the Heart Action. *International Journal of Applied Mathematics and Computer Science*, 24(4):853–863, 2014.

[60] H. Giacomini and S. Neukirch. Number of Limit Cycles of the Liénard Equation. *Physical Review E*, 56(4):3809, 1997.

[61] G. Sansone and R. Conti. *Non-Linear Differential Equations: International Series of Monographs in Pure and Applied Mathematics*, volume 67. Elsevier, 2014.

[62] M. Sabatini and G. Villari. On the Uniqueness of Limit Cycles for Liénard Equations: the Legacy of G. Sansone. *Le Matematiche*, 65(2):201–214, 2010.

[63] T. Carletti and G. Villari. A Note on Existence and Uniqueness of Limit Cycles for Liénard Systems. *J. Math. Anal. Appl*, 307:763–773, 2005.

[64] A. Palit and D.P. Datta. Existence of Limit Cycles in a Class of Non-symmetric Lienard Systems. *Indian Journal of Mathematics*, 58:59–93, 2016.

[65] Z. Zhang. On the Uniqueness of the Limit Cycles of Some Nonlinear Oscillation Equations. *Doki. Acad. Nauk. SSSR*, 119:659–662, 1958.

[66] A.F. Filippov. A Sufficient Condition for the Existence of a Stable Limit Cycle for an Equation of the Second Order. *Matematicheskii Sbornik*, 72(1):171–180, 1952.

[67] J.L. Lopez, S. Abbasbandy and R. Lopez-Ruiz. Formulas for the Amplitude of the Van der Pol Limit Cycle. *arXiv preprint arXiv:0806.1634*, 2008.

[68] S. Liao. *Beyond Perturbation: Introduction to the Homotopy Analysis Method*. CRC Press, 2003.

[69] S. Liao. An Analytic Approximate Approach for Free Oscillations of Self-excited Systems. *International Journal of Non-Linear Mechanics*, 39(2):271–280, 2004.

[70] M.E. Machacek and M.T. Vaughn. Two-loop Renormalization Group Equations in a General Quantum Field Theory:(I). Wave

Function Renormalization. *Nuclear Physics B*, 222(1):83–103, 1983.

[71] J.J. Binney, N.J. Dowrick, A.J. Fisher and M. Newman. *The Theory of Critical Phenomena: An Introduction to the Renormalization Group*. Oxford University Press, Inc., 1992.

[72] K.G. Wilson. Renormalization Group and Critical Phenomena. I. Renormalization Group and the Kadanoff Scaling Picture. *Physical review B*, 4(9):3174, 1971.

[73] L.Y. Chen, N. Goldenfeld and Y. Oono. Renormalization Group Theory for Global Asymptotic Analysis. *Physical Review Letters*, 73(10):1311, 1994.

[74] P.M. Chaikin and T.C. Lubensky. *Principles of Condensed Matter Physics*, volume 1. Cambridge Univ Press, 2000.

[75] G. Grosso and G.P. Parravicini. *Solid State Physics*. Elsevier Science, 2013.

[76] D.P. Datta and S. Raut. The Arrow of Time, Complexity and The Scale Free Analysis. *Chaos, Solitons & Fractals*, 28(3):581–589, 2006.

[77] D.P. Datta. Novel Late Time Asymptotics: Applications to Anomalous Transport in Turbulent Flows. *Radiation Effects and Defects in Solids*, 168(10):789–798, 2013.

[78] D.P. Datta, S. Raut and A. Raychoudhuri. Ultrametric Cantor Sets and Growth of Measure. *P-Adic Numbers, Ultrametric Analysis, and Applications*, 3(1):7–22, 2011.

[79] F. Jiang and J. Sun. On the uniqueness of limit cycles in discontinuous Liénard-type systems. *Electron. J. Qual. Theory Differ. Equ*, 71:1–12, 2014.

[80] F. Jiang, J. Shi and J. Sun. On the Number of Limit Cycles for Discontinuous Generalized Liénard Polynomial Differential Systems. *International Journal of Bifurcation and Chaos*, 25(10):1550131, 2015.